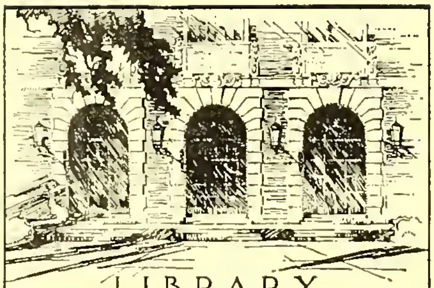

LIBRARY
OF THE
UNIVERSITY
OF ILLINOIS
538.767
Il6a
no. 1-5

Digitized by the Internet Archive
in 2011 with funding from
University of Illinois Urbana-Champaign

http://www.archive.org/details/impedanceofshort02balm

UNIVERSITY OF ILLINOIS
URBANA

AERONOMY REPORT
NO. 2

THE IMPEDANCE OF A SHORT DIPOLE ANTENNA IN A MAGNETOPLASMA

by
K. G. Balmain

July 1, 1964

ssued under
ational Aeronautics and
pace Administration
rant NsG-511

Department of Electrical Engineering
Engineering Experiment Station
University of Illinois
Urbana, Illinois

AERONOMY REPORT NO. 2

THE IMPEDANCE OF A SHORT DIPOLE ANTENNA IN A MAGNETOPLASMA

by

K. G. Balmain

July, 1964

Issued under
National Aeronautics and
Space Administration
Grant NsG-511

Department of Electrical Engineering
Engineering Experiment Station
University of Illinois
Urbana, Illinois

ACKNOWLEDGEMENT

The author is indebted to Professor G. A. Deschamps for his helpful advice and guidance. He is grateful to the members of the University of Illinois Antenna Laboratory for their assistance. The author also wishes to thank Messrs. J. C. Wissmiller and G. L. Duff for their contributions to the experimental apparatus and numerical computations.

The work described in this report was supported by the Geophysics Research Directorate, Air Force Cambridge Research Laboratories under Contract No. AF19(604)-5565. Support was also provided by the National Aeronautics and Space Administration under Grants NsG-395 and NsG-511. This report was first printed, and received limited distribution, in May 1963.

ABSTRACT

A formula for the impedance of a short, cylindrical dipole in a magnetoplasma is derived using quasi-static electromagnetic theory. The formula is valid in a lossy plasma and for any dipole orientation with respect to the magnetic field. It is shown that the quasi-static theory can be interpreted in terms of scaled coordinates and that a cylindrical dipole in a magnetoplasma has a free space equivalent with a distorted shape. The dipole impedance is found to have a positive real part under lossless conditions when the quasi-static differential equation is hyperbolic; this indicates that the quasi-static theory predicts a form of radiation. The effects of plasma wave excitation and various assumed current distributions are discussed. Laboratory measurements of monopole impedance are found to agree fairly well with the theoretical calculations.

CONTENTS

Page

1. Introduction 1

2. The Quasi-Static Theory for a Short Dipole Antenna in a Magnetoplasma 5

    2.1 Derivation of the Basic Equations 5
    2.2 The Field of a Short Dipole 32
    2.3 The Impedance of a Short Dipole 44
    2.4 The Poynting Theorem and Calculation of Radiation Resistance 57
    2.5 Derivation of the Impedance Formula by Dimensional Scaling 68
    2.6 The Effect of a Cylindrical Current Assumption on the Computed Impedance 80
    2.7 The Effect of a Smooth Current Assumption on the Computed Impedance 85

3. Validity of the Theoretical Model 93

    3.1 A First-Order Correction to the Quasi-Static Theory 93
    3.2 The Effect of Plasma Waves on Impedance 104
    3.3 The Effect of a Non-Uniform Electron Density 117

4. Laboratory Measurement of Monopole Impedance 124

    4.1 Experimental Apparatus and Measurement Technique 124
    4.2 Comparison of Experimental and Theoretical Impedance 135

5. Conclusions 154

References 157

Additional References on Related Topics 159

Appendix 160

LIST OF ILLUSTRATIONS

Figure Number		Page
2.1.1	The elliptic and hyperbolic regions. Note: θ is the angle (with respect to the Z axis) of the characteristic cone when the differential equation is hyperbolic	30
2.2.1	The co-ordinate system	35
2.2.2	The assumed current distribution	37
2.2.3	The charge distribution	38
2.2.4	Integration Contours	42
2.3.1	Derivation of the impedance formula	46
2.3.2	The cylindrical co-ordinate system	48
2.4.1	Radiation fields of a monopole	60
2.5.1	The co-ordinate system in the magnetoplasma	75
2.5.2	The free space co-ordinate system	77
2.7.1	Electric field discontinuities for two current distributions	91
3.2.1	The source distribution	105
3.3.1	The assumed electron density distribution between two parallel conducting plates	118
3.3.2	The impedance of a non-uniform, isotropic plasma between parallel plates as a function of peak electron density. Collision parameter: Z=.10	120
3.3.3	The impedance of a non-uniform, isotropic plasma between parallel plates as a function of peak electron density. Collision parameter: Z=.05	121
4.1.1	The vacuum system	125
4.1.2	The experimental apparatus	126
4.1.3	The discharge tube and RF probe	128
4.1.4	Determination of electron density by the "Resonance Probe" technique	129

LIST OF ILLUSTRATIONS (continued)

Figure Number Page

4.1.5 Method of plotting an impedance locus using a square-law detector 130

4.1.6a Slotted line voltage as a function of time. (Neon at 4.3 mm. pressure. Time scale: 320 μs/cm.) 131

4.1.6b Slotted line voltage as a function of time. (Neon at 4.3 mm. pressure. Time scale: 320 μs/cm.) 132

4.1.7 Vacuum system leakage 134

4.2.1 Theoretical impedance loci for neon at 2.3 mm. pressure 139

4.2.2 Experimental impedance loci for neon at 2.2 mm. pressure 140

4.2.3 Experimental impedance loci for neon (0.5% argon) at 2.0 mm. pressure 141

4.2.4 Theoretical impedance loci for neon at 4.3 mm. pressure 142

4.2.5 Experimental impedance loci for neon at 4.3 mm. pressure 143

4.2.6 Experimental impedance loci for neon (0.5% argon) at 4.2 mm. pressure 144

4.2.7 Experimental impedance loci for neon (0.5% argon, 0.03% air) at 4.3 mm. pressure 145

4.2.8 Experimental impedance loci for neon (0.5% argon, 0.15% air) at 4.3 mm. pressure 146

4.2.9 Theoretical impedance loci for neon at 10.3 mm. pressure 147

4.2.10 Experimental impedance loci for neon (0.5% argon) at 10.3 mm. pressure 148

4.2.11 Theoretical impedance loci for helium at 2.2 mm. pressure 149

4.2.12 Experimental impedance loci for helium at 2.2 mm. pressure 150

1. INTRODUCTION

When an antenna is immersed in some medium, knowledge of its impedance is important whether the antenna is regarded as part of a communications system or as a probe for studying the properties of the medium. For the former application, energy reflection from the antenna must be minimized and for the latter, the relationship between impedance and medium properties must be well established. The foregoing statements apply especially to rocket and satellite exploration of the ionosphere and also to plasma diagnostics in the laboratory. For these reasons it was decided to study both theoretically and experimentally the impedance of a short cylindrical dipole antenna immersed in a magnetoplasma. Only linear (low RF level) phenomena will be discussed in this report.

The analysis is limited to short antennas (short compared to a wavelength) in order to avoid the problem of obtaining theoretically the antenna current distributions. If the antenna is short enough, the current may be assumed to vary linearly from a maximum at the center to zero at both ends. Furthermore a short antenna may be conveniently analyzed using quasi-static electromagnetic theory, a method which (in free space at least) gives good impedance results but does not predict radiation. In this report the quasi-static theory is derived by means of a low frequency approximation and is used to calculate dipole impedance for any orientation of the dipole with respect to the steady magnetic field. Furthermore it is shown that the first near field term of Mittra and Deschamps[1] is the quasi-static field.

Laboratory impedance measurements also are simplified by limiting the experimentation to short antennas. Since a short antenna radiates little energy, the reflection of this energy from nearby obstacles has negligible effect on the impedance. This is especially important when the antenna is immersed in a laboratory plasma because the walls of the plasma container must necessarily be close to the antenna. The measurements to be described were performed on a monopole antenna having a length of approximately a twentieth of a free space wavelength and inserted in the end of a cylindrical glass discharge tube. For experimental convenience, measurements are limited to the case in which the steady magnetic field is parallel to the monopole axis. The impedance measurements agree reasonably well with the quasi-static theoretical predictions.

An unexpected result of the quasi-static theory is the prediction of radiation which occurs when the quasi-static differential equation is hyperbolic. The effect of this radiation on impedance is not only predicted theoretically but also detected experimentally. Electromagnetic effects such as radiation were not expected because, in free space, a quasi-static (irrotational) electric field cannot induce a magnetic field. In a magnetoplasma, however, the electric field does induce a magnetic field and radiation can take place.

The validity of the theoretical model is examined from several viewpoints. An impedance correction is computed, using a second order term arising in the derivation of the quasi-static field theory. The problem of the influence of the assumed current distribution is treated by computing the effects of two different current distributions. In addition, the effect of the excitation of longitudinal plasma waves is computed for the isotropic case. However, as far as the laboratory experiment is concerned these corrections are of negligible importance compared to the problem of non-uniform electron density resulting from plasma diffusion to the antenna surface and to the container walls. The magnitude of this effect is estimated by calculating the impedance of a non-uniform, isotropic plasma between parallel conducting plates.

There are relatively few published papers dealing with the impedance of antennas in anisotropic media. Kononov et al,[2] have applied quasi-static theory to the problem of an infinitesimal dipole but their field and impedance expressions differ with those in this report due to their choice of an integration contour. Katzin and Katzin[3] have derived an impedance formula for longer dipoles but a great deal of numerical integration would be necessary to extract impedance values from their formula. Whale[4] has discussed some aspects of the problem, including the effect of plasma wave excitation on radiation resistance. Bramley[5] has obtained an impedance expression valid for low electron density or weak magnetic field. Kaiser[6] has observed a real part in the input impedance of a biconical dipole but he believes this to be the result of energy storage rather than radiation.

Some papers on related topics should be mentioned for the sake of completeness. The impedance of antennas in conducting, isotropic media has been studied by King and Harrison[7] and also by Deschamps[8] whose impedance relation is particularly simple and useful. Quasi-static theory has been applied to propagation problems in plasmas by Trivelpiece and Gould[9] and in ferrites by Trivelpiece et al,[10] and several other authors.[11,12]

A thorough discussion of source problems in isotropic, warm plasma has been presented by Cohen[13] in a series of three articles.

2. THE QUASI-STATIC THEORY FOR A SHORT DIPOLE ANTENNA IN A MAGNETOPLASMA

2.1 Derivation of the Basic Equations

In a plasma with a z- directed DC magnetic field, Maxwell's equations are

$$\nabla \times \overline{H} = j\,\omega\,\epsilon_o K\,\overline{E} + \overline{J} \tag{2.1.1}$$

$$\nabla \times \overline{E} = -j\,\omega\,\mu_o\,\overline{H} \tag{2.1.2}$$

The relative permittivity tensor K is

$$K = \begin{bmatrix} K' & jK'' & 0 \\ -jK'' & K' & 0 \\ 0 & 0 & K_o \end{bmatrix} \tag{2.1.3}$$

in which

$$K_o = 1 - \frac{X}{U}$$

$$K' = 1 - \frac{X\ U}{U^2 - Y^2}$$

$$K'' = -\frac{X\ Y}{U^2 - Y^2}$$

$X = \frac{\omega_N^2}{\omega^2}$ $\omega_N^2 = \frac{Ne^2}{m\epsilon_o}$

$Y = \frac{\omega_H}{\omega}$ $\omega_H = \frac{eB_o}{m}$

$U = 1 - jZ = 1 - j\frac{\nu}{\omega}$ ν = collision frequency

N = electron density

B_o = DC magnetic flux density

ω = angular frequency of signal source

e = magnitude of electron charge

m = electron mass

ϵ_o = permittivity of free space = $(36\pi \times 10^9)^{-1}$ fd./m.

μ_o = permeability of free space = $4\pi \times 10^{-7}$ hy./m.

$k_o = \omega\sqrt{\mu_o \epsilon_o} = \frac{\omega}{c} = \frac{2\pi}{\lambda_o}$ = free space propagation constant

c = velocity of light in a vacuum

λ_o = free space wavelength

M.K.S. units (rationalized) are used throughout.

The impedance analysis of an antenna requires knowledge of its near field. If all the dimensions of the antenna are small compared to a wavelength, the use of an approximate near field theory is indicated in order to simplify the otherwise complicated calculations. Such an approximate theory can be obtained by first formulating general near field expressions and then letting the antenna dimensions become very small in terms of wavelengths. An equivalent process involves letting the frequency become arbitrarily small while maintaining the antenna size and the properties of the medium constant (i.e., the dispersive nature of the medium is not considered). This low frequency limit is employed in the following paragraphs to derive quasi-static expressions for the electric field, the magnetic field and Poynting's theorem.

The first step is to obtain a general field formulation valid for electromagnetic problems in a magnetoplasma. It is desired to derive $\overline{E}$ and $\overline{H}$ from a pair of potentials chosen in such a manner as to display the quasi-static electric field as a distinct part of the total electric field. The total electric field can be expressed in terms of a scalar potential ψ and a vector potential $\overline{A}$.

$$\overline{E} = - \nabla \psi - j \omega \overline{A} \qquad (2.1.4)$$

Substitution of Equation (2.1.4) in Equation (2.1.2) gives

$$\mu_o \overline{H} = \nabla \times \overline{A} \qquad (2.1.5)$$

The above two relations, together with Equation (2.1.1) give

$$\nabla \times \nabla \times \overline{A} - k_o^2 K \overline{A} = -j \omega \mu_o \epsilon_o K \nabla \psi + \mu_o \overline{J} \qquad (2.1.6)$$

Operation on Equation (2.1.6) with the divergence operator gives

$$\nabla \cdot K \nabla \psi + j \omega \nabla \cdot K \bar{A} = \frac{\nabla \cdot \bar{J}}{j\omega\epsilon_o} \tag{2.1.7}$$

This equation can be simplified by introducing the following restriction on $\bar{A}$:

$$\nabla \cdot K \bar{A} = 0 \tag{2.1.8}$$

This is a modification of the Coulomb gauge condition and is discussed in the Appendix. Equation (2.1.7) becomes

$$\nabla \cdot K \nabla \psi = \frac{\nabla \cdot \bar{J}}{j\omega\epsilon_o} \tag{2.1.9}$$

This differential equation can be used to obtain the potential ψ due to a current density $\bar{J}$. If q is the charge density, the equation of continuity ($\nabla \cdot \bar{J} + j \omega q = 0$) puts Equation (2.1.9) into the form

$$\nabla \cdot K \nabla \psi = - \frac{q}{\epsilon_o} \tag{2.1.10}$$

which may be regarded as a modified Poisson's equation.* A complete solution for all the fields would involve solving Equation (2.1.9) or Equation (2.1.10) for ψ, substituting ψ in Equation (2.1.6) and solving for $\bar{A}$. Expressions for $\bar{E}$ and $\bar{H}$ could then be derived using Equations (2.1.4) and (2.1.5).

---

* Equation (2.1.10) is widely used and is the quasi-static differential equation for the scalar potential ψ.

Solution of the above equations can be facilitated by the use of spatial Fourier transforms. A transform will be indicated with a wavy line (~) and the transform variables will be represented by the vector $\bar{k}$. Transformation of Equation (2.1.6) gives

$$M \tilde{\bar{A}} = \omega \mu_o \epsilon_o K \bar{k} \tilde{\psi} + \mu_o \tilde{\bar{J}} \tag{2.1.11}$$

where

$$-M = \bar{k} \times \bar{k} \times + k_o^2 K.$$

Transformation of Equation (2.1.9) gives

$$\tilde{\psi} = -\frac{1}{\omega \epsilon_o} \frac{\bar{k} \cdot \tilde{\bar{J}}}{\bar{k} \cdot K \bar{k}} \tag{2.1.12}$$

Substitution of Equation (2.1.12) in Equation (2.1.11) gives

$$\tilde{\bar{A}} = \mu_o M^{-1} \left(- \frac{K \bar{k} \bar{k} \cdot \tilde{\bar{J}}}{\bar{k} \cdot K \bar{k}} + \tilde{\bar{J}} \right) \tag{2.1.13}$$

The electric field $\tilde{E}$ can be expressed in terms of the potentials and consequently in terms of the current density $\tilde{\tilde{J}}$ by transforming Equation (2.1.4):

$$\tilde{\tilde{E}} = -j\left(\bar{k}\,\tilde{\psi} + \omega\,\tilde{\tilde{A}}\right) \tag{2.1.14}$$

Similarly, transformation of Equation (2.1.5) gives an expression for the magnetic field:

$$\tilde{\tilde{H}} = \frac{j}{\mu_o}\,\bar{k} \times \tilde{\tilde{A}} \tag{2.1.15}$$

Thus the electric and magnetic fields can be expressed in terms of a scalar potential and a vector potential which can be derived from the source current in a straightforward manner. The gauge condition on the potentials is chosen so that the scalar potential ψ satisfies the relatively simple quasi-static differential equation.

An examination of the equations in the preceding paragraph suggests that some simplification may result if $\tilde{\tilde{E}}$ and $\tilde{\tilde{J}}$ are each separated into two parts as follows:

$$\begin{aligned} \tilde{E} &= \tilde{\tilde{E}}_o + \tilde{\tilde{E}}_1 \\ \tilde{\tilde{J}} &= \tilde{\tilde{J}}_o + \tilde{\tilde{J}}_1 \end{aligned} \tag{2.1.16}$$

in which

$$\tilde{\tilde{\bar{E}}}_o = -\, j\, \bar{k}\, \tilde{\psi}$$

$$\tilde{\tilde{\bar{E}}}_1 = -\, j\, \omega\, \tilde{\tilde{\bar{A}}}$$

$$\tilde{\tilde{\bar{J}}}_o = \frac{K\, \bar{k}\, \bar{k} \cdot \tilde{\tilde{\bar{J}}}}{\bar{k} \cdot K\, \bar{k}}$$

$$\tilde{\tilde{\bar{J}}}_1 = \tilde{\tilde{\bar{J}}} - \frac{K\, \bar{k}\, \bar{k} \cdot \tilde{\tilde{\bar{J}}}}{\bar{k} \cdot K\, \bar{k}} \qquad (2.1.17)$$

The following relations may be deduced readily:

$$\bar{k} \times K^{-1}\, \tilde{\tilde{\bar{J}}}_o = 0 \qquad (2.1.18)$$

$$\bar{k} \cdot \tilde{\tilde{\bar{J}}}_1 = 0 \qquad (2.1.19)$$

$\tilde{\tilde{\bar{J}}}_1$ is clearly a transverse vector. However it is not the entire transverse part of the current density since the other part $\tilde{\tilde{\bar{J}}}_o$ is not longitudinal; rather, $K^{-1}\, \tilde{\tilde{\bar{J}}}_o$ is longitudinal. Equation (2.1.13) for the vector potential becomes

$$\tilde{\tilde{\bar{A}}} = \mu_o\, M^{-1}\, \tilde{\tilde{\bar{J}}}_1 \qquad (2.1.20)$$

Equations (2.1.20), (2.1.14) and (2.1.12) permit the two parts of $\tilde{\bar{E}}$ to be expressed as

$$\tilde{\bar{E}}_o = \frac{j}{\omega\epsilon_o} K^{-1} \tilde{\bar{J}}_o \qquad (2.1.21)$$

$$\tilde{\bar{E}}_1 = - j \omega \mu_o M^{-1} \tilde{\bar{J}}_1 \qquad (2.1.22)$$

Equation (2.1.18) shows that $\tilde{\bar{E}}_o$ is a longitudinal vector. However it is not the entire longitudinal part of $\tilde{\bar{E}}$ since in general $\bar{k} \cdot \tilde{\bar{E}}_1 \neq 0$. Rather $K \tilde{\bar{E}}_1$ is transverse, a fact which may be deduced from the gauge condition. An expression for the magnetic field follows from Equations (2.1.20) and (2.1.15). It is

$$\tilde{\bar{H}} = j \bar{k} \times M^{-1} \tilde{\bar{J}}_1 \qquad (2.1.23)$$

Another expression for $\tilde{\bar{H}}$ may be derived by noting that

$$-M \bar{k} = \bar{k} \times \bar{k} \times \bar{k} + k_o^2 K \bar{k}$$

from which

$$-\bar{k} = k_o^2 M^{-1} K \bar{k} \qquad (2.1.24)$$

Substitution of Equation (2.1.24) in Equation (2.1.13) gives

$$\overset{\approx}{\bar{A}} = \frac{1}{\omega^2 \epsilon_o} \frac{\bar{k}\,\bar{k} \cdot \overset{\approx}{\bar{J}}}{\bar{k} \cdot K\,\bar{k}} + \mu_o M^{-1} \overset{\approx}{\bar{J}} \qquad (2.1.25)$$

from which

$$\overset{\approx}{\bar{H}} = j\,\bar{k} \times M^{-1} \overset{\approx}{\bar{J}} \qquad (2.1.26)$$

A comparison of Equation (2.1.26) with Equation (2.1.23) leads to the conclusion that

$$\bar{k} \times M^{-1} \overset{\approx}{\bar{J}}_o = 0 \qquad (2.1.27)$$

The decomposition of the current density into two parts (a procedure suggested by Professor G. A. Deschamps) evidently simplifies the equations considerably. Furthermore it is clear that $\bar{E}_o$ is derived entirely from $\bar{J}_o$ and that both $\bar{E}_1$ and $\bar{H}$ are derived entirely from $\bar{J}_1$. Similarly ψ and $\bar{A}$ are derived from $\bar{J}_o$ and $\bar{J}_1$ respectively. Thus the entire field problem has been divided into two distinct halves, one with the source $\bar{J}_o$ and the other with the source $\bar{J}_1$. Although $\bar{J}$ may be confined to a finite region in space, $\bar{J}_o$ and $\bar{J}_1$ both exist outside that region.

The theory developed above does not use any approximations and is valid as long as the constant permittivity tensor K is a valid representation for the properties of the medium. However, the near field analysis of a short antenna can be simplified greatly by the use of a low frequency approximation to the general theory. Since k_o is a parameter proportional to frequency, the low frequency approximation can be effected by letting k_o approach zero. As discussed before, the low frequency approximation is not applied to the elements of the permittivity tensor K; that is, the elements of K are to be considered fixed as k_o approaches zero. It will be shown that the first term of the approximation gives an electric field equal to $\bar{E}_o$ (the quasi-static electric field). Furthermore it will be shown that the low frequency approximation gives a magnetic field consisting of two parts. One part is the familiar magnetic field obtainable from the DC form of Ampere's law and the other part is an induced magnetic field which is non-zero only in an anisotropic medium.

The low frequency approximation (the limit as k_o^2 approaches zero) can now be applied to the vector potential $\tilde{\bar{A}}$. Equation (2.1.25) shows that $\tilde{\bar{A}}$ can be expressed as follows:

$$\tilde{\bar{A}} = \frac{\bar{k}\,\bar{k}\cdot\tilde{\bar{J}}}{\omega^2\,\epsilon_o\,\bar{k}\cdot K\,\bar{k}} + \mu_o\,M^{-1}\,\tilde{\bar{J}}$$

$$= \frac{\mu_o}{k_o^2}\left(\frac{\bar{k}\,\bar{k}\quad\tilde{\bar{J}}}{\bar{k}\cdot K\,\bar{k}} + k_o^2\,M^{-1}\,\tilde{\bar{J}}\right) \qquad (2.1.28)$$

If the rectangular components of $\bar{k}$ are k_1, k_2, k_3, then the matrix M is

$$M = \begin{bmatrix} k_2^2 + k_3 - k_o^2 K' & -k_1 k_2 - jk_o^2 K'' & -k_1 k_3 \\ -k_1 k_2 + jk_o^2 K'' & k_1^2 + k_3^2 - k_o^2 K' & -k_2 k_3 \\ -k_1 k_3 & -k_2 k_3 & k_1^2 + k_2^2 - k_o^2 K_o \end{bmatrix} \qquad (2.1.29)$$

The inverse of M can be expressed as $M^{-1} = \frac{N}{D}$

$$= \frac{N_o + k_o^2 N_1 + k_o^4 N_2}{k_o^2 (a + k_o^2 b + k_o^4 c)} \qquad (2.1.30)$$

in which D is the determinant of M. In order to consider the low frequency limit, it is necessary to know the scalars a, b, c and the matrices N_o, N_1, N_2. They are

$$a = -(k_1^2 + k_2^2 + k_3^2) \left[K' (k_1^2 + k_2^2) + K_o k_3^2 \right]$$

$$= -\overline{k}^2\, \overline{k} \cdot K\, \overline{k} \qquad (2.1.31)$$

$$b = (K'^2 - K''^2)(k_1^2 + k_2^2) + K' K_o (k_1^2 + k_2^2 + 2 k_3^2) \qquad (2.1.32)$$

$$c = K_o (K''^2 - K'^2)$$

$$= - \det K$$

$$N_o = (k_1^2 + k_2^2 + k_3^2) \begin{bmatrix} k_1^2 & k_1 k_2 & k_1 k_3 \\ k_1 k_2 & k_2^2 & k_2 k_3 \\ k_1 k_3 & k_2 k_3 & k_3^2 \end{bmatrix}$$

$$= \overline{k^2}\ \overline{k}\ \overline{k}. \qquad (2.1.33)$$

$$N_1 = - \begin{bmatrix} K'(k_1^2 + k_2^2) + K_o(k_1^2 + k_3^2) & K_o k_1 k_2 - jK''(k_1^2 + k_2^2) & K' k_1 k_3 - jK'' k_2 k_3 \\ K_o k_1 k_2 + jK''(k_1^2 + k_2^2) & K'(k_1^2 + k_2^2) + K_o(k_2^2 + k_3^2) & K' k_2 k_3 + jK'' k_1 k_3 \\ K' k_1 k_3 + jK'' k_2 k_3 & K' k_2 k_3 - jK'' k_1 k_3 & K'(k_1^2 + k_2^2 + 2k_3^2) \end{bmatrix} \qquad (2.1.34)$$

$$N_2 = K_o \begin{bmatrix} K' & -jK'' & 0 \\ jK'' & K' & 0 \\ 0 & 0 & \dfrac{K'^2 - K''^2}{K_o} \end{bmatrix} \qquad (2.1.35)$$

The vector potential expression, Equation (2.1.28), now can be written as

$$\tilde{\tilde{A}} = \frac{\mu_o}{k_o^2} \left[- \frac{N_o}{a} + k_o^2 \; M^{-1} \right] \tilde{\tilde{J}} \qquad (2.1.36)$$

$$= \mu_o \left[\frac{-(b+k_o^2 c) \dfrac{N_o}{a} + N_1 + k_o^2 N_2}{a + k_o^2 b + k_o^4 c} \right] \tilde{\tilde{J}} \qquad (2.1.37)$$

In the limit as k_o approaches zero, Equation (2.1.37) becomes

$$\tilde{\tilde{A}}_o = \frac{\mu_o}{a} \left(N_1 - \frac{b N_o}{a} \right) \tilde{\tilde{J}} \qquad (2.1.38)$$

It should be noted that the above expression for $\tilde{\tilde{A}}_o$ is independent of the parameter k_o.

Low frequency expressions for $\tilde{\tilde{E}}$ and $\tilde{\tilde{H}}$ now can be derived using Equation (2.1.38).

$$\tilde{\tilde{E}} = \tilde{\tilde{E}}_o + \tilde{\tilde{E}}_1$$

$$= -j\,(\bar{k}\,\tilde{\psi} + \omega\,\tilde{\bar{A}}_o)$$

$$= \frac{-j}{\omega\epsilon_o}\left[\frac{N_o}{a} + \frac{k_o^2}{a}\left(N_1 - \frac{bN_o}{a}\right)\right]\tilde{\tilde{J}} \qquad (2.1.39)$$

If k_o^2 is sufficiently small, the second term can be neglected (see Section 3.1). Under such conditions

$$\tilde{\tilde{E}} = \frac{-j\,N_o\,\tilde{\tilde{J}}}{\omega\epsilon_o a}$$

$$= \tilde{\tilde{E}}_o \qquad (2.1.40)$$

Equation (2.1.40) asserts that the predominant low frequency electric field can be derived entirely from the scalar potential ψ. Thus $\tilde{\tilde{E}}_o$ is the well-known quasi-static electric field. The preceding derivation not only displays the quasi-static electric field as a low frequency limit but also provides a first order correction term (the second term in Equation (2.1.39)).

It will now be shown that the two terms of Equation (2.1.39) are identical to the two near field terms which can be derived by the method of Mittra and Deschamps[1]. In their work, Mittra and Deschamps derive an expression for one electric field component by going through two long divisions; the following electric field derivation makes use of this approach. In the notation of this report, the transformed electric field may be expressed as

$$\tilde{\bar{E}} = - j \omega \mu_o M^{-1} \tilde{\bar{J}} \tag{2.1.41}$$

$$= \frac{-j}{\omega \epsilon_o} k_o^2 M^{-1} \tilde{\bar{J}}$$

$$= \frac{-j}{\omega \epsilon_o} \left[\frac{N_o + k_o^2 N_1 + k_o^4 N_2}{a + k_o^2 b + k_o^4 c} \right] \tilde{\bar{J}} \tag{2.1.42}$$

The first long division gives

$$\tilde{\bar{E}} = \frac{-j}{\omega \epsilon_o} \left[\frac{N_o}{a} + k_o^2 \left\{ \frac{\left(N_1 - \frac{bN_o}{a} \right) + k_o^2 \left(N_2 - \frac{cN_o}{a} \right)}{a + k_o^2 b + k_o^4 c} \right\} \right] \tilde{\bar{J}} \tag{2.1.43}$$

The second long division gives

$$\tilde{\bar{E}} = \frac{-j}{\omega\epsilon_o}\left[\frac{N_o}{a} + \frac{k_o^2}{a}\left(N_1 - \frac{bN_o}{a}\right) + k_o^4\left\{\frac{N_2 - bN_1 + (b^2 - c)\frac{N_o}{a} + k_o^2\, c\left(\frac{bN_o}{a} - N_1\right)}{a + k_o^2\, b + k_o^4\, c}\right\}\right]\tilde{\bar{J}} \tag{2.1.44}$$

The first two terms of Equation (2.1.44) are interpreted by Mittra and Deschamps as near field terms because they are singular at the origin. Note that Equation (2.1.39) is identical to the first two terms of Equation (2.1.44).

The transformed magnetic field was given by Equation (2.1.23); it is

$$\tilde{\bar{H}} = j\,\bar{k} \times M^{-1}\,\tilde{\bar{J}}_1 \tag{2.1.45}$$

Equation (2.1.30) shows that this can be expressed as

$$\tilde{\bar{H}} = j\,\bar{k} \times \left[\frac{N_o + k_o^2\, N_1 + k_o^4\, N_2}{k_o^2\,(a + k_o^2\, b + k_o^4 c)}\right]\tilde{\bar{J}}_1 \tag{2.1.46}$$

However,

$$\begin{aligned}\bar{k} \times N_o\,\tilde{\bar{J}} &= \bar{k} \times (\bar{k}^{-2}\,\bar{k}\,\bar{k}\cdot\tilde{\bar{J}}_1) \\ &= 0\end{aligned} \tag{2.1.47}$$

Thus a general expression for the transformed magnetic field is

$$\tilde{\bar{H}} = j\ \bar{k} \times \left[\frac{N_1 + k_o^2 N_2}{a + k_o^2 b + k_o^4 c} \right] \tilde{\bar{J}}_1 \qquad (2.1.48)$$

A comparison of Equation (2.1.23) with Equation (2.1.26) shows that Equation (2.1.48) can be written as

$$\overset{\approx}{\bar{H}} = j\ \bar{k} \times \left[\frac{N_1 + k_o^2 N_2}{a + k_o^2 b + k_o^4 c} \right] \overset{\approx}{\bar{J}} \qquad (2.1.49)$$

In the limit as $k_o^2 \longrightarrow 0$, Equation (2.1.48) becomes

$$\overset{\approx}{\bar{H}}_o = j\ \frac{\bar{k} \times N_1\ \overset{\approx}{\bar{J}}_1}{a} \qquad (2.1.50)$$

and similarly, Equation (2.1.49) becomes

$$\tilde{\bar{H}}_o = j\ \frac{\bar{k} \times N_1\ \overset{\approx}{\bar{J}}}{a} \qquad (2.1.51)$$

Further insight into the meaning of Equations (2.1.50) and (2.1.51) can be obtained by employing a different derivation. One of Maxwell's equations is

$$\nabla \times \bar{H} = j \omega \epsilon_o K \bar{E} + \bar{J} \qquad (2.1.52)$$

Taking the curl of Equation (2.1.52) and setting $\nabla \cdot \bar{H} = 0$ gives

$$\nabla^2 \bar{H} = - j \omega \epsilon_o \nabla \times K \bar{E} - \nabla \times \bar{J} \qquad (2.1.53)$$

In the low frequency or quasi-static limit, $\bar{E} = - \nabla \psi$. Substitution of this in Equation (2.1.53) gives

$$\nabla^2 \bar{H}_o' = j \omega \epsilon_o \nabla \times K \nabla \psi - \nabla \times \bar{J} \qquad (2.1.54)$$

If K is a scalar the first term on the right hand side is identically zero and $\bar{H}_o'$ and $\bar{J}$ are related only by the point form of Ampère's law for direct currents. If K is a tensor, the term containing K is not zero in general and thus contributes to $\bar{H}_o'$. Evidently in an anisotropic medium an irrotational electric field can contribute to the magnetic field. A convenient expression for the magnetic field can be obtained by taking the Fourier transform of Equation (2.1.54). This gives

$$\tilde{\bar{H}}'_o = \frac{j}{\bar{k}^2}\left(\omega\,\epsilon_o\,\bar{k}\times K\,\bar{k}\,\tilde{\psi} + \bar{k}\times\tilde{\bar{J}}\right)$$

$$= \frac{j}{\bar{k}^2}\left(-\frac{\bar{k}\times K\,\bar{k}\;\bar{k}\cdot\tilde{\bar{J}}}{\bar{k}\cdot K\,\bar{k}} + \bar{k}\times\tilde{\bar{J}}\right) \tag{2.1.55}$$

$$\tilde{\bar{H}}'_o = \frac{j}{\bar{k}^2}\,\bar{k}\times\tilde{\bar{J}}_1 \tag{2.1.56}$$

Equation (2.1.55) can be written in rectangular components as follows:

$$\tilde{\bar{H}}'_o = \frac{j}{k_1^2+k_2^2+k_3^2}\left\{-\frac{k_1\tilde{J}_x+k_2\tilde{J}_y+k_3\tilde{J}_z}{K'(k_1^2+k_2^2)+K_o k_3^2}\begin{bmatrix}(K'-K_o)k_2k_3-jK''k_1k_3\\ -(K'-K_o)k_1k_3-jK''k_2k_3\\ jK''(k_1^2+k_2^2)\end{bmatrix}+\begin{bmatrix}k_2\tilde{J}_z-k_3\tilde{J}_y\\ k_3\tilde{J}_x-k_1\tilde{J}_z\\ k_1\tilde{J}_y-k_2\tilde{J}_x\end{bmatrix}\right\} \tag{2.1.57}$$

It can be shown that this low frequency expression for $\tilde{\bar{H}}'_o$ is identical to Equation (2.1.51) (i.e. $\bar{H}'_o = \bar{H}_o$). The advantage of this derivation is that it displays the low frequency magnetic field as the sum of two terms (see Equation (2.1.55)), the first term being identically zero in isotropic media and the second simply a statement of Ampère's law for direct currents. The meaning of the first term can be clarified be relating it to the induced current which flows in the medium due to the quasi-static electric field. Equation (2.1.21) shows that

$$\tilde{\bar{J}}_o = - j \omega \epsilon_o K \tilde{\bar{E}}_o$$

$$= - j \omega \epsilon_o \left(1 + \frac{\sigma}{j\omega\epsilon_o}\right) \tilde{\bar{E}}_o$$

$$= -j \omega \epsilon_o \tilde{\bar{E}}_o - \sigma \tilde{\bar{E}}_o \qquad (2.1.58)$$

in which σ is the conductivity tensor. If the electric field $\bar{E}_o$ induces a current density $\bar{J}_1$ in the medium, $\bar{J}_1$ is given by

$$\tilde{\bar{J}}_1 = \sigma \tilde{\bar{E}}_o$$

$$= - \tilde{\bar{J}}_o - j \omega \epsilon_o \tilde{\bar{E}}_o$$

$$= - \frac{K \bar{k} \bar{k} \cdot \tilde{\bar{J}}}{\bar{k} \cdot K \bar{k}} - j \omega \epsilon_o \tilde{\bar{E}}_o \qquad (2.1.59)$$

The induced current is seen to consist of two parts; the first part is irrotational only when K is a scalar and the second is always irrotational. The magnetic field resulting from the quasi-static induced current is given by

$$\tilde{\bar{H}}_i = \frac{j}{\bar{k}^2} \bar{k} \times \tilde{\bar{J}}_i$$

$$= \frac{-j}{\bar{k}^2} \frac{\bar{k} \times K \bar{k} \bar{k} \cdot \tilde{\bar{J}}}{\bar{k} \cdot K \bar{k}} \qquad (2.1.60)$$

This expression is exactly the first term of Equation (2.1.55) which now may be written

$$\tilde{\bar{H}} = \tilde{\bar{H}}_i + \frac{j}{\bar{k}^2} \bar{k} \times \tilde{\bar{J}} \qquad (2.1.61)$$

The existence of an induced magnetic field $\overline{H}_1$ in the low frequency limit suggests that unusual electromagnetic effects may be predicted by quasi-static theory when it is applied to problems in anisotropic media. Propagation effects in magnetoplasmas and ferrites have been described in the literature in connection with source-free problems;[9,10] a problem which includes sources is the subject of this report and it will be shown in Sections 2.3 and 2.4 that the quasi-static theory predicts a form of radiation

The low frequency behaviour of the field quantities may be summarized by noting their proportionality with respect to frequency when expressed in terms of an operation on an assumed current density $\overline{J}$:

$$\begin{array}{ll} \psi \propto \frac{1}{\omega}, & E \propto \frac{1}{\omega}, \\ A = \text{const.}, & H = \text{const} \end{array} \qquad (2.1\ 62)$$

The infinities in ψ and E at $\omega = 0$ arise from the fact that $\overline{J}$ is assumed to remain constant as $\omega \rightarrow 0$ It would be more realistic to base field calculations at $\omega = 0$ on some assumed charge distribution. Since an oscillating charge distribution ρ is related to a current distribution by the equation of continuity

$$\nabla \cdot \overline{J} + j \omega \rho = 0 \qquad (2.1\ 63)$$

it is clear that an assumed charge distribution would produce a finite ψ and E at $\omega = 0$.

The existence of quasi-static field expressions suggests that the Poynting theorem might also be expressed in a quasi-static form. The Poynting theorem is often written as follows:

$$\int_V \bar{E} \cdot \bar{J}^* \, dv = j\omega \int_V \left(\bar{E} \cdot \bar{D}^* - \bar{B} \cdot \bar{H}^* \right) dv - \int_S \left(\bar{E} \times \bar{H}^* \right) \cdot \hat{n} \, ds \qquad (2.1.64)$$

In the quasi-static limit the relations of Equation (2.1.62) indicate that the $\bar{B} \cdot \bar{H}^*$ term is negligible. A more useful limiting form of the Poynting theorem may be derived by substituting

$$\bar{E} = - \nabla \psi - j \omega \bar{A} \qquad (2.1.65)$$

in the surface integral. This gives

$$\int_V \bar{E} \cdot \bar{J}^* \, dv = j\omega \int_V \left(\bar{E} \cdot \bar{D}^* - \bar{B} \cdot \bar{H}^* \right) dv + \int_S \left(\nabla \psi \cdot \bar{H}^* \right) \cdot \hat{n} \, ds + j\omega \int_S \left(\bar{A} \times \bar{H}^* \right) \cdot \hat{n} \, ds \qquad (2.1.66)$$

The first surface integral can be simplified using the vector indentity

$$\nabla \psi \times \overline{H}^* = \nabla \times \psi \, \overline{H}^* - \psi \, \nabla \times \overline{H}^* \qquad (2.1.67)$$

and the conjugate of one of Maxwell's equations,

$$\nabla \times \overline{H}^* = - j \, \omega \, \overline{D}^* + \overline{J}^* \qquad (2.1.68)$$

If it is assumed that $\overline{J} = 0$ on the surface S, Poynting's theorem becomes

$$\int_V \overline{E} \cdot \overline{J}^* dv = j\omega \int_V \left(\overline{E} \cdot \overline{D}^* - \overline{B} \cdot \overline{H}^* \right) dv + j\omega \int_S \left(\psi \, \overline{D}^* + \overline{A} \times \overline{H}^* \right) \cdot \hat{n} \, ds \qquad (2.1.69)$$

In the quasi-static limit the relations of Equation (2.1.62) indicate that the $\overline{B} \cdot \overline{H}^*$ and $\overline{A} \times \overline{H}^*$ terms are negligible Thus a quasi-static form for Poynting's theorem is

$$\int_V \overline{E} \cdot \overline{J}^* dv = j\omega \int_V \overline{E} \cdot \overline{D}^* dv + j\omega \int_S \psi \, \overline{D}^* \cdot \hat{n} \, ds \qquad (2.1.70)$$

This formula is similar to the well known energy expression to be found in textbooks on electrostatics. A similar formula for the magnetostatic limit may be derived if $\overline{H}$ is expressed in terms of a magnetic scalar potential. The surface integral of the magnetostatic formula gives a result identical to that obtained by Trivelpiece and Gould[9] in their equation numbered (A.10).

The quasi-static field equations and Poynting theorem discussed above constitute a body of theory sufficient for a study of the near fields of a short antenna in a magnetoplasma. Before proceeding to the antenna problem, it is worthwhile to examine the form of the quasi-static differential equation. Equation (2.1.9) may be expressed as

$$\psi_{xx} + \psi_{yy} + \frac{1}{a^2} \psi_{zz} = \frac{\nabla \cdot \overline{J}}{j \omega \epsilon_o K'} \tag{2.1.71}$$

where
$$a = \sqrt{\frac{K'}{K_o}}$$

Let us consider the lossless case in which both K' and K_o are real. Some information about the potential ψ may be obtained from a study of the characteristic surfaces of the above differential equation (see Sneddon[14], for instance). The nature of the characteristic surfaces depends on whether a^2 is positive or negative; the equation is elliptic when a^2 is positive and hyperbolic when a^2 is negative (see Figure 2.1.1).

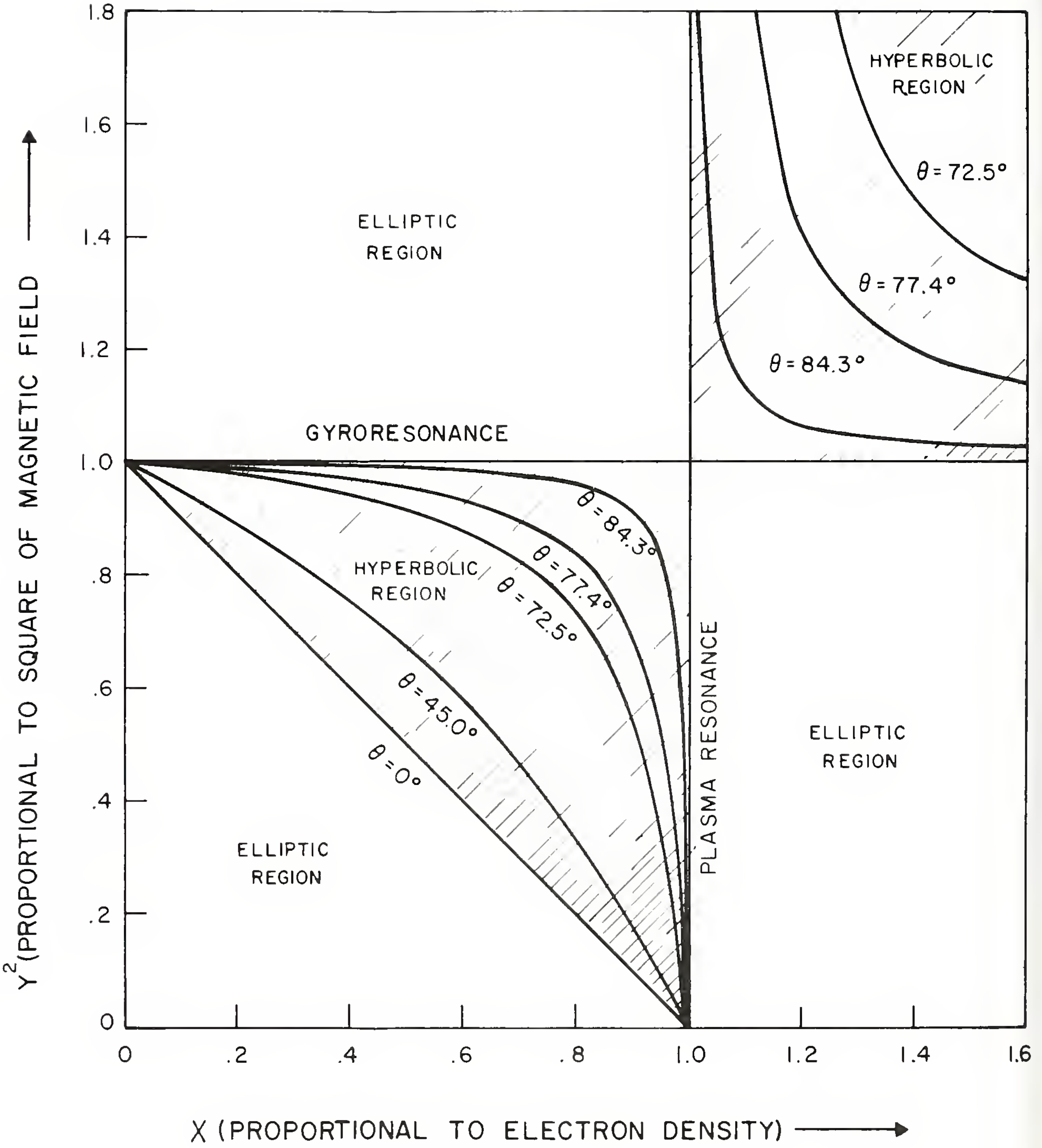

Figure 2.1.1 The elliptic and hyperbolic regions. Note: θ is the angle (with respect to the Z axis) of the characteristic cone when the differential equation is hyperbolic

An elliptic equation has complex characteristic surfaces and thus no physical significance can be attached to them. A hyperbolic equation has real characteristic surfaces along which discontinuities "propagate" (i.e. cannot vanish). Thus under hyperbolic conditions any discontinuity in $\nabla \cdot \bar{J}$ will cause a discontinuity in the electric field $(-\nabla \psi)$ extending outward from the region where the source current $\bar{J}$ is localized.

The equation of the family of characteristic surfaces may be derived easily by writing the quasi-static differential equation in cylindrical co-ordinates for the axially symmetric case. If r is the radial variable and z is the axial variable, Equation (2.1.71) becomes

$$\psi_{rr} + \frac{1}{r} \psi_{r} + \frac{1}{a^2} \psi_{zz} = \frac{\nabla \cdot \bar{J}}{j \omega \epsilon_o K'} \qquad (2.1.72)$$

The equation for the characteristic surface as given by Sneddon is

$$\dot{z}^2 + \frac{1}{a^2} \dot{r}^2 = 0 \qquad (2.1.73)$$

in which the dot represents differentiation with respect to some parameter. The solution is

$$z = \pm j \frac{1}{a} r + \text{const.} \tag{2.1.74}$$

which represents a family of cones when a^2 is negative. Therefore any source discontinuity at a point will result in a conical field discontinuity emanating from that point. Under hyperbolic conditions the field of a short dipole should contain three discontinuity cones, two emanating from its ends and one from its center. These cones are evident in the field formula to be derived in Section 2.2. Thus the most prominent feature of the field solution has been obtained without a detailed solution.

2.2 The Field of a Short Dipole

As shown in Section 2.1, the quasi-static differential equation is

$$K'(\psi_{xx} + \psi_{yy}) + K_o \psi_{zz} = - \frac{q}{\epsilon_o} \tag{2.2.1}$$

This may be written as

$$\psi_{xx} + \psi_{yy} = \frac{1}{a^2} \psi_{zz} = - \frac{q}{\epsilon_o K'} \tag{2.2.2}$$

where $$a = \sqrt{\frac{K'}{K_o}}$$

The solution will be obtained using the Fourier transform pair

$$\tilde{f}(\bar{k}) = \iiint_{-\infty}^{\infty} f(\bar{r}) e^{-j\bar{k}\cdot\bar{r}} \, dx \, dy \, dz$$

$$f(\bar{r}) = \frac{1}{(2\pi)^3} \iiint_{-\infty}^{\infty} \tilde{f}(\bar{k}) e^{j\bar{k}\cdot r} \, dk_1 \, dk_2 \, dk_3 \qquad (2.2.3)$$

The transforms can be used to solve Equation (2.2.2) and the solution can be expressed as

$$\psi(\bar{r}) = \frac{1}{\epsilon_o K' (2\pi)^3} \iiint_{-\infty}^{\infty} \frac{\tilde{q}(\bar{k}) e^{j\bar{k}\cdot\bar{r}}}{k_1^2 + k_2^2 + \frac{k_3^2}{a^2}} \, dk_1 \, dk_2 \, dk_3 \qquad (2.2.4)$$

The transform of the charge distribution is

$$\tilde{q}\,(\bar{k}) = \iiint_{-\infty}^{\infty} q\,(\bar{r})\,e^{-j(k_1 x + k_2 y + k_3 z)}\,dx\,dy\,dz \qquad (2.2.5)$$

This can be written in the (u, y, v) coordinate system as shown in Figure 2.2.1. Both $\bar{r}$ and $\bar{k}$ can be transformed as follows:

$$\begin{aligned} x &= u \sin\theta - v \cos\theta \\ z &= u \cos\theta + v \sin\theta \end{aligned} \qquad (2.2.6)$$

$$\begin{aligned} k' &= k_1 \sin\theta + k_3 \cos\theta \\ k'' &= -k_1 \cos\theta + k_3 \sin\theta \end{aligned} \qquad (2.2.7)$$

Now $\tilde{q}$ can be expressed as

$$\tilde{q}\,(\bar{k}) = \iiint_{-\infty}^{\infty} q\,(u, y, v)\,e^{-j(k' u + k_2 y + k'' v)}\,du\,dy\,dv \qquad (2.2.8)$$

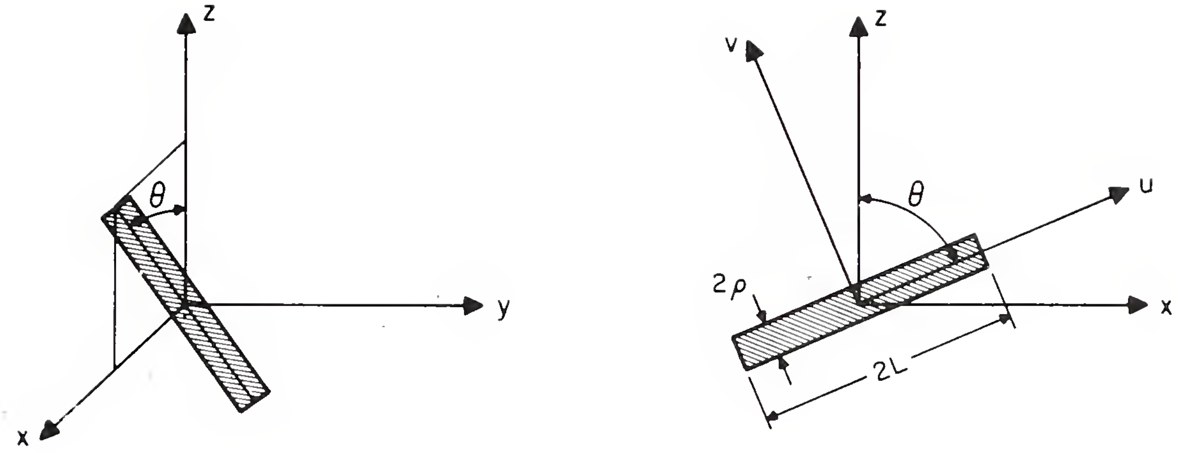
z
θ
y
x
v
z
θ
u
2ρ
x
2L

Figure 2.2.1 The co-ordinate system

The dipole field will be derived from the filamentary, triangular current distribution shown in Figure 2.2.2. The corresponding charge distribution is obtained from the equation of continuity.

$$q(\bar{r}) = -\frac{1}{j\omega}\frac{\partial J_u}{\partial u}\,\delta(y)\,\delta(v)$$

$$= \frac{1}{j\omega L}\,T(u)\,\delta(y)\,\delta(v) \qquad (2.2.9)$$

The function T(u) is shown in Figure 2.2.3. The transform of the charge distribution is

$$\tilde{q}(\bar{k}) = \frac{1}{\omega L k'}\left(e^{-jk'L} + e^{jk'L} - 2\right) \qquad (2.2.10)$$

This can be substituted into Equation (2.2.4) and integration will result in an expression for the potential ψ. However, for impedance calculation, the electric field parallel to the current (E_u) is required.

$$E_u(\bar{r}) = -\frac{\partial\psi}{\partial u}$$

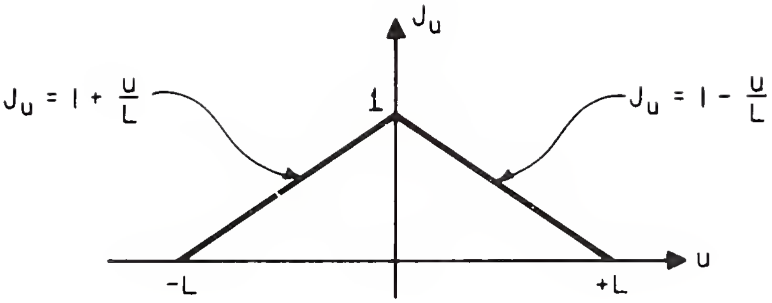
J_u
$J_u = 1 + \frac{u}{L}$
1
$J_u = 1 - \frac{u}{L}$
u
-L
+L

Figure 2.2.2 The assumed current distribution

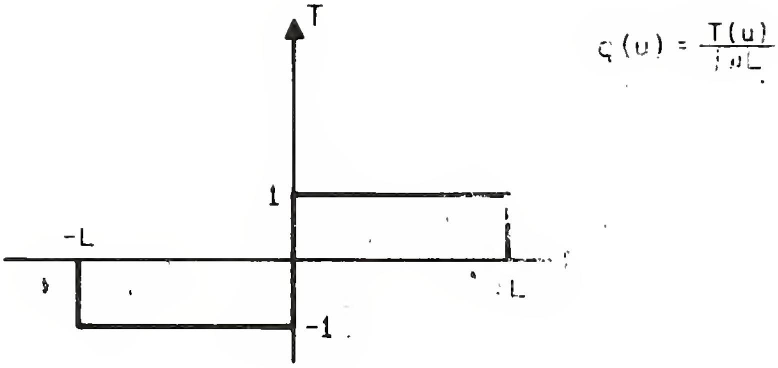
T
ς (u) = T(u) / jωL
1
-L
L
-1

Figure 2.2.3 The charge distribution

$$= \frac{1}{j\omega(2\pi)^3 \epsilon_o K' L} \iiint_{-\infty}^{\infty} \left(e^{-jk' L} + e^{jk' L} - 2\right) \frac{e^{j(k' u + k_2 y + k'' v)}}{k_1^2 + k_2^2 + \frac{k_3^2}{a^2}} \, dk_1 \, dk_2 \, dk_3$$

$$= \frac{1}{j\omega \epsilon_o K' L} \left[I_{(L)} + I_{(-L)} - 2I_{(o)} \right] \tag{2.2.11}$$

The integral $I_{(L)}$ can be expressed as

$$I_{(L)} = \frac{1}{(2\pi)^3} \iiint_{-\infty}^{\infty} \frac{e^{j\left[k_1 (x - L \sin\theta) + k_2 y + k_3 (z - L \cos\theta)\right]}}{k_1^2 + k_2^2 + \frac{k_3^2}{a^2}} \, dk_1 \, dk_2 \, dk_3 \tag{2.2.12}$$

Employing a transformation to cylindrical coordinates,

$$\begin{aligned} x - L \sin\theta &= \rho_1 \cos\phi_1 & k_1 &= \gamma \cos\eta \\ y &= \rho_1 \sin\phi_1 & k_2 &= \gamma \sin\eta \\ z - L \cos\theta &= z_1 & k_3 &= k_3 \quad , \end{aligned} \tag{2.2.13}$$

we can write

$$I_{(L)} = \frac{1}{(2\pi)^3} \int_{-\infty}^{\infty} \int_{0}^{\infty} \int_{0}^{2\pi} \frac{e^{j[\gamma \rho_1 \cos(\eta - \phi_1) + k_3 z_1]}}{\gamma^2 + \frac{k_3^2}{a^2}} \gamma \, d\eta \, d\gamma \, dk_3$$

$$= \frac{1}{(2\pi)^2} \int_{-\infty}^{\infty} \int_{0}^{\infty} \frac{e^{jk_3 z_1} J_o(\gamma \rho_1) \gamma}{\gamma^2 + \frac{k_3^2}{a^2}} \, d\gamma \, dk_3 \qquad (2.2.14)$$

since

$$J_o(\gamma \rho_1) = \frac{1}{2\pi} \int_{0}^{2\pi} e^{j\gamma \rho_1 \cos(\eta - \phi_1)} \, d\eta \, . \qquad (2.2.15)$$

The next step involves contour integration with respect to k_3. It is convenient to designate by "a" the square root of K'/K_o which has a positive real part, however small. Under lossless hyperbolic conditions (a^2 negative with $\nu=0$) the correct choice for "a" must be made by taking the limit as the collision frequency (ν) approaches zero.

The contour integration gives

$$\frac{1}{2\pi}\int_{-\infty}^{\infty}\frac{e^{jk_3 z_1}}{\gamma^2+\frac{k_3^2}{a^2}}\,dk_3 = \frac{a^2}{2\pi}\int_{-\infty}^{\infty}\frac{e^{jk_3 z_1}}{(k_3+ja\gamma)\,(k_3-ja\gamma)}\,dk_3$$

$$= \frac{a}{2}\,\frac{e^{-a\gamma|z_1|}}{\gamma} \qquad (2.2.16)$$

The integration contours are shown in Figure (2.2.4)

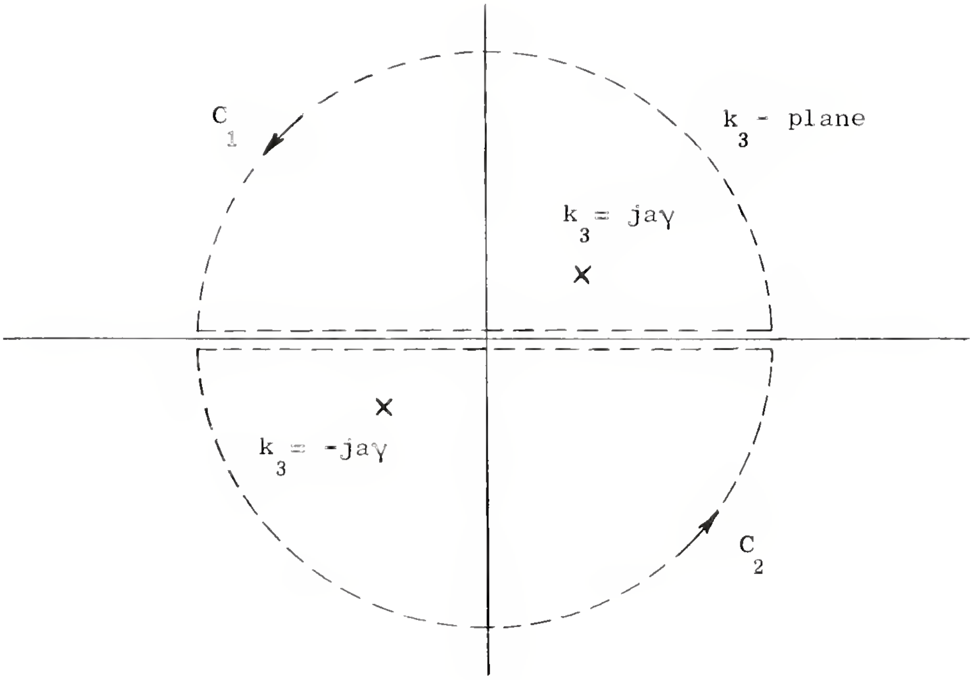
C_1
k_3 - plane
$k_3 = ja\gamma$
$k_3 = -ja\gamma$
C_2

Figure 2.2.4 Integration Contours

C_1 is used for z_1 positive and C_2 for z_1 negative.

Integration with respect to γ completes the evaluation of $I_{(L)}$.

$$I_{(L)} = \frac{a}{4\pi} \int_0^\infty e^{-a\gamma |z_1|} J_o(\gamma \rho_1)\, d\gamma$$

$$= \frac{a}{4\pi} (\rho_1^2 + a^2 z_1^2)^{-\frac{1}{2}} \qquad (2.2.17)$$

Similar expressions for $I_{(-L)}$ and $I_{(o)}$ may be derived. Using the nomenclature

$$\begin{aligned} \rho_1^2 &= (x-L\sin\theta)^2 + y^2 & z_1 &= z - L\cos\theta \\ \rho_2^2 &= (x+L\sin\theta)^2 + y^2 & z_2 &= z + L\cos\theta \\ \rho_o^2 &= x^2 + y^2 & z_o &= z \quad , \end{aligned} \qquad (2.2.18)$$

we may express the electric field parallel to the dipole as

$$E_u = \frac{a}{j\,\omega 4\pi\,\epsilon_o K' L}\left[\frac{1}{\sqrt{\rho_1^2 + a^2 z_1^2}} + \frac{1}{\sqrt{\rho_2^2 + a^2 z_2^2}} - \frac{2}{\sqrt{\rho_o^2 + a^2 z_o^2}}\right] \qquad (2.2.19)$$

Under lossless hyperbolic conditions (a^2 real and negative), E_u becomes infinite on the surfaces $\rho_1^2 + a^2 z_1^2 = 0$, $\rho_2^2 + a^2 z_2^2 = 0$, and

$\rho_o^2 + a^2 z_o^2 = 0$ These surfaces are cones emanating from the ends and center of the dipole. Their discovery was anticipated by the discussion of the differential equation characteristics in Section 2.1. In addition, inspection of Equation (2.2.19) shows that phase shifts across the conical surfaces occur under hyperbolic conditions.

2.3 The Impedance of a Short Dipole

For an input current of unit magnitude, the input impedance of an antenna with a conducting surface is given by

$$Z_{in} = - \int_S \overline{J} \;\; \overline{E} \; ds \qquad (2.3.1)$$

where S is the antenna surface. In this formula $\overline{J}$ is the current density on the antenna surface and $\overline{E}$ is the electric field at the antenna surface when the conducting material in the antenna is removed. This impedance formula may be derived using the "reaction concept" and such derivations have been discussed recently by Richmond[15] for isotropic media. These derivations are based on the Lorentz integral relation between any two solutions of Maxwell's equations (the solutions are numbered 1 and 2)

$$\int_A (\overline{E}_1 \times \overline{H}_2 - \overline{E}_2 \times \overline{H}_1) \;\; \overline{n} \; da = \int_V (\overline{J}_1 \;\; \overline{E}_2 - \overline{K}_1 \cdot \overline{H}_2 - \overline{J}_2 \cdot \overline{E}_1 + \overline{K}_2 \cdot \overline{H}_1) \; dv \qquad (2.3.2)$$

where $\overline{J}$ and $\overline{K}$ are electric and magnetic current respectively. This relation may be written for a magneto-ionic medium only if the sense of the magnetic field is reversed for one solution (say number 2). If the volume V is the entire space exterior to the antenna, the surface integral at infinity vanishes and there remains

$$\int_S (\overline{E}_1 \times \overline{H}_2 - \overline{E}_2 \times \overline{H}_1) \cdot \overline{n}\, ds = 0 \qquad (2.3.3)$$

where **S** is the antenna surface (see Figure 2.3.1). If $\overline{n} \times \overline{H}_1 = \overline{J}_1$ and $-\overline{n} \times \overline{E}_1 = \overline{K}_1$, then

$$\int_S \overline{K}_1 \cdot \overline{H}_2\, ds = \int_S \overline{J}_1 \quad \overline{E}_2\, ds \qquad (2.3.4)$$

If the gap is narrow,

$$\int_S \overline{K}_1 \cdot \overline{H}_2\, ds = - V_1 I_2 \qquad (2.3.5)$$

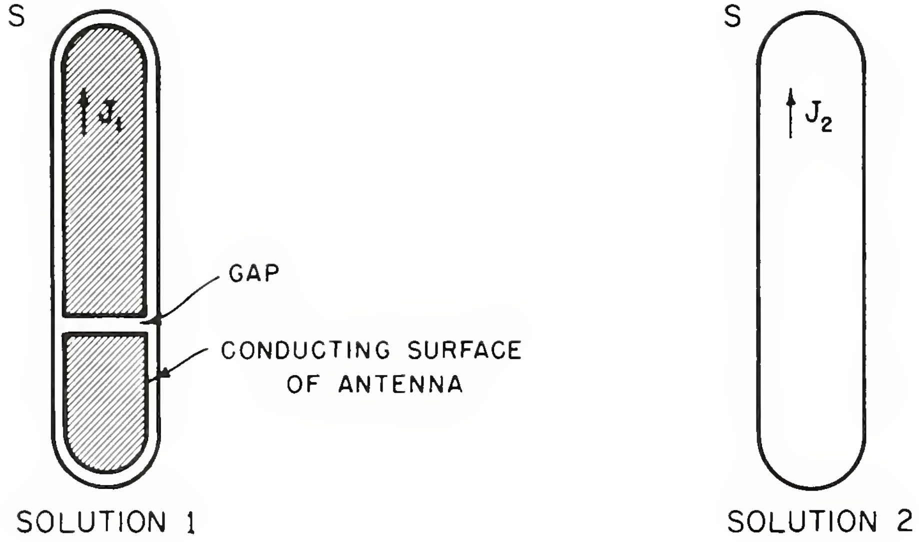
S
J_1
GAP
CONDUCTING SURFACE OF ANTENNA
SOLUTION 1
S
J_2
SOLUTION 2

Figure 2.3.1 Derivation of the impedance formula

where V and I represent source voltage and current. If $J_1 = J_2 = J$ and $I_1 = I_2 = I$ and the input impedance is defined by $Z_{in} = \frac{V_1}{I}$, then

$$Z_{in} = - \frac{1}{I^2} \int_S \bar{J} \cdot \bar{E}_2 \, ds \qquad (2.3.6)$$

which reduces to Equation (2.3.1) for unit source current. Since solution 2 requires reversal of the DC magentic field, $\bar{E}_2$ must be calculated under such conditions. $\bar{H}_2$ at the gap is completely determined by the source current and thus is unaffected by the DC magnetic field reversal. However in the quasi-static theory for an infinite medium all solutions for the electric field are independent of the sense of the DC magnetic field. Consequently in the impedance calculations to follow, Equation (2.3.1) may be used just as it would be in free space.

The impedance formula for unit input current (in the (u, y, v) coordinate system) is

$$Z_{in} = - \int_S J_u E_u \, ds \qquad (2.3.7)$$

Transformation to a cylindrical (u, r, ϕ) coordinate system (as in Figure 2.3.2) gives

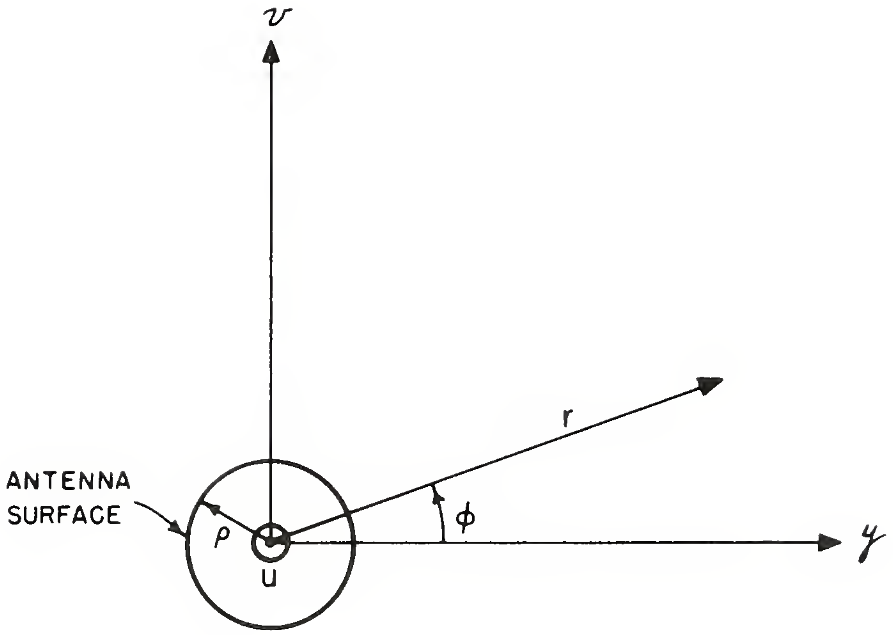
v
r
ANTENNA SURFACE
ρ
u
ϕ
y

Figure 2.3.2 The cylindrical co-ordinate system

$$y = r \cos\phi \quad , \qquad v = r \sin\phi$$

If the current is spread uniformly over the antenna surface, the current density is

$$J_u = \frac{1 - \frac{u}{L}}{2\pi\rho} \; \delta\,(r-\rho) \qquad \text{for } u > 0 \tag{2.3.8}$$

$$ = \frac{1 + \frac{u}{L}}{2\pi\rho} \; \delta\,(r-\rho) \qquad \text{for } u < 0$$

In order to simplify the calculations, one can obtain an expression for the impedance of a monopole of length L. The impedance of a dipole of length 2L is just twice the monopole impedance. The monopole impedance is

$$Z_{in} = -\frac{1}{2\pi} \int_0^{2\pi}\!\!\int_0^{L} (1 - \frac{u}{L}\,)\; E_u\;(u,\rho,\phi)\; du\; d\phi \tag{2.3.9}$$

and E_u (u,ρ,ϕ) is given in Equation (2 2 19). In the cylindrical coordinate system,

$$\begin{aligned}
\rho_1^2 &= \left[(u-L)\sin\theta - \rho\cos\theta\sin\phi \right]^2 + \left[\rho\cos\phi\right]^2 \\
\rho_2^2 &= \left[(u+L)\sin\theta - \rho\cos\theta\sin\phi \right]^2 + \left[\rho\cos\phi\right]^2 \\
\rho_o^2 &= \left[u\sin\theta - \rho\cos\theta\sin\phi \right]^2 + \left[\rho\cos\phi\right]^2
\end{aligned} \tag{2.3.10}$$

$$\begin{aligned}
z_1 &= (u-L)\cos\theta + \rho\sin\theta\sin\phi \\
z_2 &= (u+L)\cos\theta + \rho\sin\theta\sin\phi \\
z_o &= u\cos\theta + \rho\sin\theta\sin\phi
\end{aligned} \tag{2.3.11}$$

The expression for E_u may be simplified by introducing

$$\begin{aligned}
F &= 1 + (a^2-1)\cos^2\theta \\
G &= 2\rho(a^2-1)\sin\theta\cos\theta\sin\phi \\
H &= \rho^2\left[1 + (a^2-1)\sin^2\theta\sin^2\phi\right]
\end{aligned} \tag{2.3.12}$$

Thus,

$$\rho_1^2 + a^2\ z_1^2 = F(u-L)^2 + G(u-L) + H$$

$$\rho_2^2 + a^2\ z_2^2 = F(u+L)^2 + G(u+L) + H$$

$$\rho_o^2 + a^2\ z_o^2 = Fu^2 + Gu + H \qquad (2.3.13)$$

The monopole impedance is

$$Z_{in} = \frac{-a}{j\omega\ 4\pi\epsilon_o K' L} \cdot \frac{1}{2\pi} \int_0^{2\pi} (I_1 + I_2 - 2I_3)\ d\phi \qquad (2.3.14)$$

where

$$I_1 = \int_0^L \frac{\left(1 - \frac{u}{L}\right) du}{\sqrt{F(u-L)^2 + G(u-L) + H}}$$

(2.3.15)

$$= -\frac{1}{L} \left\{ \frac{\sqrt{F\alpha^2 + G\alpha + H}}{F} - \frac{G}{2F} \cdot \frac{1}{\sqrt{F}} \ln\left[2\sqrt{F(F\alpha^2 + G\alpha + H)} + 2F\alpha + G \right] \right\}_{\alpha=-L}^{\alpha=0}$$

$$I_2 = \int_0^L \frac{\left(1 - \frac{u}{L}\right) du}{\sqrt{F(u+L)^2 + G(u+L) + H}}$$

$$= -\frac{1}{L}\left\{\frac{\sqrt{F\,a^2 + G\,a + H}}{F} - \frac{G}{2F} \cdot \frac{1}{\sqrt{F}} \ln\left[2\sqrt{F(F\,a^2 + G\,a + H)} + 2F\,a + G\right]\right\}_{a=L}^{a=2L}$$

$$+ 2\left\{\frac{1}{\sqrt{F}} \ln\left[2\sqrt{F(F\,a^2 + G\,a + H)} + 2F\,a + G\right]\right\}_{a=L}^{a=2L} \qquad (2.3.16)$$

$$I_3 = \int_0^L \frac{\left(1 - \frac{u}{L}\right) du}{\sqrt{Fu^2 + Gu + H}}$$

$$= -\frac{1}{L}\left\{\frac{\sqrt{F\,a^2 + G\,a + H}}{F} - \frac{G}{2F} \cdot \frac{1}{\sqrt{F}} \ln\left[2\sqrt{F(F\,a^2 + G\,a + H)} + 2F\,a + G\right]\right\}_{a=0}^{a=L}$$

$$+\left\{\frac{1}{\sqrt{F}} \ln\left[2\sqrt{F(F\,a^2 + G\,a + H)} + 2F\,a + G\right]\right\}_{a=0}^{a=L} \qquad (2.3.17)$$

In order to make the expressions more compact, let

$$N(a) = \sqrt{F a^2 + G a + H}$$

$$M(a) = 2\sqrt{F(F a^2 + G a + H)} + 2 F a + G \qquad (2.3.18)$$

The sum of the above integrals is

$$I_1 + I_2 - 2I_3 = \frac{-1}{FL}\left[3N(o) - 3N(L) + N(2L) - N(-L)\right]$$

$$+ \frac{G}{2FL} \cdot \frac{1}{\sqrt{F}} \ln \frac{M(o)^3\ M(2L)}{M^3(L)\ M(-L)}$$

$$+ \frac{2}{\sqrt{F}} \ln \frac{M(o)\ M(2L)}{M^2(L)} \qquad (2.3.19)$$

If it is assumed that $\rho \ll L$, then the above formula can be greatly simplified:

$$I_1 + I_2 - 2I_3 = \frac{2}{\sqrt{F}}\left[1 - \ln\frac{FL}{\rho} + \ln\left(\sqrt{F}\sqrt{1+(a^2-1)\sin^2\theta\ \sin^2\phi} + (a^2-1)\sin\theta\ \cos\theta\ \sin\phi\right)\right] \tag{2.3.20}$$

Substitution of the above in Equation (2.3.14) gives

$$Z_{in} = \frac{a}{j\omega 2\pi\epsilon_0 K' L \sqrt{F}}\left[\ln\frac{L}{\rho} - 1 + \ln F - \frac{1}{2\pi}\int_0^{2\pi} \ln\left(\sqrt{F}\sqrt{1+(a^2-1)\sin^2\theta\ \sin^2\phi} + (a^2-1)\sin\theta\ \cos\theta\ \sin\phi\right)d\phi\right] \tag{2.3.21}$$

It can be shown that

$$\frac{1}{2\pi}\int_0^{2\pi} f(\sin^2\phi,\ \sin\phi)\ d\phi = \frac{1}{\pi}\int_0^{\pi/2}\left[f(\sin^2\phi,\ -\sin\phi) + f(\sin^2\phi,\ \sin\phi)\right]d\phi \tag{2.3.22}$$

from which

$$\frac{1}{2\pi}\int_{0}^{2\pi} \ln\left(\sqrt{F}\sqrt{1+(a^2-1)\sin^2\theta\ \sin^2\phi} + (a^2-1)\sin\theta\ \cos\theta\ \sin\phi\right) d\phi$$

$$= \frac{1}{\pi}\int_{0}^{\pi/2} \ln\left\{F\left[1+(a^2-1)\sin^2\theta\ \sin^2\phi\right] - (a^2-1)^2\ \sin^2\theta\ \cos^2\theta\ \sin^2\phi\right\} d\phi$$

$$= \ln\frac{\sqrt{F} + a}{2} \qquad (2.3.23)$$

Substitution of the above in Equation (2.3.21) gives

$$Z_{in} = \frac{a}{j\omega 2\pi\epsilon_o K' L\sqrt{F}}\left[\ln\frac{L}{\rho} - 1 - \ln\frac{a+\sqrt{F}}{2F}\right] \qquad (2.3.24)$$

where $F = \sin^2\theta + a^2\cos^2\theta$ and $a^2 = \frac{K'}{K_o}$

This formula gives the input impedance of a short, thin monopole making an angle θ with the DC magnetic field. Two special cases are of interest,

$\theta = 0$ (monopole parallel to $\overline{H}_{DC}$) and $\theta = \pi/2$ (monopole perpendicular to $\overline{H}_{DC}$).

Parallel case:

$$Z_{in} = \frac{1}{j\omega 2\pi\epsilon_o K' L}\left[\ln\frac{L}{\rho} - 1 + \ln a\right] \tag{2.3.25}$$

Perpendicular case:

$$Z_{in} = \frac{a}{j\omega 2\pi\epsilon_o K' L}\left[\ln\frac{L}{\rho} - 1 - \ln\frac{a+1}{2}\right] \tag{2.3.26}$$

In free space ($K_o = K' = 1$) the above impedance formulas reduce to

$$Z_{in} = \frac{1}{j\omega 2\pi\epsilon_o L}\left[\ln\frac{L}{\rho} - 1\right] \tag{2.3.27}$$

which can be found in any discussion of short, cylindrical antennas (Schelkunoff and Friis[16] for instance).

It is interesting to observe that impedance formula, Equation (2.3.24), can be re-written in the same form as the free space impedance (Equation (2.3.27)) if the dimensions L and ρ are suitably scaled. That is,

$$Z_{in} = \frac{1}{j\omega 2\pi \epsilon_o L'} \left[\ln \frac{L'}{\rho'} - 1 \right]$$

where

$$L' = L \sqrt{K'} \sqrt{K_o \sin^2\theta + K' \cos^2\theta}$$

and

$$\rho' = \frac{\rho}{2} \left(\frac{K' \sqrt{K_o}}{\sqrt{K_o \sin^2\theta + K' \cos^2\theta}} + \sqrt{K' K_o} \right)$$

The significance of this scaling will be discussed further in Section 2.5.

The above impedance expressions all contain the logarithm of a function of "a". When the medium is lossless and hyperbolic, the logarithm produces a positive, real part in the input impedance. This indicates that the antenna transmits energy irreversibly into the magnetoplasma. It will be shown in Section 2.4 that this energy transmission is in fact a form of radiation.

Numerical impedance calculations will be presented in Chapter 3 along with the experimental results.

2.4 The Poynting Theorem and Calculation of Radiation Resistance

The radiation resistance of an antenna can be obtained by integrating the real part of the Poynting vector over a closed surface surrounding the antenna. Since the quasi-static theory for a lossless plasma predicts a dipole impedance having a positive real part, this real part should be the radiation resistance. Therefore, as a check on the impedance calculation, it should be possible to compute an identical radiation resistance by integrating over a surface at an arbitrary distance from the antenna. In addition, it is important to establish that the total outward power flow is independent of the distance between the source and the surface of integration; this assures that the power flow has the characteristics of radiation and not of "intrinsic loss"[17] (apparent power dissipation in a finite lossless region).

It is necessary first of all to write the Poynting theorem in a form readily applicable to quasi-static analysis. Equation (2.1.60) is in such a form and is repeated here for convenience:

$$\int_V \overline{E} \cdot \overline{J}^{\,*} \, dv = j\omega \int_V \overline{E}\,\overline{D}^{*} \, dv + j\omega \int_S \psi \, \overline{D}^{*} \cdot \hat{n} \, ds \qquad (2.4.1)$$

In quasi-static theory, the addition of a constant to the scalar potential ψ leaves the electric field unchanged. In Equation (2.4.1), the addition of a constant to ψ leaves the equation unchanged provided that there is zero net charge within the surface S.

Let us now compute the outward power flow from a short monopole (or dipole) which is oriented parallel to the DC magnetic field. This restriction simplifies the computation while preserving the essential features of the analysis. The outward power flow P through a surface S is given by

$$P = -j\omega \int_S \psi \, \bar{D}^* \cdot \hat{n} \, ds \qquad (2.4.6)$$

in the quasi-static limit. For a monopole, the surface S can be a closed cylinder as shown in Figure 2.4.1. For P to have a real part, the product $\psi \, \bar{D}^* \cdot \hat{n}$ must have an imaginary part. This can occur only under hyperbolic conditions and then only between the characteristic cones emanating from the ends of the antenna. Thus P will have a real part only over the shaded region of S_1. The surface S_2 can be removed to infinity and then neglected, at least for the computation of real power flow.

The necessary field expressions are

$$E_z(\rho, z) = \frac{a}{jM}\left[\frac{1}{\sqrt{\rho^2+a^2(z+L)^2}} + \frac{1}{\sqrt{\rho^2+a^2\,(z-L)^2}} - \frac{2}{\sqrt{\rho^2+a^2\,z^2}}\right] \qquad (2.4.7)$$

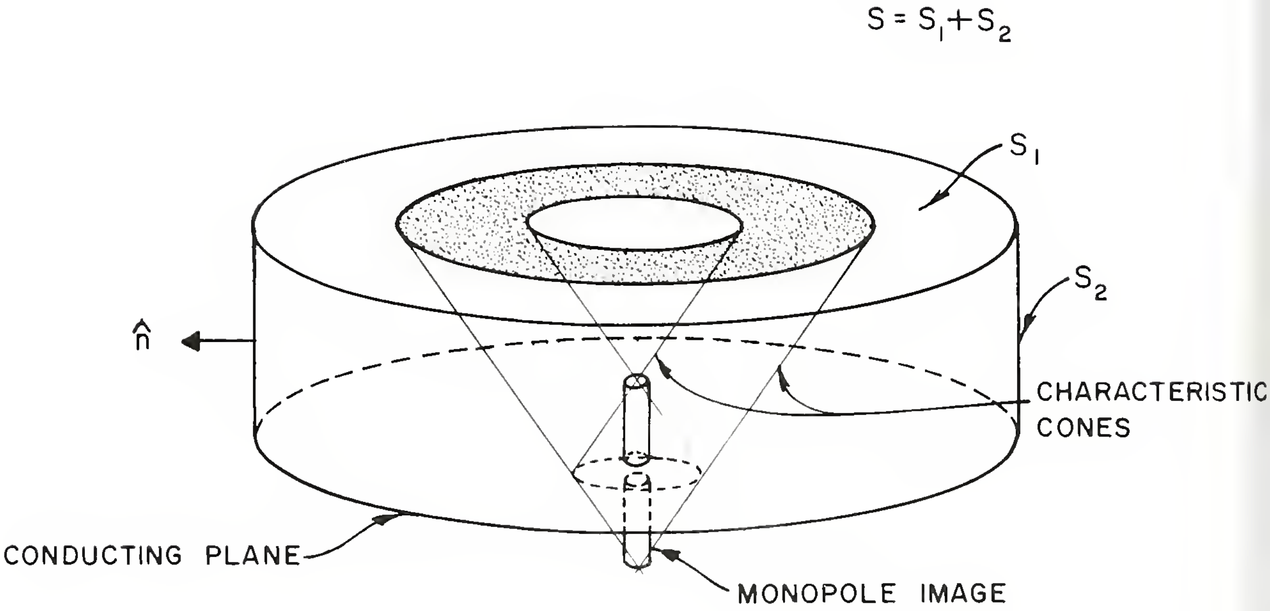
S = S₁+S₂
S₁
S₂
n̂
CHARACTERISTIC CONES
CONDUCTING PLANE
MONOPOLE IMAGE

Figure 2.4.1 Radiation fields of a monopole

$$\psi\ (\rho, z) = \frac{-a}{jM} \int_0^L \left[\frac{1}{\sqrt{\rho^2 + a^2\ (z+u)^2}} - \frac{1}{\sqrt{\rho^2 + a^2\ (z-u)^2}} \right] du \qquad (2.4.8)$$

where $M = \omega 4\pi\epsilon_o K' L$

The power flow through S_1 is designated P_1 where

$$P_1 = -j\omega \int_{S_1} \psi\ \bar{D}^* \cdot \hat{n}\ ds \qquad (2.4.9)$$

$$= -j\omega\epsilon_o K_o \int_0^\infty \int_0^{2\pi} \psi(\rho, z)\ E_z^*\ (\rho, z)\ \rho d\phi\ d\rho$$

$$= Q \int_0^\infty \psi(\rho, z)\ E_z^*\ (\rho, z)\ d\rho^2$$

where

$$Q = -j\omega\pi\epsilon_o K_o$$

$$P_1 = \frac{-Q|a|^2}{M^2} \int_0^L \int_0^\infty \left[\frac{1}{\sqrt{\rho^2 + a^2 (z+u)^2}} - \frac{1}{\sqrt{\rho^2 + a^2 (z-u)^2}} \right] \left[\frac{1}{\sqrt{\rho^2 + a^2 (z+L)^2}} + \frac{1}{\sqrt{\rho^2 + a^2 (z-L)^2}} - \frac{2}{\sqrt{\rho^2 + a^2 z^2}} \right]^* d\rho^2 \, du$$

$$= \frac{-Q|a|^2}{M^2} \int_0^L \sum_{ij} I_{ij} \, du \quad \text{where } i=1,2 \text{ and } j=1,2,3 \qquad (2.4.10)$$

Here, I_{ij} indicates an integral formed from one of the six products indicated above. In general the real part of P_1 comes from the imaginary parts of the integrals I_{ij}. Imaginary parts arise when a^2 is negative (say $a^2 = -C^2$) and over a limited range of the variable ρ^2. For instance, consider the integral I_{11}

$$I_{11} = \int_0^\infty \frac{d\rho^2}{\sqrt{\rho^2 - C^2 (z+u)^2} \left(\sqrt{\rho^2 - C^2 (z+L)^2} \right)^*} \qquad (2.4.11)$$

It is evident that the imaginary part of I_{11} is given by

$$j\,\mathrm{Im}\,I_{11} = \int_{\rho^2=C^2(z+u)^2}^{\rho^2=C^2(z+L)^2} \frac{d\rho^2}{\sqrt{\rho^2-C^2(z+u)^2}\left(\sqrt{\rho^2-C^2(z+L)^2}\right)^*} \qquad (2.4.12)$$

$$= j\,2\tan^{-1}\sqrt{\frac{\rho^2-C^2(z+u)^2}{C^2(z+L)^2-\rho^2}}\,\Bigg|_{\rho^2=C^2(z+u)^2}^{\rho^2=C^2(z+L)^2}$$

$$= j\,2\left[\tan^{-1}\infty - \tan^{-1}0\right]$$

$$= \pm j\,n\pi \quad \text{where } n \text{ is an odd integer} \qquad (2.4.13)$$

It can be shown readily that $\mathrm{Im}\,I_{21} = -\,\mathrm{Im}\,I_{11}$, $\mathrm{Im}\,I_{22} = -\,\mathrm{Im}\,I_{12}$, and $\mathrm{Im}_{23} = +\,\mathrm{Im}\,I_{13}$. Thus

$$j \ \mathrm{Im} \sum_{1j} I_{1j} = 2 \ j \ \mathrm{Im} \ I_{13} \qquad (2.4.14)$$

$$= -4 \int_{\rho^2=C^2 z^2}^{\rho^2=C^2 (z+u)^2} \frac{d\rho^2}{\sqrt{\rho^2 - C^2 (z+u)^2} \left(\sqrt{\rho^2 - C^2 z^2} \right)^*}$$

$$= 4j \int_{\rho^2=C^2 z^2}^{\rho^2=C^2 (z+u)^2} \frac{d\rho^2}{\sqrt{C^2 (z+u)^2 - \rho^2} \ \sqrt{\rho^2 - C^2 z^2}}$$

$= \pm n \, 4j\pi$ where n is an odd integer. (2.4.15)

The correct value for $\pm$ n can be determined by introducing a small loss and observing the locations of the points $\rho^2 = C^2 z^2$ and $\rho^2 = C^2 (z+u)^2$ in the complex ρ^2-plane. There are two cases of interest, $K' < 0$ and $K' > 0$. These cases correspond to the two hyperbolic regions in a Y^2 vs. X graph (compare with Figure 2.1.1):

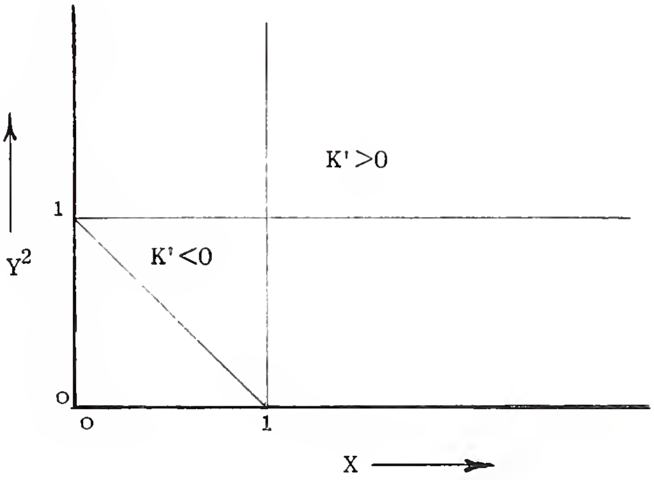

In the complex ρ^2-plane, the real axis is the path of integration. If $K' > 0$ the points $C^2 z^2$ and $C^2 (z+u)^2$ are below the real axis. If $K' < 0$, the two points are above the real axis. Thus the imaginary part of the integral (the "phase change") is negative for $K' > 0$ and positive for $K' < 0$. In addition the total phase change of the integral can be no greater than π in magnitude so that $n = 1$.

Thus
$$j \,\mathrm{Im} \sum_{ij} I_{ij} = 4 j \pi \quad \text{if } K' > 0 \tag{2.4.16}$$
$$= - 4 j \pi \quad \text{if } K' < 0$$

If P_r is the real outward power flow through the surface S_1,

$$P_r = -\frac{Q|a|^2}{M^2}\int_0^L j\ \mathrm{Im}\ \sum_{ij}\ I_{ij}\ du \qquad (2.4.17)$$

$$= -\frac{Q|a|^2}{M^2}(\pm 4\ j\ \pi)\ L \qquad \begin{cases} + \text{ sign for } K' > 0 \\ - \text{ sign for } K' < 0 \end{cases}$$

$$= \frac{-(-j\omega\pi\epsilon_0 K_0)}{(\omega 4\pi\epsilon_0 K' L)^2}\left(-\frac{K'}{K_0}\right)\left(\pm 4j\pi\right) L$$

$$= \frac{1}{4\omega L\epsilon_0 |K'|} \qquad (2.4.18)$$

If the input current is unity then the radiation resistance is given by

$$R_{rad} = \frac{1}{4\omega L\epsilon_0 |K'|} \qquad (2.4.19)$$

From the former impedance calculations for a monopole we have

$$\mathrm{Re}(Z_{in}) = \frac{\ln a}{j\omega 2\pi\epsilon_o K' L} \tag{2.4.20}$$

$$= \frac{\pm j\ \pi/2}{j\omega 2\pi\epsilon_o K' L} \qquad \begin{cases} + \text{ sign for } K' > o \\ - \text{ sign for } K' < o \end{cases}$$

$$= \frac{1}{4\omega L\epsilon_o |K'|}$$

$$= R_{rad}. \tag{2.4.21}$$

It has been shown that the real power flow is independent of the height "z" of the surface S_1 and that the radiation resistance is equal to the real part of the input impedance. This indicates presence of a mode of radiation which is most unusual because it can have a pronounced effect even for a very short antenna. The explanation for this phenomenon was suggested in Section 2.1 where it was shown that an irrotational electric field induces a magnetic field in a magnetoplasma, making possible electromagnetic effects such as radiation. However it remains to be shown that it is the induced magnetic field $\overline{H}_1$ which is totally responsible for the real part of the total outward power flow P. This can be done by writing

$$P = \int_S \overline{E} \times \overline{H}^* \cdot \hat{n}\ ds \tag{2.4.22}$$

and using the quasi-static electric field together with the total low frequency magnetic field. The latter is given in Equation (2.1.61) as

$$\tilde{\bar{H}} = \tilde{\bar{H}}_1 + \frac{j}{\bar{k}^2} \bar{k} \times \tilde{\bar{J}} \qquad (2.4.23)$$

Evaluation of Equation (2.4.22) for the case of a monopole parallel to the DC magnetic field gives the same integral already evaluated (Equation (2.4.10)). Furthermore the real part of the outward power flow arises entirely from the induced magnetic field $\bar{H}_i$.

2.5 Derivation of the Impedance Formula by Dimensional Scaling

Consider the problem of transforming the anisotropic differential equations into equations having the same form as the free space differential equations. In the quasi-static theory three equations are important, any two of which are independent. They are

$$K_1 \phi_{xx} + K_2 \phi_{yy} + K_3 \phi_{zz} = -\frac{q}{\epsilon_0} \qquad (2.5.1)$$

$$\nabla \cdot \bar{J} + j\omega q = 0 \qquad (2.5.2)$$

$$K_1 \phi_{xx} + K_2 \phi_{yy} + K_3 \phi_{zz} = \frac{1}{j\omega\epsilon_0} \nabla \cdot \bar{J} \qquad (2.5.3)$$

where K_1, K_2, K_3 are the relative permittivities in the x, y, z coordinate directions (respectively), q is the charge density and $\bar{J}$ is the current density. A time factor $e^{j\omega t}$ is understood.

Dimensional scaling of the following form will be considered:

$$x' = \alpha x, \qquad y' = \beta y, \qquad z' = \gamma z . \tag{2.5.4}$$

In order to transform the "anistropic Laplacian" into an "isotropic" or ordinary Laplacian, it is required that

$$K_1 \phi_{xx} + K_2 \phi_{yy} + K_3 \phi_{zz} = C\,(\phi_{x'x'} + \phi_{y'y'} + \phi_{z'z'}) \tag{2.5.5}$$

$$= C \,\Delta' \phi$$

where C is some constant. Substituting the scaled variables on the left side and equating the coefficients gives

$$\frac{\alpha^2 K_1}{C} = \frac{\beta^2 K_2}{C} = \frac{\gamma^2 K_3}{C} = 1 \tag{2.5.6}$$

or

$$\alpha^2 = \frac{C}{K_1}, \quad \beta^2 = \frac{C}{K_2}, \quad \gamma^2 = \frac{C}{K_3} \tag{2.5.7}$$

After transformation, the divergence of the current density becomes

$$\nabla \cdot \bar{J} = \alpha \beta \gamma \quad \nabla' \cdot \bar{J}' \tag{2.5.8}$$

Equations (2.5.1) and (2.5.2) can be expressed as

$$C \, \Delta' \, \phi = \frac{-q}{\epsilon_o} \tag{2.5.9}$$

$$\alpha \beta \gamma \nabla' \cdot \bar{J}' + j \omega q = 0 \tag{2.5.10}$$

If it is assumed that C and $\alpha \beta \gamma$ are not zero, Equations (2.5.9) and (2.5.10) become

$$\Delta' \, \phi = - \frac{q}{\epsilon_o C} \tag{2.5.11}$$

$$\Delta' \cdot \bar{J} + j \frac{\omega q}{\alpha b \gamma} = 0 \qquad (2.5.12)$$

These can be reduced to the free-space form if ω and q are suitably transformed, say to ω' and q'.

$$q' = \frac{q}{C} \qquad (2.5.13)$$

$$\omega' q' = \frac{\omega q}{\alpha \beta \gamma} \qquad (2.5.14)$$

It is necessary to put some restriction on the frequency and charge scaling. First let it be assumed that $\omega' = \omega$ (frequency-invariant scaling). Equations (2.5.13) and (2.5.14) give

$$C = \alpha \beta \gamma . \qquad (2.5.15)$$

Equations (2.5.6) and (2.5.15) can be solved for α, β, γ, and C, giving

$$\alpha = \sqrt{K_2 K_3}, \qquad \beta = \sqrt{K_1 K_3}, \qquad \gamma = \sqrt{K_1 K_2}, \qquad C = \sqrt{K_1 K_2 K_3} . \qquad (2.5.16)$$

Now let it be assumed that $q' = q$ (charge-invariant scaling). It is apparent that

$$C = 1 \tag{2.5.17}$$

and from Equation (2.5.7),

$$\alpha = \frac{1}{\sqrt{K_1}}, \qquad \beta = \frac{1}{\sqrt{K_2}}, \qquad C = \frac{1}{\sqrt{K_3}}. \tag{2.5.18}$$

To summarize, there are two principal types of scaling, one frequency-invariant and one charge-invariant.

a) Frequency-invariant scaling:

$$\begin{aligned} x' &= \sqrt{K_2 K_3}\, x & \omega' &= \omega \\ y' &= \sqrt{K_1 K_3}\, y & q' &= \frac{q}{K_1 K_2 K_3} \\ z' &= \sqrt{K_1 K_2}\, z \end{aligned} \tag{2.5.19}$$

b) Charge-invariant scaling:

$$\begin{aligned} x' &= x/\sqrt{K_1} & \omega' &= \omega\sqrt{K_1 K_2 K_3} \\ y' &= y/\sqrt{K_2} & q' &= q \\ z' &= z/\sqrt{K_3} \end{aligned} \tag{2.5.20}$$

Either of these two methods of scaling converts the equations of free-space form

$$\Delta' \phi = - \frac{q'}{\epsilon_o} \qquad (2.5.21)$$

$$\nabla' \cdot \overline{J}' + j \omega' q' = 0 \qquad (2.5.22)$$

$$\Delta' \phi = \frac{1}{j\omega' \epsilon_o} \nabla' \cdot \overline{J}' \qquad (2.5.23)$$

to Equations (2.5.1), (2.5.2), (2.5.3), respectively, Since frequency (rather than charge) appears explicitly in the quasi-static impedance formulas, frequency-invariant scaling is to be preferred.

For a magnetized plasma with the DC magnetic field oriented along with the z axis, the scaling is somewhat simplified.

a) Frequency-invariant scaling:

$$x' = \sqrt{K' K_o} \; x \qquad \omega' = \omega \qquad (2.5.24)$$

$$y' = \sqrt{K' K_o} \; y \qquad q' = \frac{q}{K'^2 K_o}$$

$$z' = K' \; z$$

b) Charge-invariant scaling:

$$x' = x/\sqrt{K'} \qquad \omega' = K'\sqrt{K_o} \tag{2.5.25}$$

$$y' = y/\sqrt{K'} \qquad q' = q .$$

$$z' = z/\sqrt{K_o}$$

By means of scaling, the quasi-static differential equations may be transformed into free space equations. If the scaling is applied to the dimensions of a cylindrical dipole, the equivalent free space dipole can be shown to have an elliptical cross section (for the case of real, positive scale factors). This free space dipole, in turn, has a free space equivalent with a circular cross section. Thus the impedance of a short dipole in an anisotropic medium may be found by a simple scaling of the well-known results for cylindrical antennas in free space. The details of this approach to the problem will be worked out in the following paragraphs.

Frequency-invariant scaling will be employed. The scale factors are given by

$$x' = \sqrt{K'K_o}\; x \;, \qquad y' = \sqrt{K'K_o}\; y \;, \qquad z' = K' z \tag{2.5.26}$$

The co-ordinate system is shown in Figure 2.5.1.

The length scales easily. If x', z' are the projections of the scaled length L' and x, z are the projections of L, we have

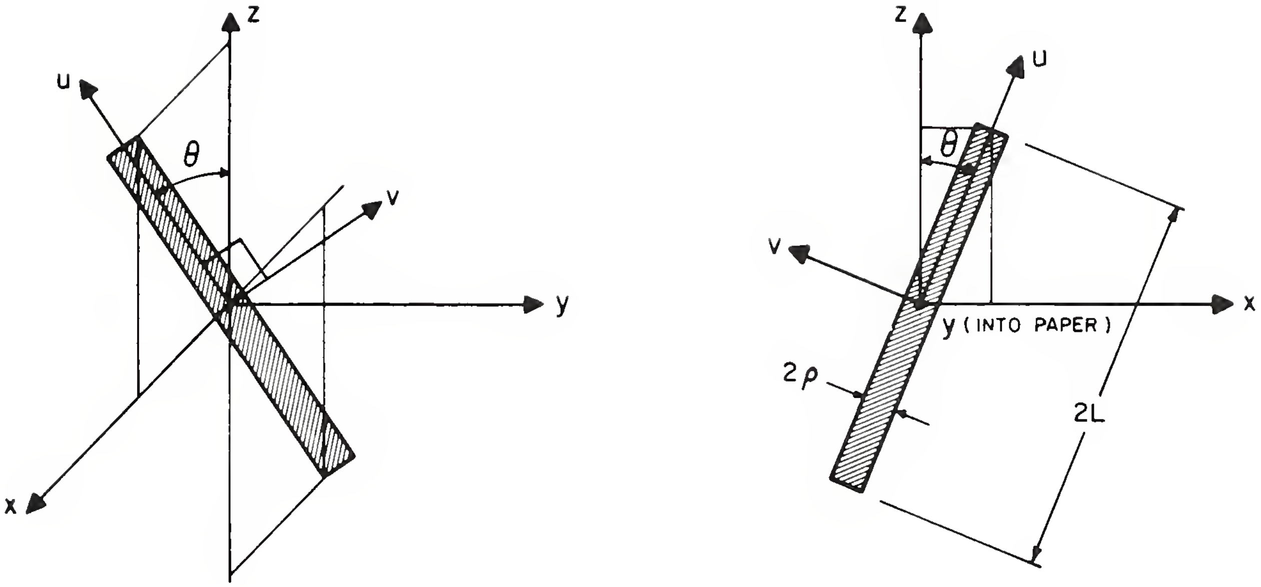
z
u
θ
v
y
x
z
u
θ
v
x
y (INTO PAPER)
2ρ
2L

Figure 2.5.1 The co-ordinate system in the magnetoplasma

$$L' = \sqrt{x'^2 + z'^2} = \sqrt{K'}\ \sqrt{K_o\ x^2 + K'\ z^2}$$

$$= \sqrt{K'}\ \sqrt{K_o\ \sin^2\theta + K'\ \cos^2\theta}\quad L \tag{2.5.27}$$

The radial scaling is somewhat more involved. The circular cross section of the dipole is given by the equation

$$v^2 + y^2 = \rho^2 \tag{2.5.28}$$

where

$$\begin{aligned} u &= z\ \cos\theta + x\ \sin\theta \\ v &= z\ \sin\theta - x\ \cos\theta \end{aligned} \tag{2.5.29}$$

After scaling, the above cross section equation becomes

$$\left(\frac{z'\ \sin\theta}{K'} - \frac{x'\ \cos\theta}{\sqrt{K' K_o}}\right)^2 + \frac{y'^2}{K' K_o} = \rho^2 \tag{2.5.30}$$

The co-ordinate system is shown in Figure 2.5.2. The co-ordinate transformation $(x', z') \longrightarrow (u', v')$ is given by

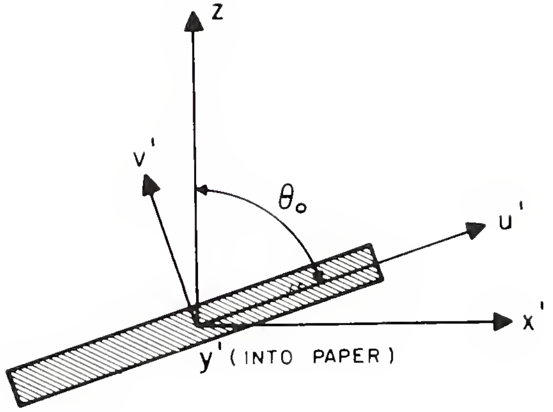
z'
v'
θ_o
u'
x'
y' (INTO PAPER)

Figure 2.5.2 The free space co-ordinate system

$$z' = u' \cos\theta_o + v' \sin\theta_o$$

$$x' = u' \sin\theta_o - v' \sin\theta_o \tag{2.5.31}$$

The relation between θ and θ_o is

$$\tan\theta_o = \frac{x'}{z'} = \sqrt{\frac{K_o}{K'}}\ \frac{x}{z} = \sqrt{\frac{K_o}{K'}}\ \tan\theta. \tag{2.5.32}$$

or

$$\sin\theta_o = \frac{\sqrt{K_o}\ \sin\theta}{\sqrt{K_o \sin^2\theta + K' \cos^2\theta}} \tag{2.5.33}$$

or

$$\cos\theta_o = \frac{\sqrt{K'}\ \cos\theta}{\sqrt{K_o \sin^2\theta + K' \cos^2\theta}} \tag{2.5.34}$$

Now the cross section equation becomes

$$v'^2 \left(\frac{K_o \sin^2\theta + K' \cos^2\theta}{K'^2 K_o} \right) + y'^2 \left(\frac{1}{K' K_o} \right) = \rho^2 \tag{2.5.35}$$

or

$$\frac{v'^2}{\left(\dfrac{\rho K' \sqrt{K_o}}{\sqrt{K_o \sin^2\theta + K' \cos^2\theta}}\right)^2} + \frac{y'^2}{\left(\rho\sqrt{K' K_o}\right)^2} = 1 \tag{2.5.36}$$

This is an ellipse with semi-axes

$$A = \frac{\rho K' \sqrt{K_o}}{\sqrt{K_o \sin^2\theta + K' \cos^2\theta}}, \quad B = \rho \sqrt{K' K_o} \tag{2.5.37}$$

Thus there exists an equivalent free space dipole having an elliptical cross section.

Y. T. Lo[18] has shown that a dipole with an elliptical cross section has an equivalent with a circular cross section, the radius of which is given by $\rho' = \frac{A+B}{2}$. Thus the radial scaling can be written as

$$\rho' = \frac{\rho}{2}\left(\frac{K' \sqrt{K_o}}{\sqrt{K_o \sin^2\theta + K' \cos^2\theta}} + \sqrt{K' K_o}\right) \tag{2.5.38}$$

The impedance of a short cylindrical monopole in free space is usually expressed (see Schelkunoff and Friis[16]) as

$$Z_{in} = \frac{1}{j\omega 2\pi\epsilon_o L'} \left[\ln \frac{L'}{\rho'} - 1 \right] \qquad (2.5.39)$$

When L' and ρ' are transformed as indicated above, the formula becomes

$$\begin{aligned} Z_{in} = \frac{1}{j\omega 2\pi\epsilon_o L \sqrt{K'}\sqrt{K_o \sin^2\theta + K' \cos^2\theta}} \Bigg[& \ln \frac{L}{\rho} - 1 \\ & + \ln \frac{2(K_o \sin^2\theta + K' \cos^2\theta)}{\sqrt{K_o}\left(\sqrt{K'} + \sqrt{K_o \sin^2\theta + K' \cos^2\theta}\right)} \Bigg] \end{aligned} \qquad (2.5.40)$$

This formula could have been derived using charge-invariant scaling, which involves the slight additional complication of a frequency scale factor. The above expression is identical to the one obtained by solving the anisotropic source problem without recourse to scaling.

2.6 The Effect of a Cylindrical Current Assumption on the Computed Impedance

The analysis in the preceding sections of Chapter 2 has uncovered unexpected phenomena associated with lossless, hyperbolic conditions in the magnetoplasma. The field of a short dipole exhibits infinite discontinuities and its impedance has a real part, indicating radiation. Since such a phenomenon may be caused by a poor choice of current distribution, this section and the following one are devoted to analyses of two different current distributions. This section considers the triangular current to be spread over the cylindrical surface of the dipole rather than being concentrated in an infinitesimal filament along the dipole axis.

For the sake of simplicity, both the dipole and the DC magnetic field are oriented in the z direction. Because of cylindrical symmetry, the differential equation may be expressed in cylindrical co-ordinates as

$$\psi_{rr} + \frac{1}{r}\psi_r + \frac{1}{a^2}\psi_{zz} = -\frac{q}{\epsilon_o K'} \qquad (2.6.1)$$

This equation is to be solved with the help of the transform pair

$$\tilde{f}(k,\gamma) = \int_{-\infty}^{\infty}\int_{o}^{\infty} f(z,r)\, e^{-jkz}\, J_o(\gamma r)\, r\, dr\, dz \qquad (2.6.2)$$

$$f(z,r) = \frac{1}{2\pi}\int_{-\infty}^{\infty}\int_{o}^{\infty} \tilde{f}(k,\gamma)\, e^{jkz}\, J_o(\gamma r)\, \gamma\, d\gamma\, dk \qquad (2.6.3)$$

If the differential equation is transformed, solved algebraically and re-transformed, the potential can be expressed as

$$\psi(z,r) = \frac{1}{2\pi\epsilon_o K'} \int_{-\infty}^{\infty}\int_{0}^{\infty} \frac{\tilde{q}\,(k,\gamma)}{\gamma^2 + \frac{k^2}{a^2}}\, e^{jkz}\, J_o(\gamma r)\gamma\, d\gamma\, dk \qquad (2.6.4)$$

In order to find $\tilde{q}$, it is necessary to consider a current distribution J which is spread uniformly over a cylinder of radius ρ. The corresponding charge distribution is

$$q = -\frac{1}{j\,\omega}\ \frac{\partial\ J(z)}{\partial\ z}\ \frac{\delta(r-\rho)}{2\pi\rho}$$

$$= \frac{1}{j\omega L}\ T(z)\ \frac{\delta(r-\rho)}{2\pi\rho} \qquad (2.6.5)$$

for which the function T is shown in Figure 2.2.3. The transform of q is

$$\tilde{q}(k,\gamma) = \frac{1}{2\pi\omega Lk}\left(e^{-jkL} + e^{jkL} - 2\right) J_o(\gamma\,\rho) \qquad (2.6.6)$$

The potential ψ at any point (z, r) now can be expressed in terms of an integral.

$$\psi(z,r) = \frac{1}{(2\pi)^2 \omega \epsilon_o K' L} \int_{-\infty}^{\infty} \int_{0}^{\infty} \frac{e^{-jkL} + e^{jkL} - 2}{k\left(\gamma^2 + \frac{k^2}{a^2}\right)} J_o(\gamma \rho) e^{jkz} J_o(\gamma r) \gamma \, d\gamma \, dk \tag{2.6.7}$$

For impedance calculation, it is necessary to have the electric field in the z direction at the dipole surface $(r=\rho)$.

$$E_z(z,\rho) = \frac{1}{(2\pi)^2 j\omega \epsilon_o K' L} \int_{-\infty}^{\infty} \int_{0}^{\infty} \frac{e^{-jkL} + e^{jkL} - 2}{\gamma^2 + \frac{k^2}{a^2}} e^{jkz} J_o^2(\gamma\rho) \, \gamma \, d\gamma \, dk \tag{2.6.8}$$

If the integration with respect to k is carried out as in Section 2.2, E_z becomes

$$E_z(z,\rho) = \frac{a}{4\pi j\omega \epsilon_o K' L} \int_{0}^{\infty} \left(e^{-a\gamma|z-L|} + e^{-a\gamma|z+L|} - 2\, e^{-a\gamma|z|}\right) J_o^2(\gamma \rho) d\gamma \tag{2.6.9}$$

The following integral relation can be used to simplify the calculations:

$$\int_0^\infty e^{-P\gamma} J_0^2 (\gamma \rho)\, d\gamma = \frac{2}{\pi} \int_0^{\pi/2} \frac{d\phi}{\sqrt{P^2 + (2\rho\cos\phi)^2}} \tag{2.6.10}$$

Now E_z can be expressed as

$$E_z(z,\rho) = \frac{a}{4\pi j\omega\epsilon_0 K' L} \cdot \frac{2}{\pi} \int_0^{\pi/2} \left[\frac{1}{\sqrt{a^2 (L-z)^2 + (2\rho\cos\phi)^2}} + \frac{1}{\sqrt{a^2 (L+z)^2 + (2\rho\cos\phi)^2}} - \frac{2}{\sqrt{a^2 z^2 + (2\rho\cos\phi)^2}} \right] d\phi \tag{2.6.11}$$

The expression inside the integral sign now has the same form as Equation (2.2.19). Integration with respect to ϕ can be delayed while the impedance calculations are carried out as in Section 2.3.

The impedance of a monopole is given by

$$Z_{in} = \int_0^L \left(1 - \frac{z}{L}\right) E_z (\rho, z)\, dz. \tag{2.6.12}$$

If the integration with respect to z is carried out and if the assumption is made that $(2\rho\cos\phi)^2 << (\,|a|L)^2$, the following formula may be written by analogy with Equation (2.3.25):

$$Z_{in} = \frac{1}{j\omega 2\pi\epsilon_o K' L} \cdot \frac{2}{\pi} \int_0^{\pi/2} \left[\ln \frac{L}{2\rho\cos\phi} - 1 + \ln a \right] d\phi \qquad (2.6.13)$$

However,

$$\frac{2}{\pi} \int_0^{\pi/2} \ln(2\rho\cos\phi)\ d\phi = \ln \rho \qquad (2.6.14)$$

Thus,

$$Z_{in} = \frac{1}{j\omega 2\pi\epsilon_o K' L} \left[\ln \frac{L}{\rho} - 1 + \ln a \right] \qquad (2.6.15)$$

which is identical to Equation (2.3.25). It may be concluded that the assumption of a filamentary current (in Section 2.2) introduces negligible error in the impedance calculation.

2.7 The Effect of a Smooth Current Assumption on the Computed Impedance

The field solution for a triangular current distribution contains infinite discontinuities along the characteristic cones emanating from the ends and center of the dipole (see Equation (2.2.19)). The discontinuities in the field are closely related to the current discontinuities at the source. In the following calculations, the current distribution chosen is filamentary but has a continuous first derivative at the ends and center of the dipole.

For simplicity, both the dipole and the DC magnetic field are oriented in the z direction. If J and q represent the corresponding current and charge distributions, it is assumed that

for $z > 0$
$$J = \delta(x)\,\delta(y)\left[1 - 3\frac{z^2}{L^2} + 2\frac{z^3}{L^3}\right] \tag{2.7.1}$$

$$q = \frac{6}{j\omega L^2}\,\frac{\delta(\rho)}{2\pi\rho}\,z\left(1 - \frac{z}{L}\right) \tag{2.7.2}$$

for $z < 0$
$$J = \delta(x)\,\delta(y)\left[1 - 3\frac{z^2}{L^2} - 2\frac{z^3}{L^3}\right] \tag{2.7.3}$$

$$q = \frac{6}{j\omega L^2}\,\frac{\delta(\rho)}{2\pi\rho}\,z\left(1 + \frac{z}{L}\right) \tag{2.7.4}$$

The transforms to be used are

$$\tilde{f}(\gamma, k) = \int_{-\infty}^{\infty}\int_{0}^{\infty} f(\rho, z)\, e^{-jkz}\, J_o(\gamma\rho)\, \rho\, d\rho\, dz \qquad (2.7.5)$$

$$f(\rho, z) = \frac{1}{2\pi}\int_{-\infty}^{\infty}\int_{0}^{\infty} \tilde{f}(\gamma, k)\, e^{jkz} J_o(\gamma\rho)\, \gamma\, d\gamma\, dk \qquad (2.7.6)$$

The transform of the charge distribution is

$$\tilde{q} = \frac{6}{j\omega 2\pi L^2}\left[\int_{-L}^{o} z\left(1+\frac{z}{L}\right) e^{-jkz}\, dz + \int_{o}^{L} z\left(1-\frac{z}{L}\right) e^{-jkz}\, dz\right] \qquad (2.7.7)$$

After combining the two integrals and integrating by parts, one obtains a convenient form of $\tilde{q}$:

$$\tilde{q} = \frac{-3}{\omega\pi L^2} \cdot \frac{1}{k}\int_{o}^{L} \left(1 - \frac{2u}{L}\right)\left(e^{jku} + e^{-jku}\right) du \qquad (2.7.8)$$

The electric field parallel to the dipole can be obtained by a transform solution of the quasi-static differential equation. The method is identical to the one employed for the previous field computations for a triangular current distribution. The inverse transformation is carried out as follows:

$$E_z(\rho, z) = \frac{-j}{2\pi\epsilon_o K'} \int_{-\infty}^{\infty}\int_{0}^{\infty} \frac{k\,\tilde{q}}{\gamma^2 + \frac{k^2}{a^2}}\, e^{jkz}\, J_o(\gamma\,\rho)\,\gamma\, d\gamma\, dk \tag{2.7.9}$$

$$E_z(\rho, z) = \frac{-3}{j\omega 2\pi^2 \epsilon_o K' L^2} \int_0^L \left(1 - \frac{2u}{L}\right) \int_{-\infty}^{\infty}\int_{0}^{\infty} \frac{e^{jk(z+u)} + e^{jk(z-u)}}{a^2 + \frac{k^2}{a^2}} J_o(\gamma\rho)\gamma\, d\gamma\, dk\, du \tag{2.7.10}$$

$$= \frac{-3a}{j\omega 2\pi\epsilon_o K' L^2} \int_0^L \left(1 - \frac{2u}{L}\right) \int_0^{\infty} \left(e^{-a\gamma|z+u|} + e^{-a\gamma|z-u|}\right) J_o(\gamma\rho)\,\gamma\, d\gamma\, du \tag{2.7.11}$$

$$= \frac{-3a}{j\omega 2\pi\epsilon_o K' L^2} \int_0^L \left(1 - \frac{2u}{L}\right) \left[\frac{1}{\sqrt{\rho^2 + a^2(z+u)^2}} + \frac{1}{\sqrt{\rho^2 + a^2(z-u)^2}}\right] du \tag{2.7.12}$$

$$= \frac{-3}{j\omega 2\pi\epsilon_o K' L^2} \left[\left(1 + \frac{2z}{L}\right) \sinh^{-1} \frac{a(L+z)}{\rho} + \left(1 - \frac{2z}{L}\right) \sinh^{-1} \frac{a(L-z)}{\rho} - 4z \sinh^{-1} \frac{az}{\rho}\right.$$

$$\left. - 2\left(\sqrt{\frac{\rho^2}{a^2L^2} + \left(1 + \frac{z}{L}\right)^2} + \sqrt{\frac{\rho^2}{a^2L^2} + \left(1 - \frac{z}{L}\right)^2} - 2\sqrt{\frac{\rho^2}{a^2L^2} + \left(\frac{z}{L}\right)^2}\right)\right] \tag{2.7.13}$$

Note that the expression for E_z has no infinite discontinuities.

If the input current is unity and the antenna surface is designated by S, the input impedance is given by

$$Z_{in} = -\int_S \bar{J} \cdot \bar{E}\, ds \tag{2.7.14}$$

After the transformations $\frac{\rho}{aL} = t$ and $\frac{z}{L} = \eta$, the impedance integral for a monopole becomes

$$Z_{in} = \frac{3}{j\omega 2\pi\epsilon_o K' L} \int_o^1 (1-3\eta^2 + 2\eta^3) \left[(1+2\eta)\sinh^{-1}\frac{1+\eta}{t} + (1-2\eta)\sinh^{-1}\frac{1-\eta}{t} \right.$$

$$\left. - 4\eta \sinh^{-1}\frac{\eta}{t} - 2\left(\sqrt{t^2 + (1+\eta)^2} + \sqrt{t^2 + (1-\eta)^2} - 2\sqrt{t^2 + \eta^2} \right) \right] d\eta \tag{2.7.15}$$

The integral has been evaluated exactly but the final answer is quite involved. To simplify the expression, it is assumed that $|\rho/a|^2 \ll L^2$. Under this assumption the impedance is given by

$$Z_{in} = \frac{1.2}{j\omega 2\pi \epsilon_o K' L} \left(\ln \frac{aL}{\rho} - 1.375 \right) \qquad (2.7.16)$$

For a triangular current distribution the corresponding monopole impedance expression as derived previously is

$$Z_{in} = \frac{1}{j\omega 2\pi \epsilon_o K' L} \left(\ln \frac{aL}{\rho} - 1 \right) \qquad (2.7.17)$$

The two impedance expressions are identical in form and only slightly different in magnitude.

The $|E_z|$ at the ground plane of a monopole is plotted in the accompanying graph (Figure 2.7.1). The field of the smoothed current distribution has no infinite discontinuity but instead it has a discontinuous slope. Despite the difference in field magnitudes, the impedance expressions are nearly identical.

Given the field calculations for the triangular current, it would be tempting to conclude that the real part of the input impedance arises from some sort of energy storage in the vicinity of the characteristic cones along which the electric field becomes infinite. In fact, such a conslusion has been reached by Kaiser[6] in his work on the biconical dipole. However the smooth current assumption produces a finite field intensity yet gives an impedance expression almost identical to the one

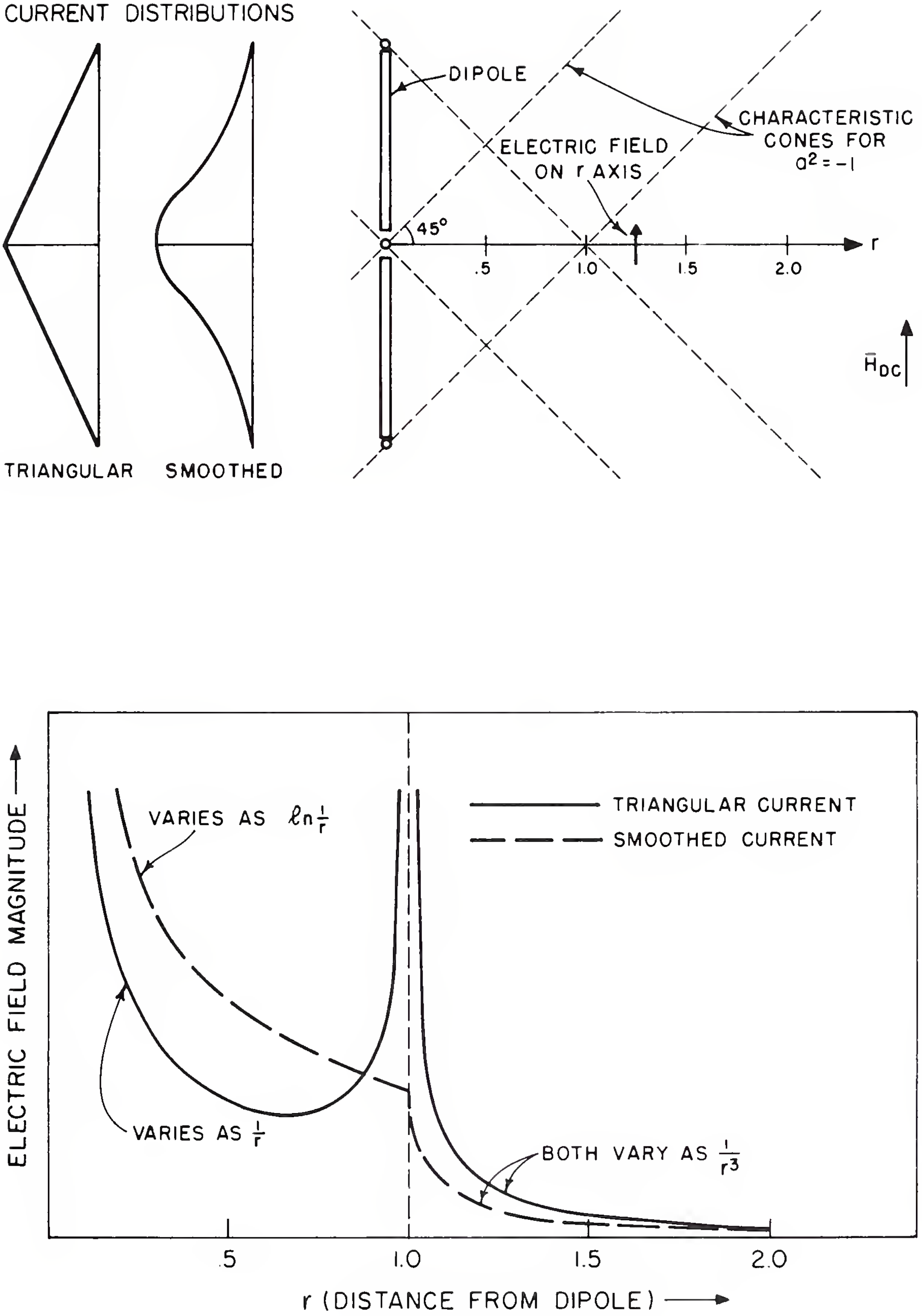

Figure 2.7.1 Electric field discontinuities for two current distributions

derived under the triangular current assumption. Thus the occurrence of field infinities is not necessary for the appearance of a real part in the input impedance. This conclusion clearly lends support to the radiation argument put forward in Section 2.4.

3. VALIDITY OF THE THEORETICAL MODEL

3.1 A first-Order Correction to the Quasi-Static Theory

It has been shown (Equation (2.1.39)) that the total electric field may be approximated at low frequencies by the quasi-static electric field plus a correction term:

$$\tilde{\bar{E}} = \frac{-j}{\omega\epsilon_o}\left[\frac{N_o}{a} + \frac{k_o^2}{a}\left(-\frac{bN_o}{a} + N_1\right)\right]\tilde{\bar{J}} \tag{3.1.1}$$

$$= \frac{j}{\omega\epsilon_o}\left[\frac{\bar{k}\,\bar{k}\cdot\tilde{\bar{J}}}{\bar{k}\cdot K\,\bar{k}} - \frac{k_o^2}{a}\left(\frac{b\,\bar{k}\,\bar{k}\cdot\tilde{\bar{J}}}{\bar{k}\cdot K\,\bar{k}} + N_1\,\tilde{\bar{J}}\right)\right] \tag{3.1.2}$$

in which

$$a = -\bar{k}^2\;\bar{k}\cdot K\,\bar{k}$$

$$b = (K'^2 - K''^2)\,(k_1^2 + k_2^2) + K'\,K_o\,(k_1^2 + k_2^2 + 2\,k_3^2)$$

The total low frequency electric field (Equation (3.1.2)) may be represented as the sum of the quasi-static field $\bar{E}^A$ and the correction term $\bar{E}^B$. Thus

$$\bar{E} = \bar{E}^A + \bar{E}^B \tag{3.1.3}$$

Using parallel notation, the low frequency input impedance may be represented by

$$Z_{in} = Z_{in}^A + Z_{in}^B \tag{3.1.4}$$

From Equation (3.1.2), the expression for $\bar{E}^B$ is

$$\tilde{\bar{E}}^B = \frac{-j\omega\mu_o}{a}\left(\frac{b\,\bar{k}\,\bar{k}\cdot\tilde{\bar{J}}}{\bar{k}\cdot K\,\bar{k}} + N_1\,\tilde{\bar{J}}\right) \tag{3.1.5}$$

The case to be considered in detail is that of finding the electric field E_z parallel to a current filament J_z. The z direction is considered in order to keep the computations as simple as possible. The electric field can be expressed as follows:

$$\tilde{E}_z^B = \frac{j\omega\mu_o}{\bar{k}^2\,\bar{k}\cdot K\,\bar{k}}\left\{\frac{\left[(K'^2 - K''^2)(k_1^2 + k_2^2) + K'K_o(k_1^2 + k_2^2 + 2\,k_3^2)\right]k_3^2}{\bar{k}\cdot K\,\bar{k}} + K'(k_1^2 + k_2^2 + 2k_3^2)\right\}\tilde{\bar{J}}_z \tag{3.1.6}$$

The expression can be simplified by a transformation to cylindrical coordinates:

$$k_1 = \gamma \cos\beta , \qquad k_1^2 + k_2^2 = \gamma^2 ,$$

$$k_2 = \gamma \sin\beta , \qquad \bar{k}^2 = \gamma^2 + k_3^2 . \tag{3.1.7}$$

Thus the electric field expression becomes

$$\tilde{E}_z^B = -j\omega\mu_o \left\{ \frac{K'^2 \ \gamma^2}{\left(K'\gamma^2 + K_o k_3^2\right)^2} + \frac{K''^2 \ \gamma^2 \ k_3^2}{\left(\gamma^2 + k_3^2\right)\left(K'\gamma^2 \ K_o k_3^2\right)^2} \right\} \tilde{J}_z \tag{3.1.8}$$

For a triangular current distribution, $\tilde{J}_z$ is given by

$$\tilde{J}_z = \frac{2 - e^{jk_3 L} - e^{-jk_3 L}}{k_3^2 \ L} = \int_o^L \left(1 - \frac{u}{L}\right) \left(e^{jk_3 u} + e^{-jk_3 u}\right) du \tag{3.1.9}$$

The electric field in space may be found by taking the Fourier transform of Equation (3.1.8). For convenience k is written in place of k_3.

$$E_z^B = \frac{1}{(2\pi)^2} \int_{\infty}^{\infty} \int_{o}^{\infty} \tilde{E}_z^B \, e^{jkz} \, J_o(\gamma\rho) \, \gamma \, d\gamma \, dk \tag{3.1.10}$$

$$= \frac{-j\omega\mu}{(2\pi)^2} \left[\left(\frac{K'}{K_o} \right)^2 I'(\rho, z) + \left(\frac{K''}{K_o} \right)^2 I''(\rho, z) \right] \tag{3.1.11}$$

where

$$I'(\rho, z) = K_o^2 \int_{-\infty}^{\infty} \int_{o}^{\infty} \int_{o}^{L} \left(1 - \frac{u}{L}\right) \frac{e^{jku} + e^{-jku}}{(K'\gamma^2 + K_o k^2)^2} \, e^{jkz} J_o(\gamma\rho) \, \gamma^3 \, du \, d\gamma \, dk \tag{3.1.12}$$

and

$$I''(\rho, z) = K_o^2 \int_{-\infty}^{\infty} \int_{o}^{\infty} \int_{o}^{L} \left(1 - \frac{u}{L}\right) \frac{k^2}{k^2 + \gamma^2} \cdot \frac{e^{jku} + e^{-jku}}{(K_o k^2 + K'\gamma^2)^2} \, e^{jkz} J_o(\gamma\rho) \gamma^3 \, du \, d\gamma \, dk \tag{3.1.13}$$

Introducing the anisotropy factor $a^2 = K'/K_o$, one may write the above two integrals as follows:

$$I'(\rho, z) = \int_0^L \left(1 - \frac{u}{L}\right) \int_0^\infty \int_{-\infty}^\infty \frac{e^{jk(z+u)} + e^{jk(z-u)}}{(k^2 + a^2\gamma^2)^2} J_o(\gamma\rho)\, \gamma^3 \, dk\, d\gamma\, du \qquad (3.1.14)$$

$$I''(\rho, z) = \int_0^L \left(1 - \frac{u}{L}\right) \int_0^\infty \int_{-\infty}^\infty \frac{k^2}{k^2+\gamma^2} \cdot \frac{e^{jk(z+u)} + e^{jk(z-u)}}{(k^2 + a^2\gamma^2)^2} J_o(\gamma\rho)\, \gamma^3 \, dk\, d\gamma\, du \qquad (3.1.15)$$

Integration with respect to k (using contour integration) gives

$$I'(\rho, z) = \frac{\pi}{2a^3} \int_0^L \left(1 - \frac{u}{L}\right) \int_0^\infty \left[\left[1 + a\gamma(z+u)\right] e^{-a\gamma(z+u)} + \left[1 + a\gamma|z-u|\right] e^{-a\gamma|z-u|} \right] J_o(\gamma\rho)\, d\gamma\, du \qquad (3.1.16)$$

$$I''(\rho, z) = \frac{\pi}{a^2-1} \int_0^L (1- \frac{u}{L}) \int_0^\infty \left[\!\left[\frac{1}{2a} \left\{ \left[\frac{a^2+1}{a^2+1} + a\gamma(z+u) \right] e^{-a\gamma(z+u)} + \left[\frac{a^2+1}{a^2-1} + a\gamma|z-u| \right] e^{-a\gamma|z-u|} \right\} \right.\right.$$

$$\left.\left. - \frac{1}{a^2-1} \left\{ e^{-\gamma(z+u)} + e^{-\gamma|z-u|} \right\} \right]\!\right] J_0(\gamma\rho)\, d\gamma\, du \qquad (3.1.17)$$

Rearranging the terms gives

$$I'(\rho, z) = \frac{\pi}{2a^2} \int_0^L (1- \frac{u}{L}) \int_0^\infty \left\{ \frac{1}{a} - \frac{\partial}{\partial a} \right\} \left\{ e^{-a\gamma(z+u)} + e^{-a\gamma|z-u|} \right\} J_0(\gamma\rho)\, d\gamma\, du \qquad (3.1.18)$$

$$I''(\rho, z) = \frac{\pi}{2(a^2-1)} \int_0^L (1- \frac{u}{L}) \int_0^\infty \left[\!\left[\left\{ \frac{a^2+1}{a(a^2-1)} - \frac{\partial}{\partial a} \right\} \left\{ e^{-a\gamma(z+u)} + e^{-a\gamma|z-u|} \right\} \right.\right.$$

$$\left.\left. - \frac{2}{a^2-1} \left\{ e^{-\gamma(z+u)} + e^{-\gamma|z-u|} \right\} \right]\!\right] J_0(\gamma\rho)\, d\gamma\, du \qquad (3.1.19)$$

After integration with respect to γ,

$$I'(\rho, z) = \frac{\pi}{2a^2}\left(\frac{1}{a} - \frac{\partial}{\partial a}\right)\int_0^L \left(1 - \frac{u}{L}\right)\left\{\frac{1}{\sqrt{\rho^2 + a^2(z+u)^2}} + \frac{\;}{\sqrt{\rho^2 + a^2\ (z-u)^2}}\right\} du \qquad (3.1.20)$$

$$I''(\rho, z) = \frac{\pi}{2(a^2-1)}\int_0^L \left(1 - \frac{u}{L}\right)\left[\!\left[\left\{\frac{(a^2+1)}{a(a^2-1)} - \frac{\partial}{\partial a}\right\}\left\{\frac{1}{\sqrt{\rho^2+a^2(z+u)^2}} + \frac{1}{\sqrt{\rho^2+a^2(z-u)^2}}\right\}\right.\right.$$

$$\left.\left. - \frac{2}{a^2-1}\left\{\frac{1}{\sqrt{\rho^2+(z+u)^2}} + \frac{1}{\sqrt{\rho^2+(z-u)^2}}\right\}\right]\!\right] du \qquad (3.1.21)$$

Recall that $E_z^B(\rho, z)$ is given by

$$E_z^B(\rho, z) = \frac{-j\omega\mu}{(2\pi)^2}\left[a^4\ I'(\rho, z) + b^4\ I''(\rho, z)\right] \qquad (3.1.22)$$

where

$$a^2 = \frac{K'}{K_o} \quad \text{and} \quad b^2 = \frac{K''}{K_o}$$

The corresponding contribution to the impedance of a short monopole is

$$Z_{in}^{B} = - \int_{0}^{L} (1 - \frac{z}{L}) \, E_{z}^{B} (\rho, z) \, dz \tag{3.1.23}$$

$$= \frac{+j\omega\mu}{(2\pi)^2} \cdot \frac{\pi}{2} \left[\left(C_1 - C_2 \frac{\partial}{\partial a} \right) \int_{0}^{L} (1 - \frac{z}{L}) \int_{0}^{L} (1 - \frac{u}{L}) \left[\frac{1}{\sqrt{\rho^2 + a^2 (z+u)^2}} + \frac{1}{\sqrt{\rho^2 + a^2 (z-u)^2}} \right] du \, dz \right.$$

$$\left. - C_3 \int_{0}^{L} (1 - \frac{z}{L}) \int_{0}^{L} (1 - \frac{u}{L}) \left[\frac{1}{\sqrt{\rho^2 + (z+u)^2}} + \frac{1}{\sqrt{\rho^2 (z-u)^2}} \right] du \, dz \right] \tag{3.1.24}$$

where $C_1 = a + \frac{b^4 (a^2+1)}{a(a^2-1)^2}$, $C_2 = a^2 + \frac{b^4}{a^2-1}$, $C_3 = \frac{2b^4}{(a^2-1)^2}$.

Note that the integrands are symmetric in u and z. Thus the impedance may be expressed as

$$Z_{in}^{B} = \frac{j\omega\mu}{(2\pi)^2} \circ \pi \left[\!\left[\left(C_1 - C_2 \frac{\partial}{\partial a}\right) \int_0^L \left(1 - \frac{z}{L}\right) \int_0^z \left(1 - \frac{u}{L}\right) \left[\frac{1}{\sqrt{\rho^2 + a^2 (z+u)^2}} + \frac{1}{\sqrt{\rho^2 + a^2 (z-u)^2}} \right] du\, dz \right.\right.$$

$$\left.\left. - C_3 \int_0^L \left(1 - \frac{z}{L}\right) \int_0^z \left(1 - \frac{u}{L}\right) \left[\frac{1}{\sqrt{\rho^2 + (z+u)^2}} + \frac{1}{\sqrt{\rho^2 + (z-u)^2}} \right] du\, dz \right]\!\right] \quad (3.1.25)$$

Integration with respect to u gives

$$Z_{in}^{B} = \frac{j\omega\mu}{4\pi} \left[\!\left[\left(C_1 - C_2 \frac{\partial}{\partial a}\right) \frac{1}{aL} \int_0^L \left(1 - \frac{z}{L}\right) \left[L \sinh^{-1} \frac{2az}{\rho} + z\left(\sinh^{-1} \frac{2az}{\rho} - 2 \sinh^{-1} \frac{az}{\rho}\right) \right.\right.\right.$$

$$\left. + 2\sqrt{\frac{\rho^2}{a^2} + z^2} - \sqrt{\frac{\rho^2}{a^2} + 4z^2} - \frac{\rho}{a} \right] dz$$

$$(3.1.26)$$

$$\left. - C_3 \circ \frac{1}{L} \int_0^L \left(1 - \frac{z}{L}\right) \left[L \sinh^{-1} \frac{2z}{\rho} + z\left(\sinh^{-1} \frac{2z}{\rho} - 2 \sinh^{-1} \frac{z}{\rho}\right) + 2\sqrt{\rho^2 + z^2} - \sqrt{\rho^2 + 4z^2} - \rho \right] dz \right]\!\right]$$

Now one can integrate with respect to z, take the derivative $\frac{\partial}{\partial a}$ and make the approximation $L \gg |\frac{\rho}{a}|$. Thus,

$$Z_{in}^{B} = \frac{j\omega\mu L}{4\pi}\left[\frac{C_1}{a}\left(\frac{1}{3}\ln\frac{aL}{\rho} + \ln 2 - \frac{11}{18}\right) + \frac{C_2}{a^2}\left(\frac{1}{3}\ln\frac{aL}{\rho} + \ln 2 - \frac{17}{18}\right) - C_3\left(\frac{1}{3}\ln\frac{L}{\rho} + \ln 2 - \frac{11}{18}\right)\right]$$

$$= \frac{j\omega\mu L}{4\pi}\left[\left(\frac{C_1}{a} + \frac{C_2}{a^2} - C_3\right)\left(\frac{1}{3}\ln\frac{L}{\rho} + \ln 2 - \frac{17}{18}\right) + \left(\frac{C_1}{a} + \frac{C_2}{a^2}\right)\frac{\ln a}{3} + \frac{1}{3}\left(\frac{C_1}{a} - C_3\right)\right] \quad (3.1.27)$$

With the help of the relation $K''^2 = (K'-K_o)(K'-1)$, it may be shown that

$$\frac{C_1}{a} = 1 + \frac{(K'-1)(K'+K_o)}{K'\ (K'-K_o)}, \quad \frac{C_2}{a^2} = 1 + \frac{K'-1}{K'}, \quad C_3 = \frac{2(K'-1)}{K'-K_o}. \quad (3.1.28)$$

from which

$$\frac{C_1}{a} + \frac{C_2}{a^2} - C_3 = 2, \quad \frac{C_1}{a} - C_3 = \frac{1}{K'}, \quad \frac{C_1}{a} + \frac{C_2}{a^2} = 2\left(1 + \frac{K'-1}{K'-K_o}\right). \quad (3.1.29)$$

Now the monopole impedance correction can be expressed as

$$Z_{in}^{B} = \frac{j\omega\mu L}{2\pi}\left[\frac{1}{3}\ln\frac{L}{\rho} + \ln 2 - \frac{17}{18} + \left(1 + \frac{K'-1}{K'-K_o}\right)\frac{\ln a}{3} + \frac{1}{6K'}\right]. \tag{3.1.30}$$

The quasi-static calculation gave

$$Z_{in}^{A} = \frac{1}{2\pi j\omega\epsilon_o LK'}\left[\ln\frac{L}{\rho} - 1 + \ln a\right] \tag{3.1.31}$$

Combining these,

$$Z_{in} \doteq Z_{in}^{A} + Z_{in}^{B}$$

$$= \frac{1}{2\pi}\cdot\frac{1}{j\omega\epsilon_o L}\left\{\frac{1}{K'}\left[\ln\frac{L}{\rho} - 1 + \ln a\right] - (2\pi)^2\left(\frac{L}{\lambda}\right)^2\left[\frac{1}{3}\ln\frac{L}{\rho} - .251\right.\right.$$

$$\left.\left. + \left(1 + \frac{K'-1}{K'-K_o}\right)\frac{\ln a}{3} + \frac{1}{6K'}\right]\right\} \tag{3.1.32}$$

where λ is the free-space wavelength.

When K', a, K_o are of the order of unity the ln $\frac{L}{\rho}$ terms dominate. Under these conditions, the quasi-static expression is accurate as long as $\frac{(2\pi)^2}{3}\left(\frac{L}{\lambda}\right)^2 \ll 1$. In other words, if L = .1λ, a correction of about 10% would be expected.

However at cyclotron resonance K' and "a" become very large, increasing the magnitude of Z_{in}^B compared to Z_{in}^A. Thus the quasi-static theory breaks down at cyclotron resonance unless the magnitudes of K' and "a" are kept low by collisional damping. As an example, consider the experimental monopole for which L = .04λ at 1.6 kmc. At $Y^2 = 1$ (cyclotron resonance), X = 1 and Z = .05, the magnitude of the correction term is 20% of the quasi-static impedance magnitude.

It is important to notice that the form of Z_{in}^B is almost identical to that of Z_{in}^A, showing that the correction term does not introduce any markedly different kind of impedance behaviour.

3.2 The Effect of Plasma Waves on Impedance

A given current distribution in a uniform, isotropic plasma generates both transverse electromagnetic waves and longitudinal plasma waves. Coupling between the two wave types occurs only in the presence of inhomogeneity or anisotropy and such coupling will not be considered here. The problem to be considered is that of a short, thin, cylindrical dipole with a triangular current distribution as shown in Figure 3.2.1. Since the electromagnetic and plasma fields are generated independently by a given current distribution (see Cohen,[13] Part I), their impedance contributions may be computed separately and added.

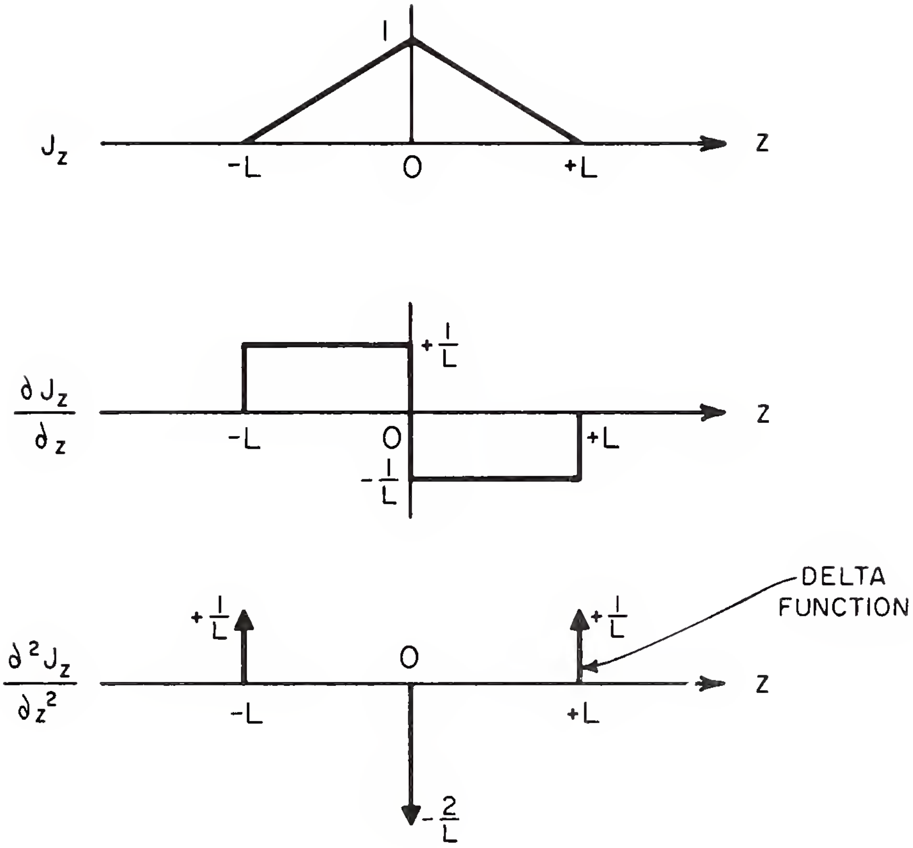
1
J_z
-L
0
+L
Z
$+\frac{1}{L}$
$\frac{\partial J_z}{\partial z}$
-L
0
+L
Z
$-\frac{1}{L}$
DELTA FUNCTION
$+\frac{1}{L}$
$+\frac{1}{L}$
$\frac{\partial^2 J_z}{\partial z^2}$
0
-L
+L
Z
$-\frac{2}{L}$

Figure 3.2.1 The source distribution

The electromagnetic problem has many well-known solutions but the plasma wave problem has received little attention. Hessel and Shmoys[19] have discussed the field problems of an infinitesimal dipole and a current distribution on a sphere. Whale[4] has calculated the radiation resistance of a short dipole and compared his calculations with the results of rocket experiments. Cohen[13] has discussed source problems in warm plasmas and has included a calculation of dipole radiation resistance. In the following paragraphs an impedance formula is derived for a cylindrical dipole; the formula is valid for a lossy medium and for any electron density.

The required differential equation can be obtained easily from the paper by Cohen[13] (Part I). If a time variation $e^{j\omega t}$ is assumed and if a collision frequency ν is introduced, Cohen's force Equation (2.6) becomes

$$j\omega\, Nm\, U\, \bar{v}_{\text{total}} = -\, Ne\, \bar{E}_{\text{total}} - m\, V^2 \nabla n \qquad (3.2.1)$$

where $V = \sqrt{\dfrac{\gamma kT}{m}}$

$\gamma = 3$
k = Boltzmann constant
T = electron temperature
m = electron mass (3.2.2)
N = average electron density
n = variation in electron density
e = magnitude of electron charge
$U = 1 - jZ = 1 - j\dfrac{\nu}{\omega}$
$\bar{v}$ = electron velocity.

Cohen's field equations can be derived for a lossy medium using the above force equation. Three of the lossy medium equations (equivalent to Cohen's Equations (3.10), (3.12) and (3.21) together with the continuity equation can be used to derive a differential equation for the plasma wave electric field $\overline{E}$ due to a source current $\overline{J}$.

$$\nabla^2 \overline{E} + \frac{U-X}{A} \overline{E} = \frac{1-K_o}{K_o} \cdot \frac{1}{j\omega\epsilon_o} \nabla \nabla \cdot \overline{J} \qquad (3.2.3)$$

where

$$A = \frac{V^2}{\omega^2}$$

$$X = \frac{\omega_N^{\;2}}{\omega^2}$$

$$\omega_N^{\;2} = \frac{Ne^2}{m\epsilon_o}$$

$$K_o = 1 - \frac{X}{U}$$

In order to carry out field and impedance calculations it is necessary to assume some current distribution $\overline{J}$. At 300°K, plasma waves have a very short wavelength (about one centimeter at ten megacycles). Since the wavelength may be comparable to a typical antenna radius, it is necessary to assume a cylindrical current distribution rather than a filamentary distribution. For a z-directed current cylinder of radius ρ, the differential equation for E_z is

$$\nabla^2 E_z - a^2 E_z = \frac{1 - K_o}{K_o} \cdot \frac{1}{j\omega\epsilon_o} \frac{\partial^2 J_z}{\partial z^2} \frac{\delta(r-\rho)}{2\pi\rho} \tag{3.2.4}$$

where

$$a^2 = -\frac{U-X}{A}$$

The longitudinal current distribution J_z is assumed to be triangular. The second derivative of a triangular current distribution is equivalent to the sum of three delta functions as shown in Figure 3.2.1.

The differential equation now can be expressed as

$$\nabla^2 E_z - a^2 E_z = \frac{1-K_o}{K_o} \cdot \frac{1}{j\omega\epsilon_o L} \left(\delta(z-L) + \delta(z+L) - 2\delta(z)\right) \frac{\delta(r-\rho)}{2\pi\rho} \tag{3.2.5}$$

The above equation can be solved using the transform pair

$$\tilde{f}(\gamma, k) = \int_{-\infty}^{\infty} \int_{0}^{\infty} f(r, z)\, e^{-jkz}\, J_o(\gamma r)\, dr\, dz \tag{3.2.6}$$

$$f(r,z) = \frac{1}{2\pi} \int_{-\infty}^{\infty} \int_{0}^{\infty} \tilde{f}(\gamma, k)\, e^{jkz} J_o(\gamma r)\, \gamma \, d\gamma \, dk \tag{3.2.7}$$

Transformation of the differential equation gives

$$-(k^2 + \gamma^2 + \alpha^2)\, \tilde{E}_z = \frac{1-K_o}{j\omega\epsilon_o K_o L} \left[e^{-jkL} + e^{jkL} - 2 \right] \frac{J_o(\gamma \rho)}{2\pi} \tag{3.2.8}$$

Now E_z can be expressed as an inverse transform.

$$E_z(rz) = \frac{K_o - 1}{j\omega\epsilon_o K_o L} \cdot \frac{1}{(2\pi)^2} \int_{-\infty}^{\infty} \int_{0}^{\infty} \frac{\left[e^{-jkL} + e^{jkL} - 2 \right]}{k^2 + \gamma^2 + \alpha^2} J_o(\gamma\rho)\, e^{jkz} J_o(\gamma r)\, \gamma \, d\gamma \, dk \tag{3.2.9}$$

If it is assumed that $\sqrt{\gamma^2 + \alpha^2}$ always has a positive real part, integration with respect to k gives

$$E_z(r,z) = \frac{K_o - 1}{j\omega 4\pi\epsilon_o K_o L} \int_{0}^{\infty} \frac{e^{-\sqrt{\gamma^2+\alpha^2}\,|z-L|} + e^{-\sqrt{\gamma^2+\alpha^2}\,(z+L)} - 2e^{-\sqrt{\gamma^2+\alpha^2}\, z}}{\sqrt{\gamma^2 + \alpha^2}} J_o(\gamma\rho)\, J_o(\gamma r)\, \gamma \, d\gamma \tag{3.2.10}$$

If one's interest is confined to impedance, one need calculate the field only at the antenna surface, that is at $r = \rho$. With the substitution

$$J_o^2(\gamma\rho) = \frac{2}{\pi}\int_0^{\pi/2} J_o(2\gamma\rho\cos\theta)\,d\theta, \qquad (3.2.11)$$

the field expression becomes

$$E_z(\rho, z) = \frac{K_o - 1}{j\omega 4\pi\epsilon_o K_o L}\cdot\frac{2}{\pi}\int_0^{\pi/2}\int_0^{\infty}\frac{e^{-\sqrt{\gamma^2+\alpha^2}\,|z-L|} + e^{-\sqrt{\gamma^2+\alpha^2}\,(z+L)} - 2e^{-\sqrt{\gamma^2+\alpha^2}\,z}}{\sqrt{\gamma^2+\alpha^2}}\,J_o(2\gamma\,\rho\cos\theta)\,\gamma\,d\gamma\,d\theta \qquad (3.2.12)$$

If it is assumed that α always has a positive real part, the integration with respect to γ can be carried out (it is a form of "Sommerfeld's integral").

$$E_z(\rho, z) = \frac{K_o - 1}{j\omega 4\pi\epsilon_o K_o L}\cdot\frac{2}{\pi}\int_0^{\pi/2}\left\{\frac{e^{-\alpha\sqrt{(z-L)^2+(2\rho\cos\theta)^2}}}{\sqrt{(z-L)^2+(2\rho\cos\theta)^2}} + \frac{e^{-\alpha\sqrt{(z+L)^2+(2\rho\cos\theta)^2}}}{\sqrt{(z+L)^2+(2\rho\cos\theta)^2}} - 2\frac{e^{-\alpha\sqrt{z^2+(2\rho\cos\theta)^2}}}{\sqrt{z^2+(2\rho\cos\theta)^2}}\right\}d\theta \qquad (3.2.13)$$

Integration with respect to θ will be delayed in order to simplify the impedance calculation.

The dipole impedance contribution due to the longitudinal plasma oscillations is twice the monopole impedance contribution. The latter may be expressed as

$$Z_{in}^{P} = -\int_{0}^{L} \left(1-\frac{z}{L}\right) E_z(\rho, z)\, dz$$

In order to express the impedance in terms of simple functions, use is made of the approximation $L^2 \gg \rho^2$. Integration with respect to z gives

$$Z_{in}^{P} = \frac{K_o - 1}{j\omega 2\pi\epsilon_o K_o L} \cdot \frac{2}{\pi} \int_{0}^{\pi/2} \left\{ \frac{1}{2\alpha L} \left[4e^{-\alpha L} - e^{-2\alpha L} - 3e^{-2\alpha\rho\cos\theta} \right] + K_o(2\alpha\rho\cos\theta) - 2E_1(\alpha L) + E_1(2\alpha L) \right\} d\theta \qquad (3.2.14)$$

where E_1 is one of the exponential integrals;

$$E_1(\alpha L) = \int_{L}^{\infty} \frac{e^{-\alpha u}}{u}\, du. \qquad (3.2.15)$$

In the derivation of Equation (3.2.14) the following integral expression for the function K_o has been used:

$$K_o(aq) = \int_q^\infty \frac{e^{-au}}{\sqrt{u^2-q^2}}\, du. \qquad (3.2.16)$$

Here it should be mentioned that the assumption of a current filament instead of a current cylinder would give the above impedance expression with the exceptions that there would be no θ integration and that $2\cos\theta$ would be replaced by unity.

Integration with respect to θ gives

$$Z_{in}^{P} = \frac{K_o - 1}{j\omega 2\pi\epsilon_o K_o L} \left\{ I_o(a\rho)\, K_o(a\rho) - 2E_1(aL) + E_1(2aL) \right.$$

$$\left. + \frac{1}{2aL}\left[4e^{-aL} - e^{-2aL} - 3I_o(2a\rho) + 3L_o(2a\rho)\right] \right\} \qquad (3.2.17)$$

where L_o is a modified Struve function. In practical cases aL is quite large but $a\rho$ may be fairly small. When $a\rho$ is small the term containing $K_o(a\rho)$ is dominant and it approaches infinity as $a\rho$ approaches zero. The large argument approximations for I_o and K_o are still useful when the argument is near unity and they give the very simple approximate result

$$Z_{in}^{P} = \frac{K_o - 1}{j\omega 2\pi\epsilon_o K_o L} \left\{ \frac{1}{2a\rho} \right\} \qquad (3.2.18)$$

Combining this with the quasi-static analysis gives

$$Z_{in} = \frac{1}{j\omega 2\pi\epsilon_o K_o L} \left\{ \ln \frac{L}{\rho} - 1 + \frac{(K_o - 1)}{2a\rho} \right\} \qquad (3.2.19)$$

From the above impedance formula, it is clear that plasma waves affect the impedance of a short monopole appreciably when $a\rho_o$ is approximately equal to unity. Taking $T = 300^oK$, we find that $V = 1.168 \times 10^5$ m/sec. In a lossless plasma

$$a = \sqrt{\frac{X-1}{A}} = \sqrt{X-1} \; \frac{\omega}{V} \qquad (3.2.20)$$

To take an example, $a\rho_o = 1.07$ when $X = 1.25$, $f = 4$ Mc. and $\rho_o = 1$ cm. Since these parameter values are representative for the maximum electron density in the F region of the ionosphere, it is clear that plasma oscillations cannot be ignored in impedance probe studies using rockets or satellites. In the laboratory experiment, however, the corresponding value of $a\rho$ would be of the order of 20. Thus it is unlikely that plasma oscillations would have a measurable effect on the impedance of the experimental monopole.

The above impedance formulation is quite general but is most convenient when the frequency is lower than the plasma frequency, that is when α is real (in the lossless case). For frequencies above the plasma frequency, α is imaginary so one can write $j\beta$ in place of α, taking care to ensure that a small loss in the medium gives $j\beta$ a positive real part. Now the input impedance contribution due to plasma oscillations can be written as

$$Z_{in}^{P} = \frac{K_o - 1}{j\omega 2\pi\epsilon_o K_o L} \cdot \frac{2}{\pi} \int_0^{\pi/2} \left\{ \frac{1}{j2\beta L} \left[4e^{-j\beta L} - e^{-j2\beta L} - 3e^{-j2\beta\rho\cos\theta} \right] \right.$$

$$- \frac{\pi}{2} \left[N_o(2\beta\rho\cos\theta) + j\, J_o(2\beta\rho\cos\theta) \right]$$

$$\left. -2 \left[Ci(\beta L) + j si(\beta L) \right] + \left[Ci(2\beta L) + j si(2\beta L) \right] \right\} d\theta \qquad (3.2.21)$$

Where the following formulas have been used:

$$-\frac{\pi}{2} N_o(q\beta) = \int_q^{\infty} \frac{\cos\beta u}{\sqrt{u^2 - q^2}}\, du, \qquad \frac{\pi}{2} J_o(q\beta) = \int_q^{\infty} \frac{\sin\beta u}{\sqrt{u^2 - q^2}}\, du$$

$$(3.2.22)$$

$$Ci(a\beta) = \int_a^{\infty} \frac{\cos\beta u}{u}\, du, \qquad -si(a\beta) = \int_a^{\infty} \frac{\sin\beta u}{u}\, du$$

Integration with respect to θ gives

$$Z_{in}^{P} = \frac{K_o - 1}{j\omega 2\pi\epsilon_o K_o L} \left\{ -\frac{\pi}{2}\left[J_o(\beta\rho)N_o(\beta\rho) + j\,J_o^2(\beta\rho)\right] - 2\left[\mathrm{Ci}(\beta L) + j\,\mathrm{si}(\beta L)\right] \right.$$

$$\left. + \left[\mathrm{Ci}(2\beta L) + j\,\mathrm{si}(2\beta L)\right] + \frac{1}{j2\beta L}\left[4e^{-j\beta L} - e^{-j2\beta L} - 3\,J_o(2\beta\rho) + 3j\,\underline{H}_o(2\beta\rho)\right]\right\} \quad (3.2.23)$$

where $\underline{H}_o$ is a Struve function.

For the case of a lossless medium, it is helpful to break up the impedance into its real and imaginary parts.

$$\mathrm{Re}\ Z_{in}^{P} = \frac{1 - K_o}{\omega 2\pi\epsilon_o K_o L} \left\{ \frac{\pi}{2} J_o^2(\beta\rho) + 2\,\mathrm{si}(\beta L) - \mathrm{si}(2\beta L) \right.$$

$$\left. + \frac{1}{2\beta L}\left[4\cos\beta L - \cos 2\beta L - 3\,J_o(2\beta\rho)\right]\right\} \quad (3.2.24)$$

$$\mathrm{Im}\ Z_{in}^{P} = \frac{1 - K_o}{\omega 2\pi\epsilon_o K_o L} \left\{ -\frac{\pi}{2} J_o(\beta\rho)\,N_o(\beta\rho) - 2\mathrm{Ci}(\beta L) + \mathrm{Ci}(2\beta L) \right.$$

$$\left. + \frac{1}{2\beta L}\left[-4\sin\beta L + \sin 2\beta L + 3\,\underline{H}_o(2\beta\rho)\right]\right\} \quad (3.2.25)$$

It should be noted that $\mathrm{Re}\ Z_{in}^{P}$ is the radiation resistance associated with the radiation of plasma waves from the antenna.

In most cases of interest $\beta\rho$ is fairly small while βL is quite large, making the terms containing $J_o^2(\beta\rho)$ and $J_o(\beta\rho)$ dominant in the above two formulas. If $\beta\rho$ is no smaller than unity, the Bessel functions can be replaced by their large argument approximations. Thus

$$\mathrm{Re}\, Z_{in}^{P} \approx \frac{1-K_o}{\omega 2\pi\epsilon_o K_o L} \cdot \frac{1+\sin 2\beta\rho}{2\beta\rho} \tag{3.2.26}$$

$$\mathrm{Im}\, Z_{in}^{P} \approx \frac{1-K_o}{\omega 2\pi\epsilon_o K_o L} \cdot \frac{\cos 2\beta\rho}{2\beta\rho} \tag{3.2.27}$$

Combining the above with the quasi-static impedance, one obtains the approximate formula

$$Z_{in} = \frac{1}{j\omega 2\pi\epsilon_o K_o L}\left\{\ln\frac{L}{\rho} - 1 + \frac{K_o-1}{2\beta\rho}\left[\cos 2\beta\rho - j(1+\sin 2\beta\rho)\right]\right\} \tag{3.2.28}$$

The preceding discussion of impedance is based on the assumption of a triangular current distribution on an antenna which is short compared to a free space wavelength. This assumption may break down, however, at the plasma frequency under near-lossless conditions. Furthermore, at high frequencies Landau damping may affect the impedance.

3.3 The Effect of a Non-Uniform Electron Density

The introduction of some surface or boundary into a plasma results in the diffusive flow of the charged particles toward the surface. Close to the surface, free diffusion predominates and an ion sheath forms. Farther away, ambipolar diffusion predominates; the electron and ion densities are nearly equal but both decrease as the point of observation approaches the surface. Since the theory in this report assumes a uniform medium with no space charge, experimental verification of the theory must depend on minimizing diffusion and on understanding its effect on antenna impedance.

The effect of non-uniform electron density on impedance can be estimated by calculating the impedance per unit area between two parallel conducting plates separated by unit distance. The space between the plates contains isotropic plasma having an electron density distribution as shown in Figure 3.3.1. The input impedance per unit area is given by

$$Z_{in} = \frac{1}{j\omega\epsilon_o} \int_0^1 \frac{1}{K_o(\gamma)} \, d\gamma \qquad (3.3.1)$$

$$= \frac{1}{j\omega\epsilon_o} \int_0^1 \frac{1}{1 - \frac{X(\gamma)}{U}} \, d\gamma \qquad \text{where } U = 1 - jZ$$

$$= \frac{U}{j\omega\epsilon_o} \left[\int_0^\beta \frac{1}{U - X_o\left(\frac{1-a}{\beta} \gamma + a\right)} \, d\gamma + \frac{1-\beta}{U - X_o} \right]$$

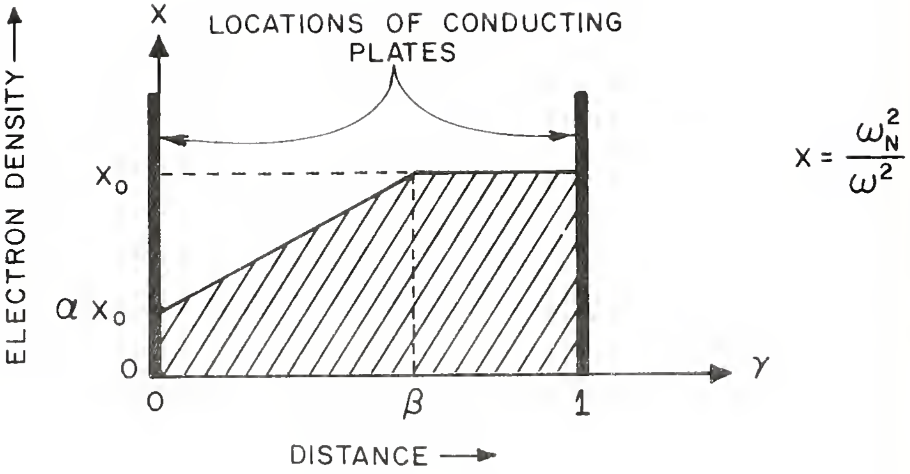
X
LOCATIONS OF CONDUCTING PLATES
ELECTRON DENSITY
X_0
αX_0
0
0
β
1
γ
DISTANCE
$X = \frac{\omega_N^2}{\omega^2}$

Figure 3.3.1 The assumed electron density distribution between two parallel conducting plates

$$= \frac{U}{j\omega\epsilon_o}\left[\frac{\beta}{(1-\alpha)\,X_o}\,\ln\frac{U-\alpha X_o}{U-X_o} + \frac{1-\beta}{U-X_o}\right] \qquad (3.3.2)$$

The results of some numerical calculations using Equation (3.3.2) are shown in Figures 3.3.2 and 3.3.3. The impedances are normalized to give a free space reactance of 5 ohms. An examination of all the curves (especially curve E) reveals that the losses in the plasma are increased considerably whenever some part of the medium is in plasma resonance. Note that curves C and F are nearly identical despite the ratio of two between their respective collision frequencies; apparently under such circumstances the electron density distribution has a greater influence on energy loss than the collision frequency. Furthermore it is evident that the effects on non-uniformity cannot be calculated from a density distribution made up of finite "steps"; only a continuous distribution will give the enhanced energy loss discussed above.

Curve E of Figure 3.3.3 exhibits an indentation for $1<X_o<2$. The similarity of this indentation to the kinks in the theoretical curves of Section 4.2 (at low values of Y^2) suggests that it may be difficult in practice to distinguish between the effects of non-uniformity and the effects of anisotropy. However, it is estimated that the conditions of curve F may be closer to the experimental conditions than those of curve E. This conclusion arises from the estimate that in the vicinity of the R.F. probe the average electron density is about four times the minimum density (see Section 4.1). Thus the ratio of maximum to minimum electron density

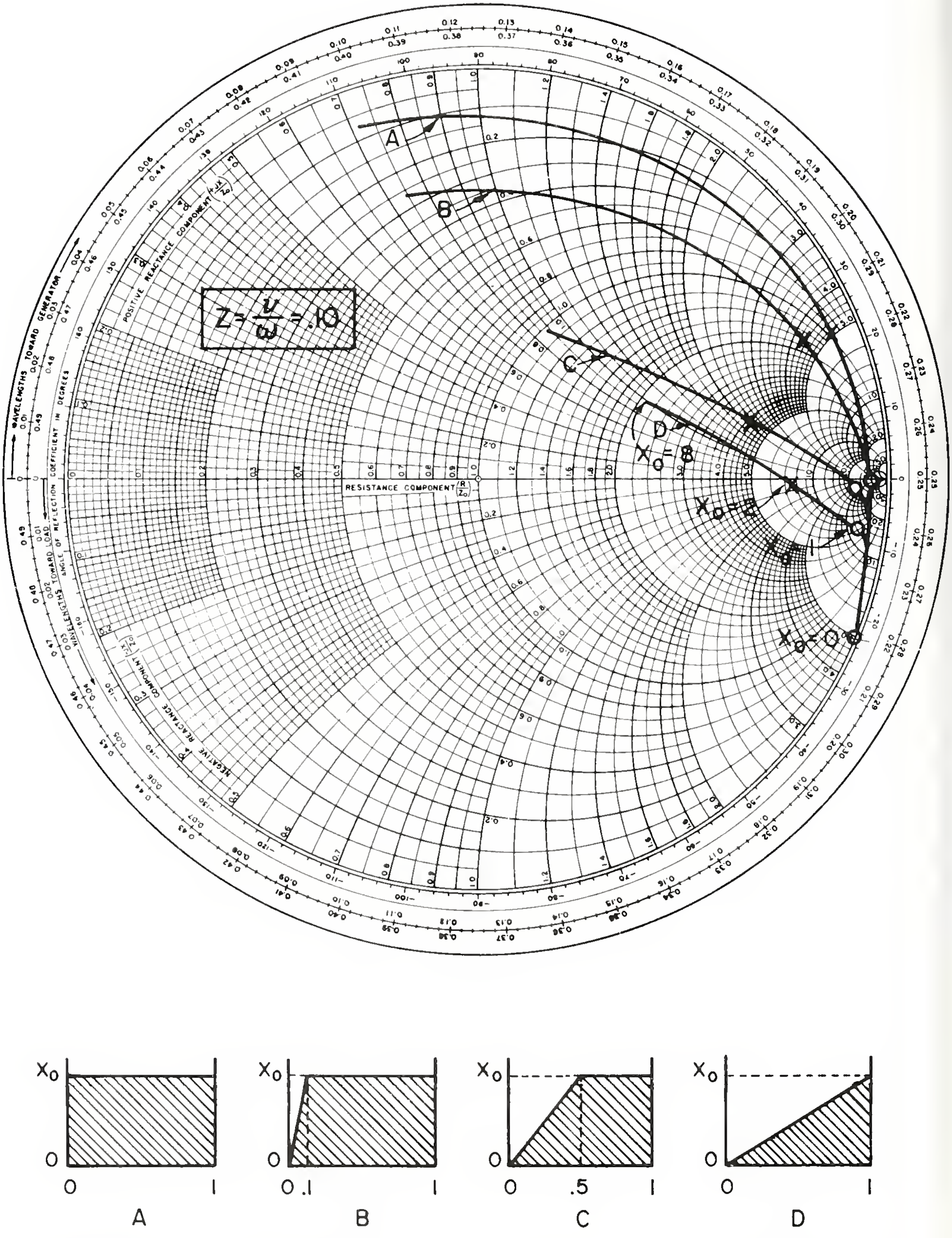

Figure 3.3.2 The impedance of a non-uniform, isotropic plasma between parallel plates as a function of peak electron density. Collision parameter: Z=.10

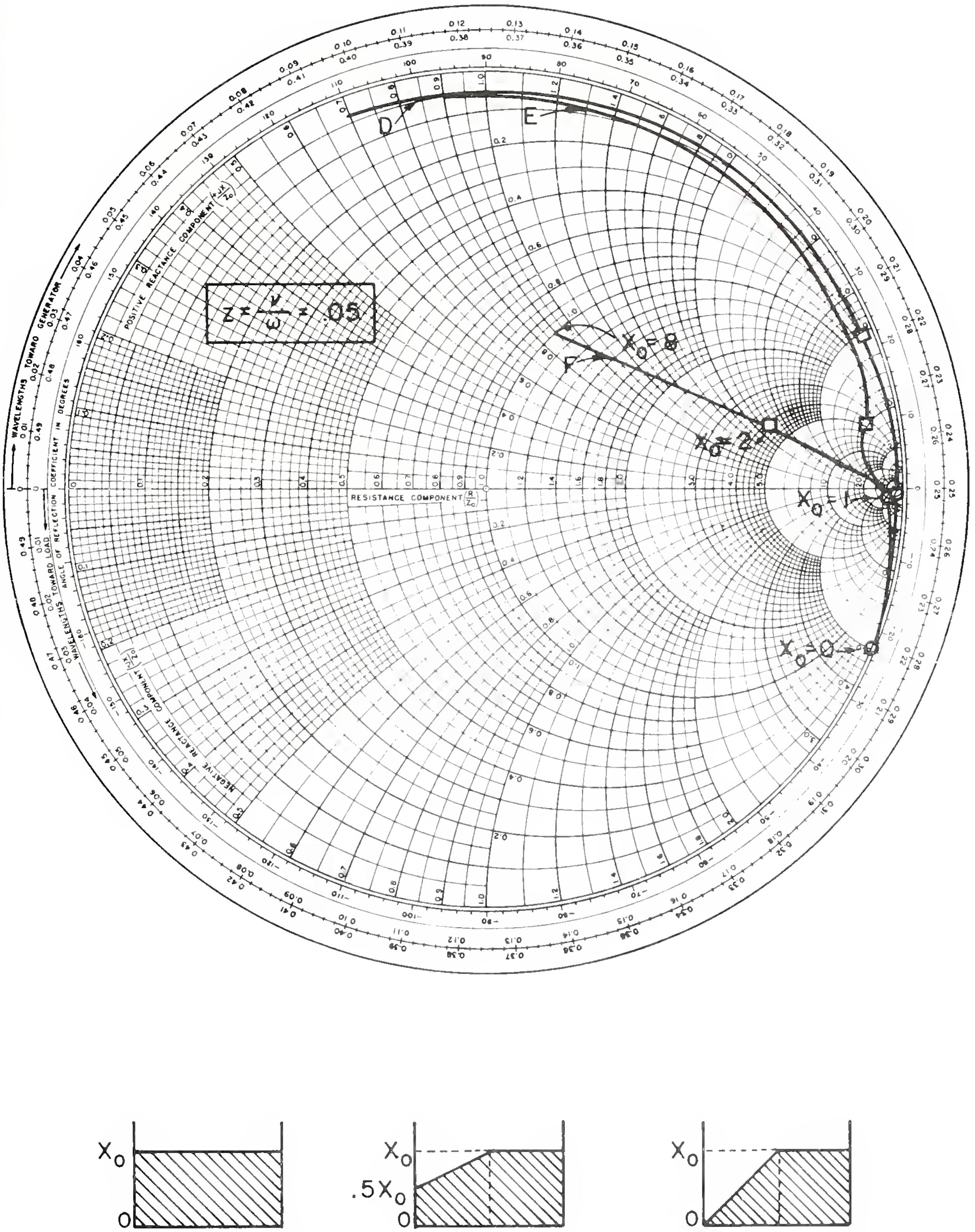

Figure 3.3.3 The impedance of a non-uniform, isotropic plasma between parallel plates as a function of peak electrondensity. Collision parameter: Z=.05

may be as high as eight. Under such conditions the impedance curve would have a very gradual indentation and would be similar to curve F. A further point is this; the experimentally observed kinks first appear for $Y^2 \geqslant .50$. For $.50 \geqslant Y^2 \geqslant .10$ the experimental curves are fairly smooth. For $.10 \geqslant Y^2 \geqslant 0$ some indentation was observed and presumably it was caused by non-uniformity. It is therefore suggested that non-uniformity in the experimental results of Section 4.2 is more likely to move the entire impedance locus toward the real axis than to cause local distortions which may be confused with anisotropic effects.

The ion sheath over a conducting surface is a type of non-uniformity which can be expanded or collapsed by the application of bias with respect to a reference electrode. When the sheath is collapsed, the plasma is essentially uniform in the region adjacent to the surface. Bias controls the sheath thickness by influencing the state of equilibrium between the electron and ion currents flowing to the surface. Consequently the surface under consideration (and also the reference electrode) must not be covered with an insulating layer. Since a state of sheath collapse is easy to achieve, it is not necessary to discuss the theory of sheath formation further in this report.

In a decaying, inactive laboratory plasma, the electron density distribution at time t_1 is a function of the deionization processes for all time before t_1 (going back to t_o, the time when the discharge was initiated). The two principal deionization processes are volume recombination and diffusion to surfaces. Recombination, being a volume process, tends to make the electron density uniform but diffusion has the opposite tendency. The experimental plasma (see Chapter 4) is initiated at t_o by a 2μs DC pulse. In the first 50 to 100μs, diffusion is dominant due to the high electron temperature. There follows a period of dominant recombination resulting from the existence of high electron and ion densities. As these densities decrease, diffusion again takes over. From the foregoing discussion it is clear that the electron density distribution around the experimental antenna will be a very complicated function of all the events in the plasma between t_o and t_1.

Measurement of the electron density distribution is difficult because any probe system disturbs the plasma around it. Because of such difficulties in measurement the best approach to the non-uniformity problem is to try to minimize diffusion. This can be accomplished by choosing a gas with a high recombination coefficient and a low diffusion coefficient (such as neon), and by using it at as high a pressure as possible. Although the choice of gas is important, the introduction of a magnetic field parallel to the diffusing surface is probably the best way to reduce diffusion, provided that the experiment can be carried out in the presence of the magnetic field.

4. LABORATORY MEASUREMENT OF MONOPOLE IMPEDANCE

4.1 Experimental Apparatus and Measurement Technique

The apparatus is designed to produce a pulsed DC discharge in neon or helium at a pressure of 1 to 10 mm. Hg. The experiments are carried out during the plasma decay period (afterglow) following each discharge pulse. The "resonance probe"[20] method is used to measure electron density and slotted-line techniques are used to measure the impedance of the monopole RF probe immersed in the plasma.

Figure 4.1.1 is a schematic drawing of the vacuum system. Pump-down procedure consists of pumping first to about 20 microns (2×10^{-2} mm) with the mechanical pump and then pumping to about 10^{-6} mm with the diffusion pump. This procedure may take from a few hours to a few days depending on the amount of contamination in the system. The application of a spark coil to the glass parts of the system speeds up the outgassing of the glass surfaces. Pump-down is followed by sealing of the system and back-filling with the required pressure of neon or helium. Operation of the discharge for a few hours completes the decontamination of the discharge tube interior. After the pump-down and back-fill procedures have been carried out again, the equipment is ready for impedance measurement experiments.

Figure 4.1.2 is a diagram of the pulse and RF system used in the experiment. The continuous discharge at the cathode end of the discharge tube assures dependable starting of the pulsed high-voltage discharge. The 2μs. discharge pulse is followed by the plasma decay which lasts for several

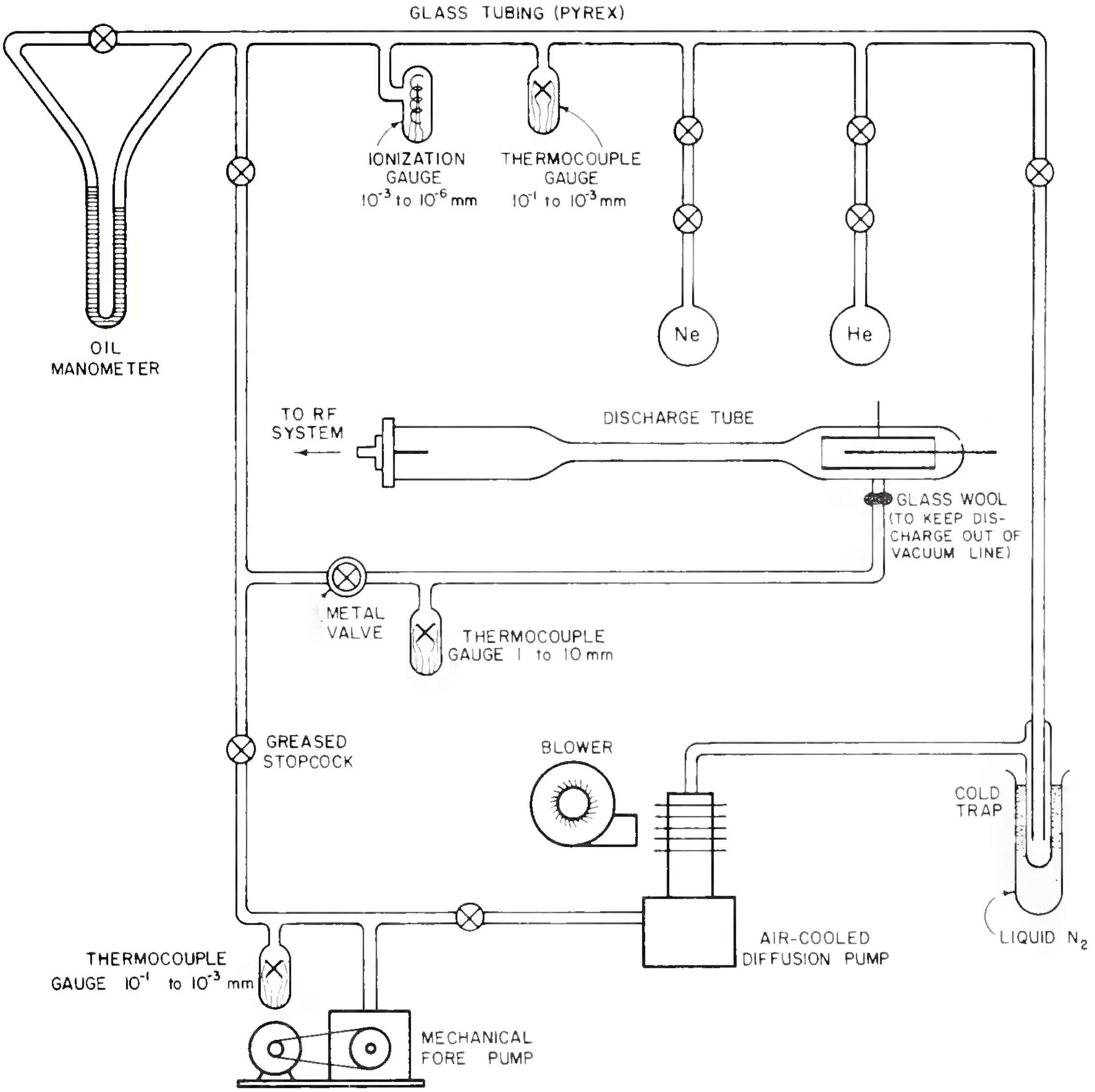
GLASS TUBING (PYREX)
OIL MANOMETER
IONIZATION GAUGE 10^{-3} to 10^{-6} mm
THERMOCOUPLE GAUGE 10^{-1} to 10^{-3} mm
Ne
He
TO RF SYSTEM
DISCHARGE TUBE
GLASS WOOL (TO KEEP DISCHARGE OUT OF VACUUM LINE)
METAL VALVE
THERMOCOUPLE GAUGE 1 to 10 mm
GREASED STOPCOCK
BLOWER
COLD TRAP
LIQUID N_2
AIR-COOLED DIFFUSION PUMP
THERMOCOUPLE GAUGE 10^{-1} to 10^{-3} mm
MECHANICAL FORE PUMP

Figure 4.1.1 The vacuum system

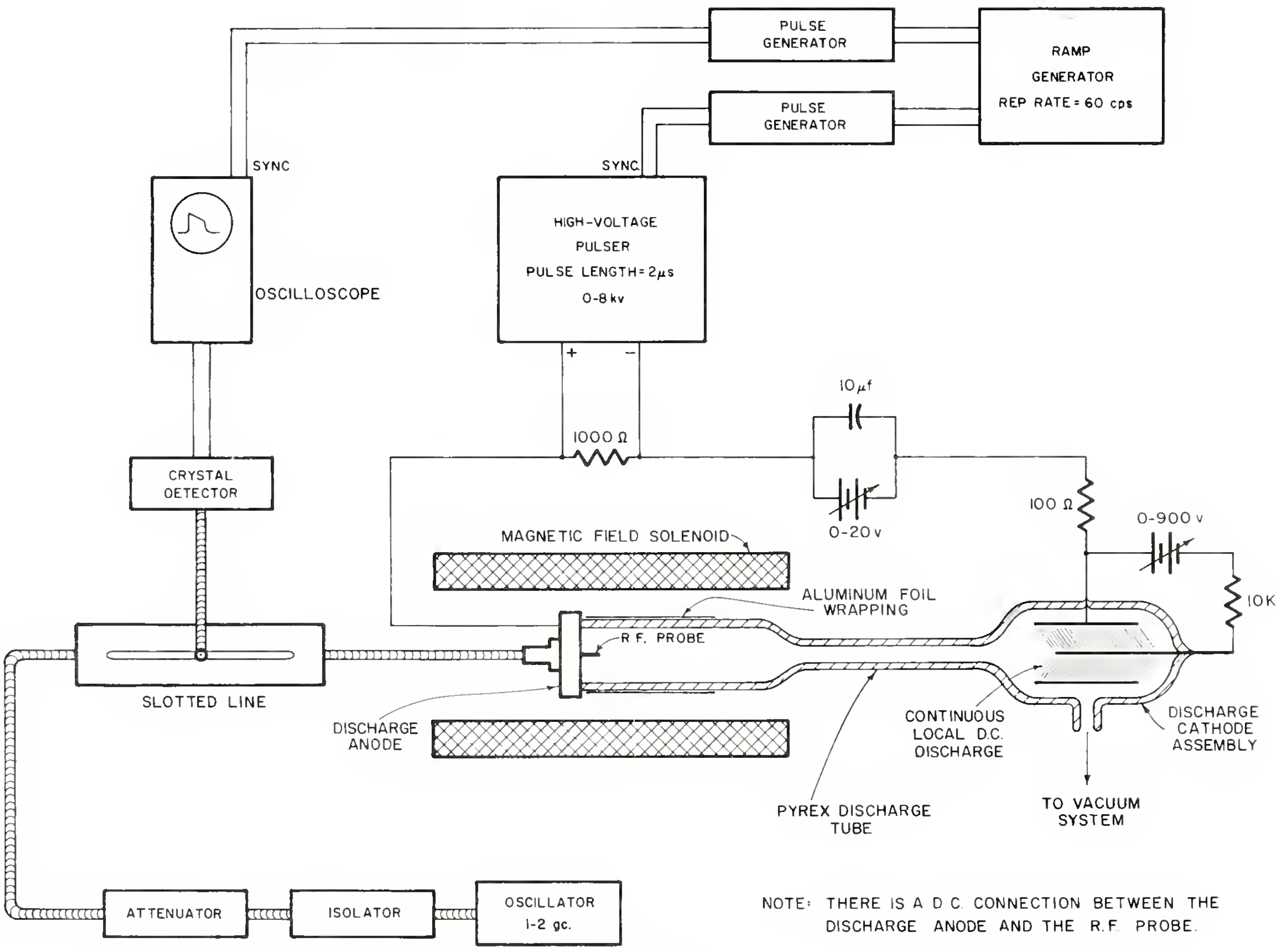
PULSE GENERATOR
RAMP GENERATOR
REP RATE = 60 cps
PULSE GENERATOR
SYNC
SYNC
HIGH-VOLTAGE PULSER
PULSE LENGTH = 2μs
0-8 kv
OSCILLOSCOPE
+
−
10μf
1000 Ω
CRYSTAL DETECTOR
100 Ω
0-20 v
0-900 v
MAGNETIC FIELD SOLENOID
ALUMINUM FOIL WRAPPING
10K
R.F. PROBE
SLOTTED LINE
DISCHARGE ANODE
CONTINUOUS LOCAL D.C. DISCHARGE
DISCHARGE CATHODE ASSEMBLY
PYREX DISCHARGE TUBE
TO VACUUM SYSTEM
ATTENUATOR
ISOLATOR
OSCILLATOR
1-2 gc.

NOTE: THERE IS A D.C. CONNECTION BETWEEN THE DISCHARGE ANODE AND THE R.F. PROBE.

Figure 4.1.2 The experimental apparatus

milliseconds. In this experiment the first one or two milliseconds of the decay are displayed on the oscilloscope.

Figures 4.1.3 and 4.1.4 show the details of the discharge tube and RF probe assembly. The coaxial line up to the RF probe is designed to minimize reflections. Both the RF probe (monopole antenna) and a flush probe (not shown but mounted flush with the surface of the brass end cap adjacent to the RF probe) are used as resonance probes to measure electron density. The electron density given by the monopole resonance probe measurement is an average density for the immediate vicinity of the monopole; the electron density given by the flush resonance probe has a much lower value and indicates the degree of plasma non-uniformity resulting from diffusion to the brass end cap. In a typical experiment the electron density adjacent to the end cap was found to be one-quarter the average electron density along the RF probe.

The method of impedance measurement is illustrated in Figure 4.1.5. The slotted line probe is positioned at four points spaced $\frac{1}{8}$ wavelength along the line. At each position a photograph of probe voltage vs. time is taken. Measurements taken from the photographs are used to plot the impedance as indicated. This method is usually referred to as the "four probe" method and is discussed in detail in the book by Ginzton[21] (page 310).

A typical set of probe voltage photographs is shown in Figure 4.1.6a and Figure 4.1.6b. The experimental conditions are as follows:

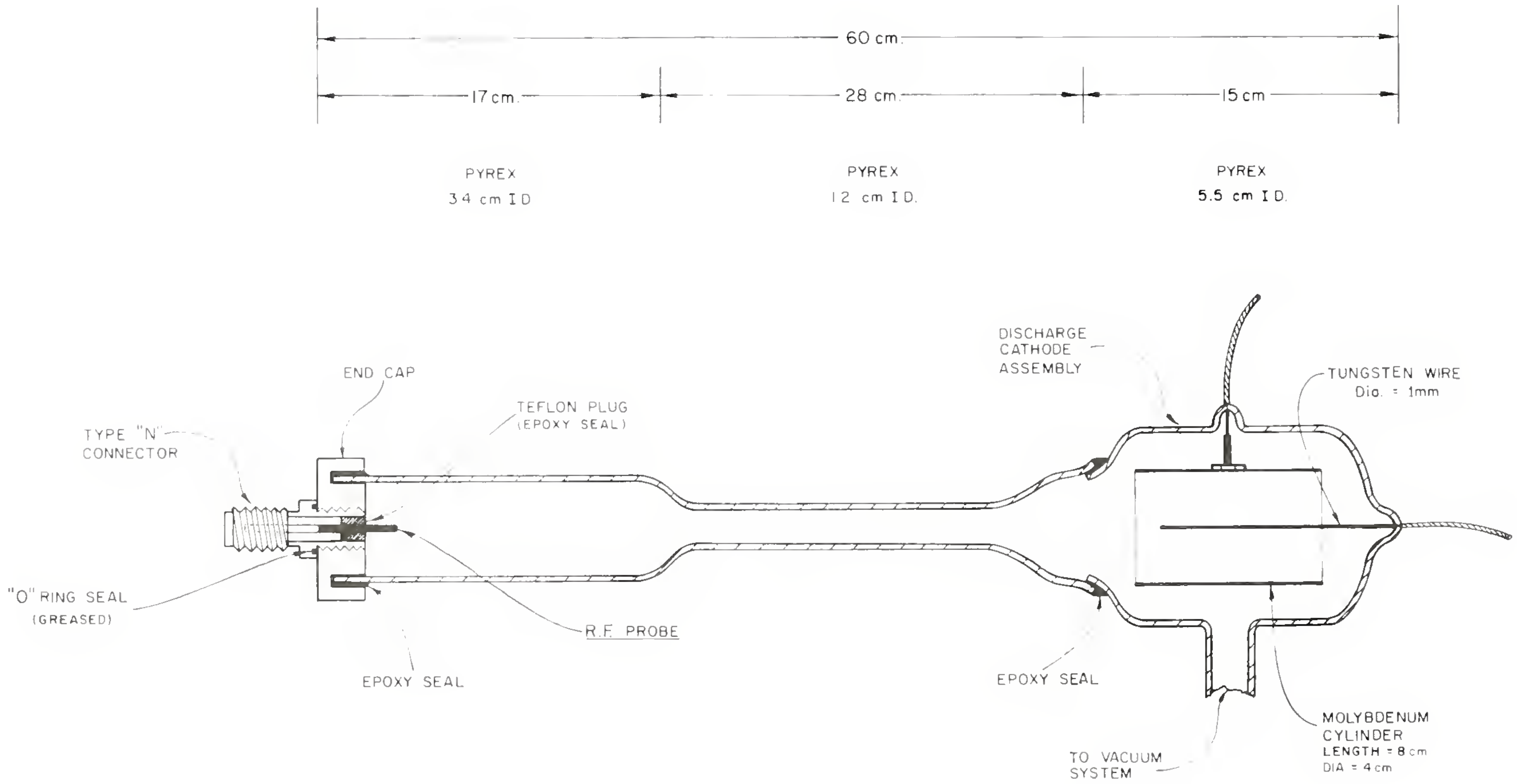
60 cm.
17 cm.
28 cm.
15 cm
PYREX
34 cm ID
PYREX
12 cm I D.
PYREX
5.5 cm I D.
END CAP
TYPE "N"
CONNECTOR
TEFLON PLUG
(EPOXY SEAL)
"O" RING SEAL
(GREASED)
R.F. PROBE
EPOXY SEAL
DISCHARGE
CATHODE
ASSEMBLY
TUNGSTEN WIRE
Dia. = 1mm
EPOXY SEAL
TO VACUUM
SYSTEM
MOLYBDENUM
CYLINDER
LENGTH = 8 cm
DIA = 4 cm

Figure 4.1.3 The discharge tube and RF probe

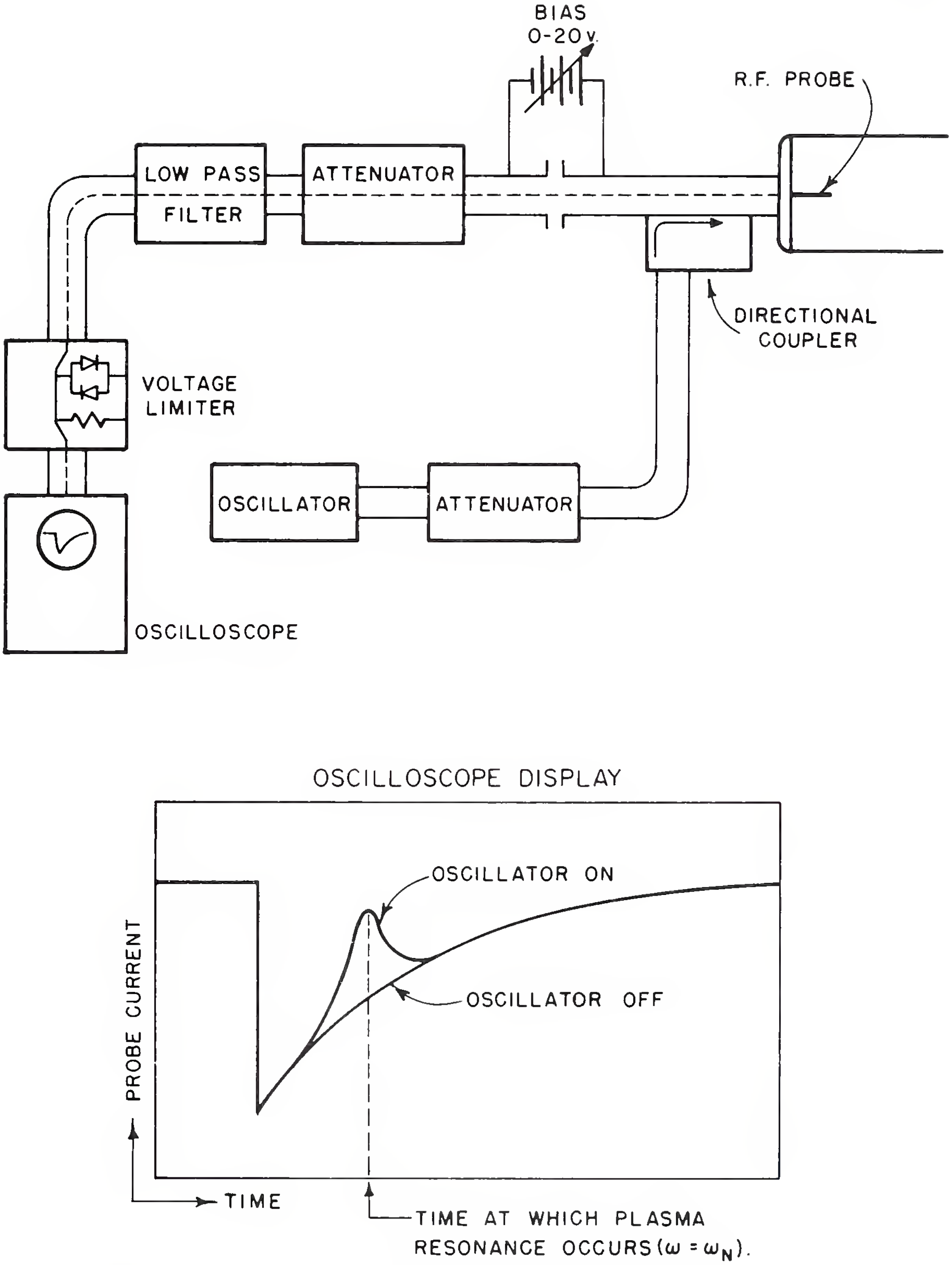
BIAS
0-20 v.
R.F. PROBE
LOW PASS
FILTER
ATTENUATOR
DIRECTIONAL
COUPLER
VOLTAGE
LIMITER
OSCILLATOR
ATTENUATOR
OSCILLOSCOPE
OSCILLOSCOPE DISPLAY
OSCILLATOR ON
OSCILLATOR OFF
PROBE CURRENT
TIME
TIME AT WHICH PLASMA
RESONANCE OCCURS ($\omega = \omega_N$).

NOTE:
THE FORMULA $\omega_N^2 = \frac{Ne^2}{m\epsilon_0}$ GIVES ELECTRON DENSITY N.

Figure 4.1.4 Determination of electron density by the "Resonance Probe" technique

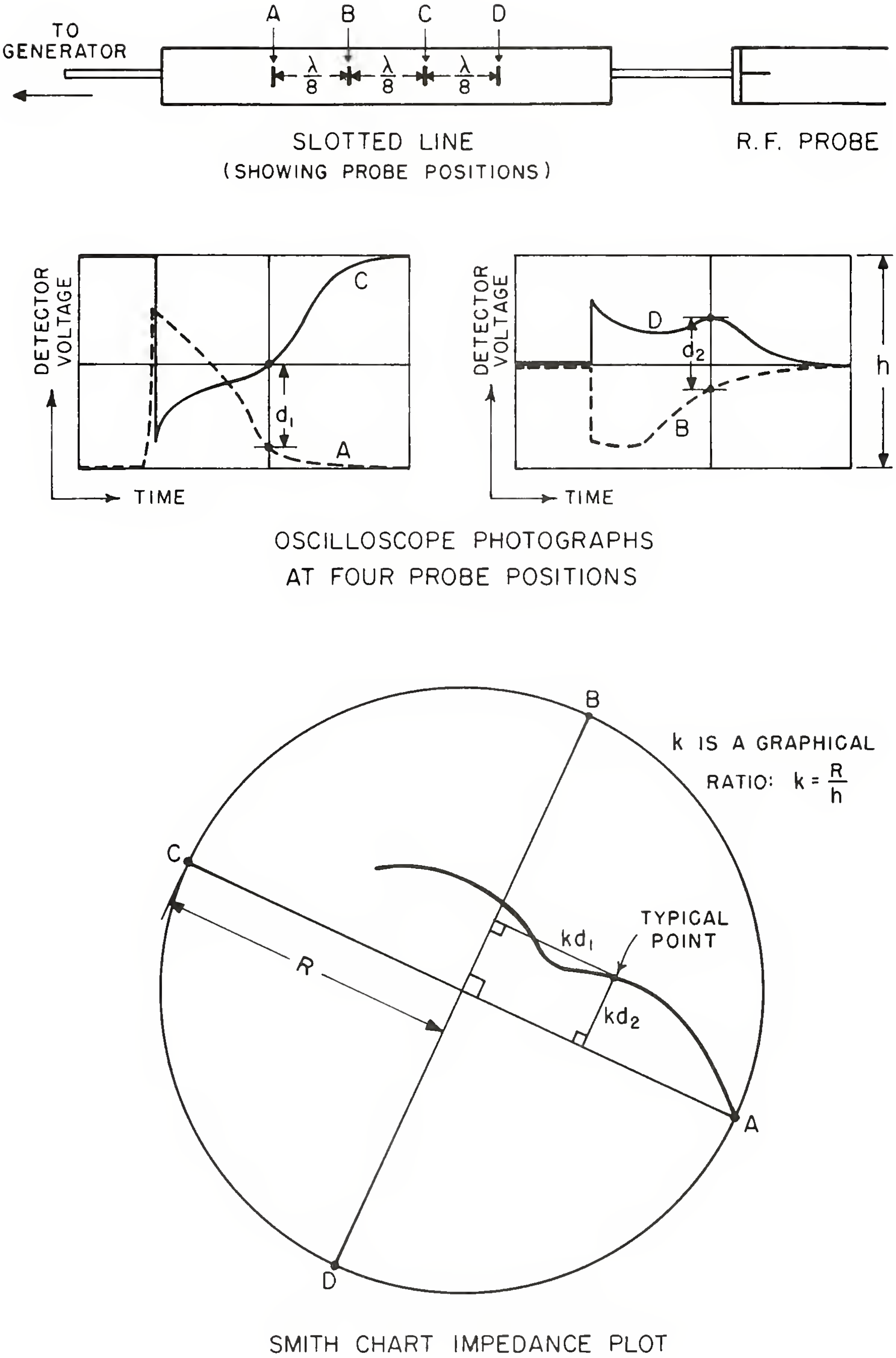
TO
GENERATOR
A
B
C
D
$\frac{\lambda}{8}$
$\frac{\lambda}{8}$
$\frac{\lambda}{8}$
SLOTTED LINE
(SHOWING PROBE POSITIONS)
R.F. PROBE
DETECTOR VOLTAGE
TIME
C
A
d_1
DETECTOR VOLTAGE
TIME
D
B
d_2
h
OSCILLOSCOPE PHOTOGRAPHS
AT FOUR PROBE POSITIONS
B
k IS A GRAPHICAL
RATIO: $k = \frac{R}{h}$
C
R
kd_1
TYPICAL
POINT
kd_2
A
D
SMITH CHART IMPEDANCE PLOT

Figure 4.1.5 Method of plotting an impedance locus using a square-law detector

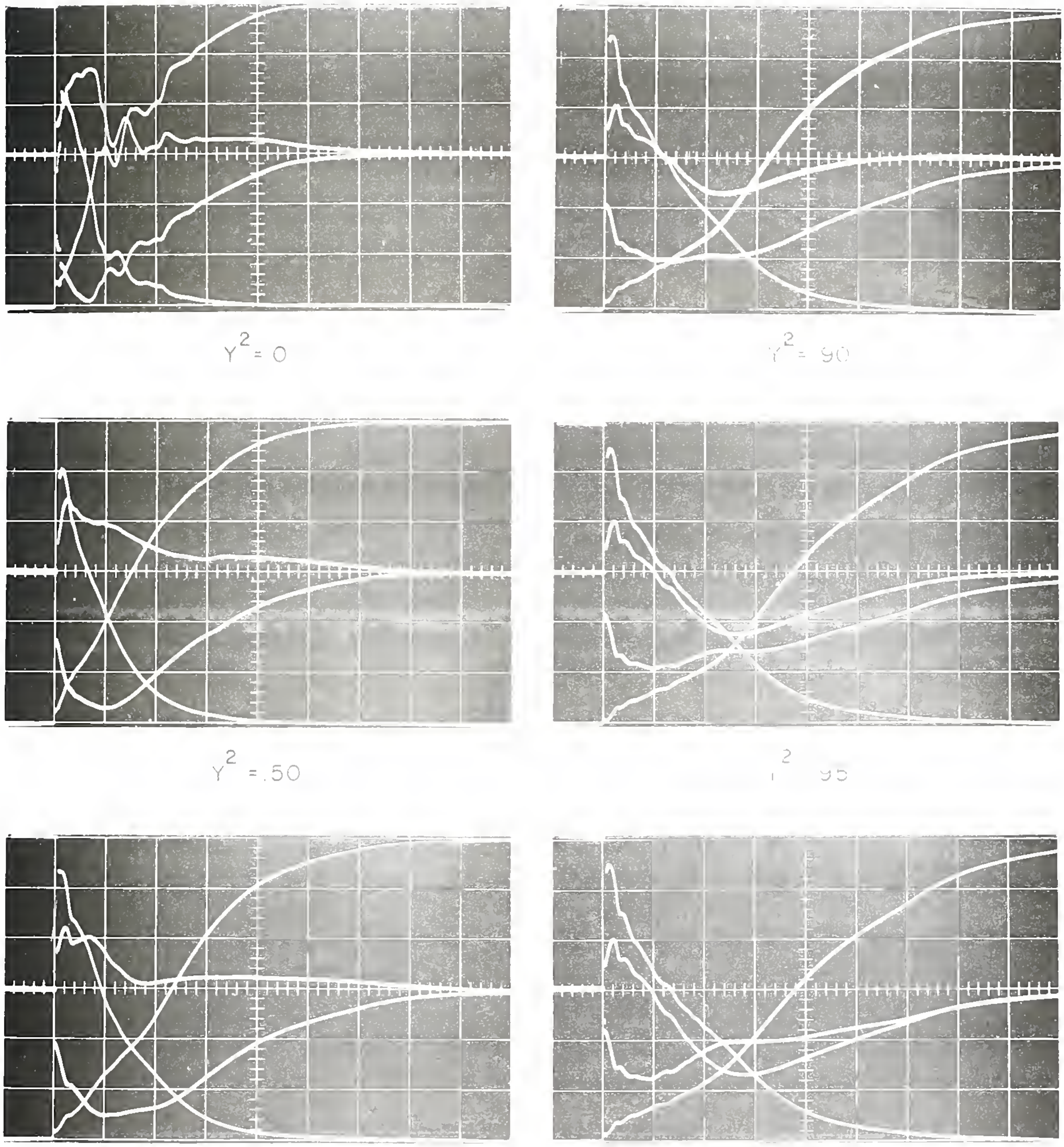

$Y^2 = 0$

$Y^2 = .90$

$Y^2 = .50$

$Y^2 = .95$

$Y^2 = .75$

$Y^2 = 1.0$

Figure 4.1.6a Slotted line voltage as a function of time. (Neon at 4.3 mm. pressure. Time scale: 320 μs/cm.)

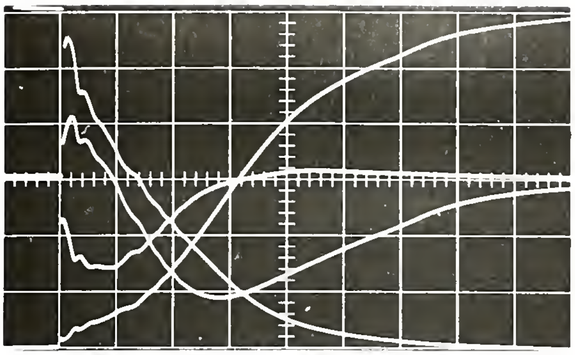

$Y^2 = 1.05$

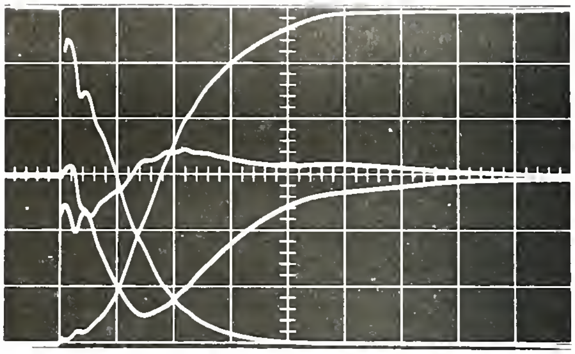

$Y^2 = 1.50$

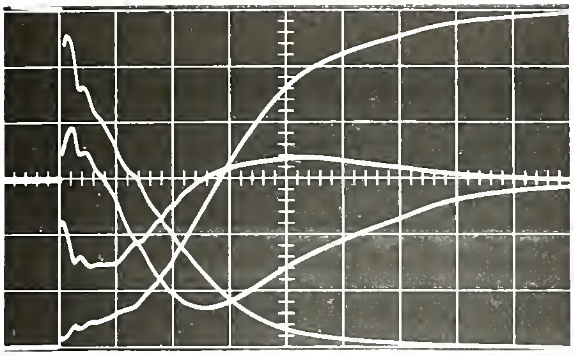

$Y^2 = 1.10$

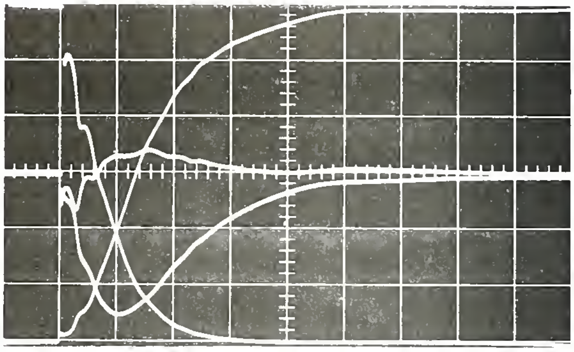

$Y^2 = 2{,}00$

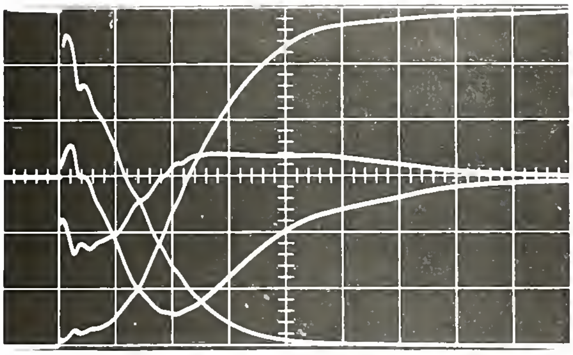

$Y^2 = 1.25$

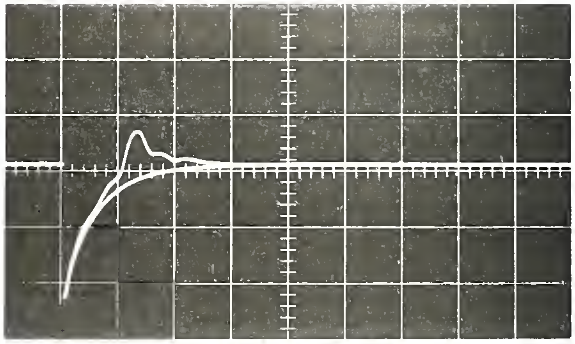

RESONANCE PROBE CURRENT

Figure 4.1.6b Slotted line voltage as a function of time. (Neon at 4.3 mm. pressure. Time scale: 320 μs/cm.)

Gas: Neon*

Pressure: 4.3 mm Hg.*

Frequency: 1.6 Gc.

Bias: 18 volts

Oscilloscope horizontal scale: 320μs./cm.*
Oscilloscope vertical scale: 2 mv./cm.

Probe dimensions: L = 8.0 mm., $L/\rho = 12.0$

The corresponding impedance loci are shown in Figure 4.2.5. The discharge pulse in each photograph is at a point one centimeter from the left side of the photograph. In the first 200 μs. after the discharge pulse the traces are irregular; thus the impedance loci of Figure 4.2.5 begin approximately 250μs. after the discharge pulse. A photograph of resonance probe current at zero magnetic field ($Y^2 = 0$) is included in Figure 4.1.6b.

It is important to estimate the leak rate of the vacuum system in order to determine the optimum period for experimentation. At a pressure of 2 to 10 mm, small changes in pressure cannot be measured accurately with the equipment of Figure 4.1.1. Thus it is necessary to measure the low pressure leak rate with the ionization gauge and assume that the leak rate is not appreciably different at a pressure of a few millimeters. Figure 4.1.7 is a graph of pressure vs. time as measured using the ionization gauge. As shown on the graph, there is a period of about one hour after pump down during which leakage contamination is negligible.

---

*Only these conditions are varied in the experiments

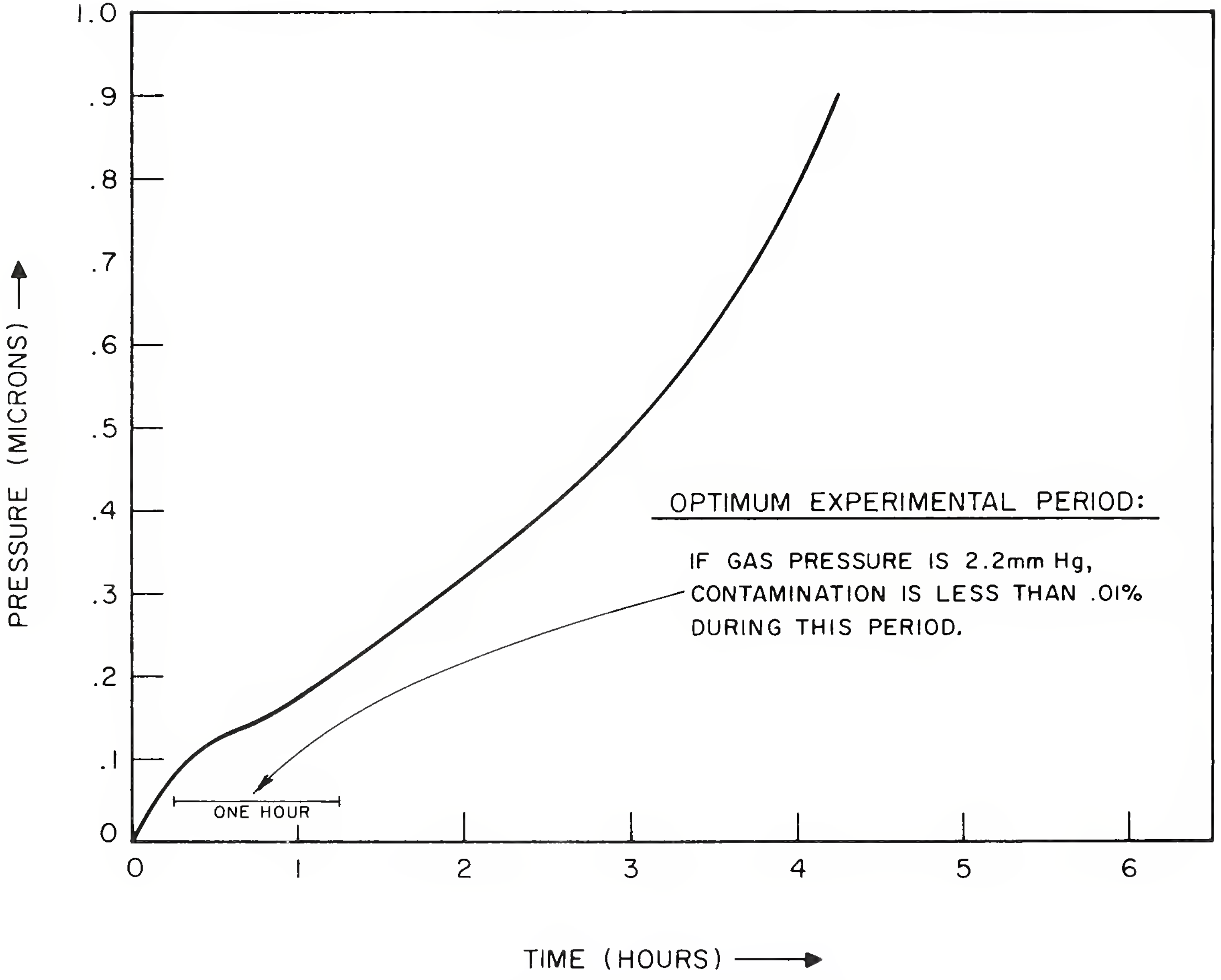

Figure 4.1.7 Vacuum system leakage

4.2 Comparison of Experimental and Theoretical Impedance

The monopole impedance measurements to be described were carried out in neon and helium gases. Some properties of these gases (at 300°K, 1 mm pressure) are summarized in the following table (CGS units):

Gas	Electron-molecule Collision probability P_c	Recombination coefficient α	Ambipolar Diffusion Coefficient D_a
Neon	3.3	2.1×10^{-7}	115
Helium	19	1.7×10^{-8}	540

The values of α and D_a are as given by Goldstein[22] and the values of P_c are as given by Brown.[23] The table indicates that neon is preferable to helium because neon has a lower diffusion coefficient and a higher recombination coefficient. This means that a neon afterglow has a greater tendency to decay by recombination instead of diffusion. Since recombination is a volume process and diffusion a surface process, afterglow decay by recombination tends to produce a uniform plasma. In addition, neon's lower value of P_c indicates that it may be used at higher pressure (for the same collision frequency) thus reducing contamination problems.

In some of the experiments a mixture of neon plus 0.5% argon is used. At 300°K the argon contributes negligibly to the collision frequency.

However the electron-molecule collision probability of argon rises sharply at higher temperatures (the Ramsauer effect). Thus the argon tends to increase the cooling rate for the electrons in the first 50 to 100μs after the discharge pulse. The presence of the argon should reduce the tendency of neon metastable excited states to maintain the electron temperature above 300°K.

The time required for the attainment of electron thermal equilibrium is of major importance and has been studied by Dougal and Goldstein.[24] For neon and helium at pressures between .5 and 5 mm., this time constant t_e is given by the following formulas:

Neon: $t_e < \frac{150}{P} + 90\ \mu s.$ for $p = 5$ mm. $t_e \leqslant 120\ \mu s.$

Helium: $t_e < \frac{8.4}{P} + 26\ \mu s.$ for $p = 1$ mm. $t_e \leqslant 36\ \mu s.$

Thus it should be possible to begin impedance measurements after the time t_e.

The theoretical calculations require an estimate of the collision frequency ν which is given by the sum of the electron-molecule collision frequency and the electron-ion collision frequency. That is,

$$\nu = \nu_{em} + \nu_{ei}$$

Similarly, the relative collision parameter $Z = \frac{\nu}{\omega}$ is given by

$$Z = Z_{em} + Z_{ei}$$

The appropriate collision frequencies are as follows (as given by Dougal and Goldstein[24] and discussed by Pfister[25]):

$$\nu_{em} = \frac{4}{3} \bar{v} \; P_c \; p_o \qquad \text{(MKS units)}$$

$$\nu_{ei} = \frac{3.62 \times 10^6 \; N_i}{T_e^{3/2}} \ln \left[\frac{3.30 \times 10^6 \; T_e^{3/2}}{N_i^{1/2}} \right]$$

in which $\bar{v} = \sqrt{\frac{8k \; T_e}{\pi \; m}}$

= average velocity of electrons with Maxwellian distribution

$p_o = \frac{273}{T} p$ = pressure reduced to 0°C

N_i = ion density

For a fixed frequency of 1.6 Gc., the electron-ion collision parameter may be approximated by the following simple function of X, the electron density parameter:

$$Z_{ei} = .010 \; X$$

The electron-molecule collision parameter values are summarized in the following table:

Gas	Pressure	Z_{em}
Neon	2.3 mm.	.010
Neon	4.3 mm.	.019
Neon	10.3 mm.	.044
Helium	2.2 mm.	.055

The theoretical and experimental results are shown as Smith chart impedance graphs in Figures 4.2.1 to 4.2.12. The theoretical graphs indicate that an increasing magnetic field sweeps the impedance locus from the top of the Smith chart nearly to the bottom. This effect is reduced by increasing the pressure. Increased pressure also tends to move the loci to the right.

A prominent feature of each theoretical locus is the presence of a "kink" in the vicinity of $X = 1$ (plasma resonance). This kink arises from the logarithm in the impedance formula and is thus related to the elliptic/hyperbolic feature of the quasi-static theory. The point $X = 1$ is always on the boundary between an elliptic and a hyperbolic region (see Figure 2.1.1). Increasing the pressure tends to smooth out the kinks in the impedance loci. In addition, the point $X = 1$ is seen to follow a nearly

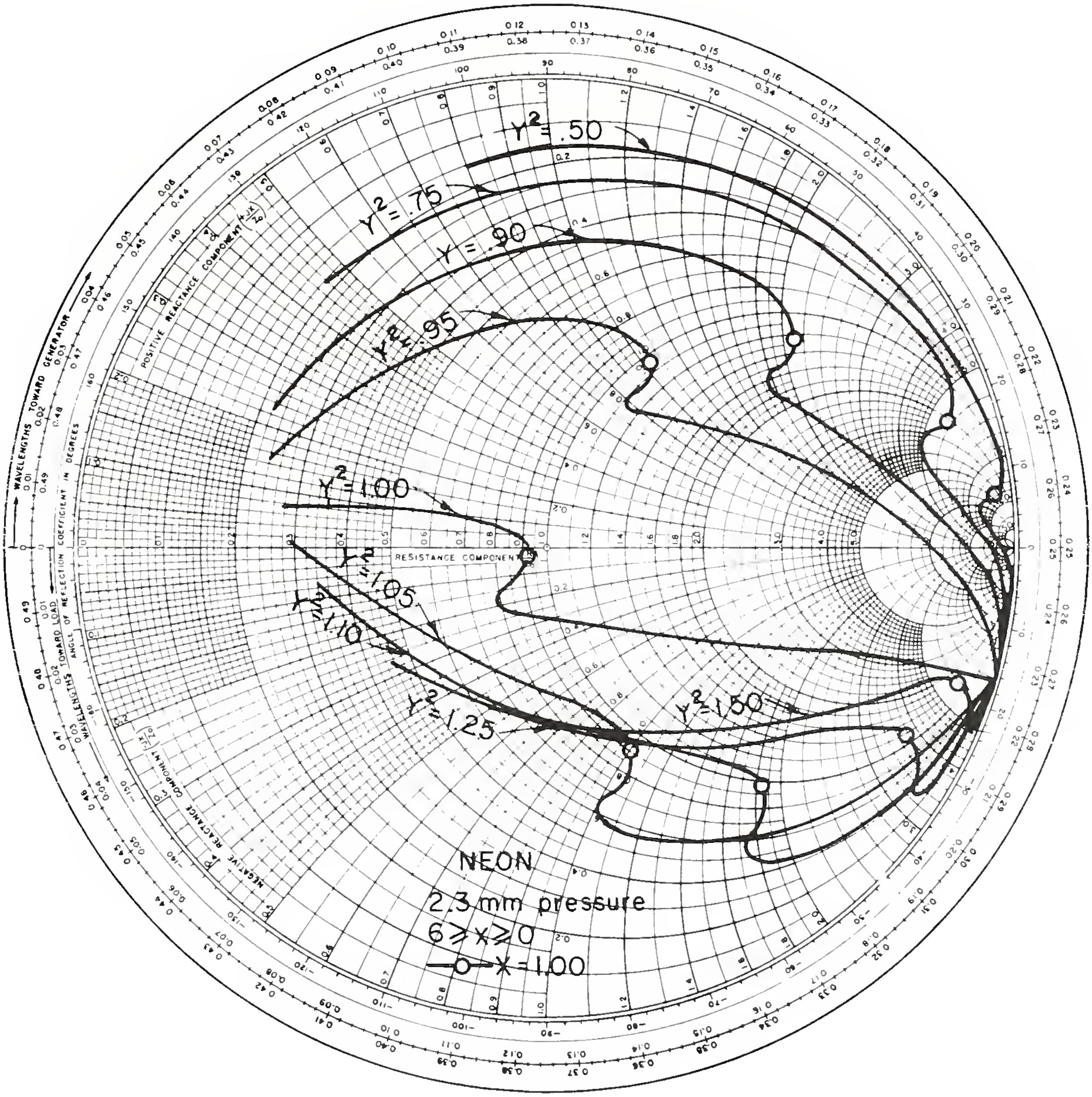

Figure 4.2.1 Theoretical impedance loci for neon at 2.3 mm. pressure

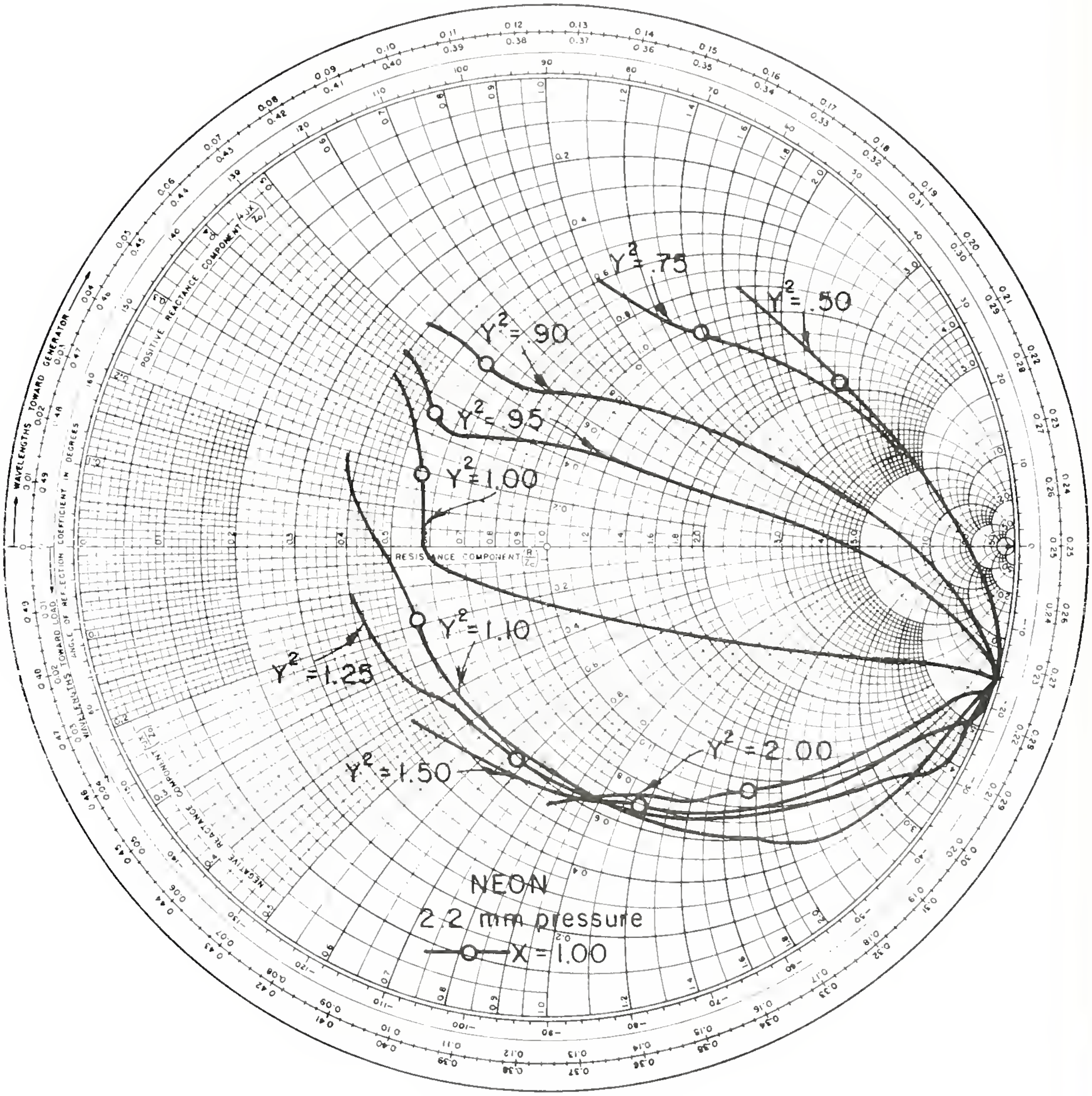

Figure 4.2.2 Experimental Impedance loci for neon at 2.2 mm. pressure

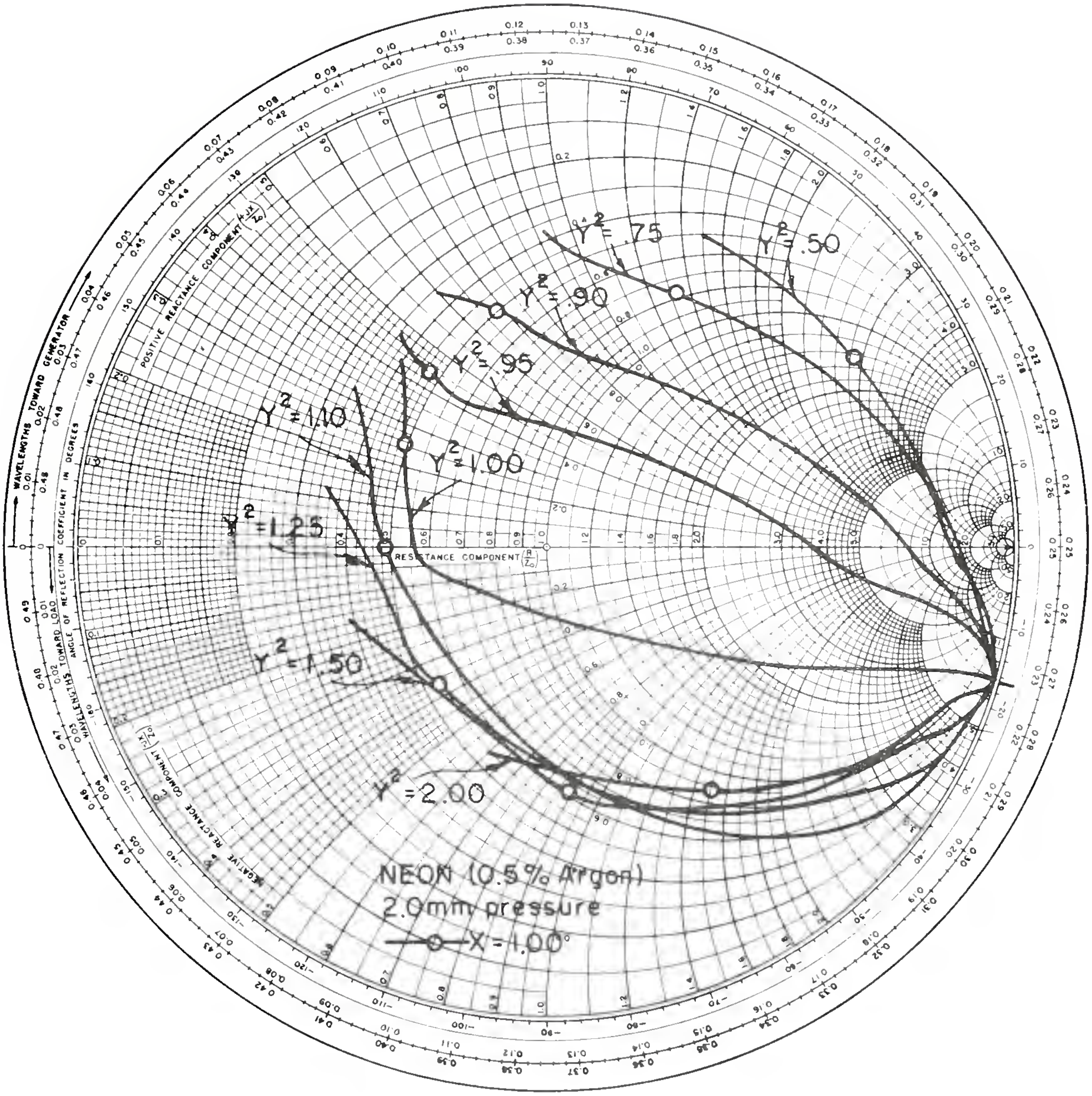

Figure 4.2.3 Experimental impedance loci for neon (0.5% argon) at 2.0 mm. pressure

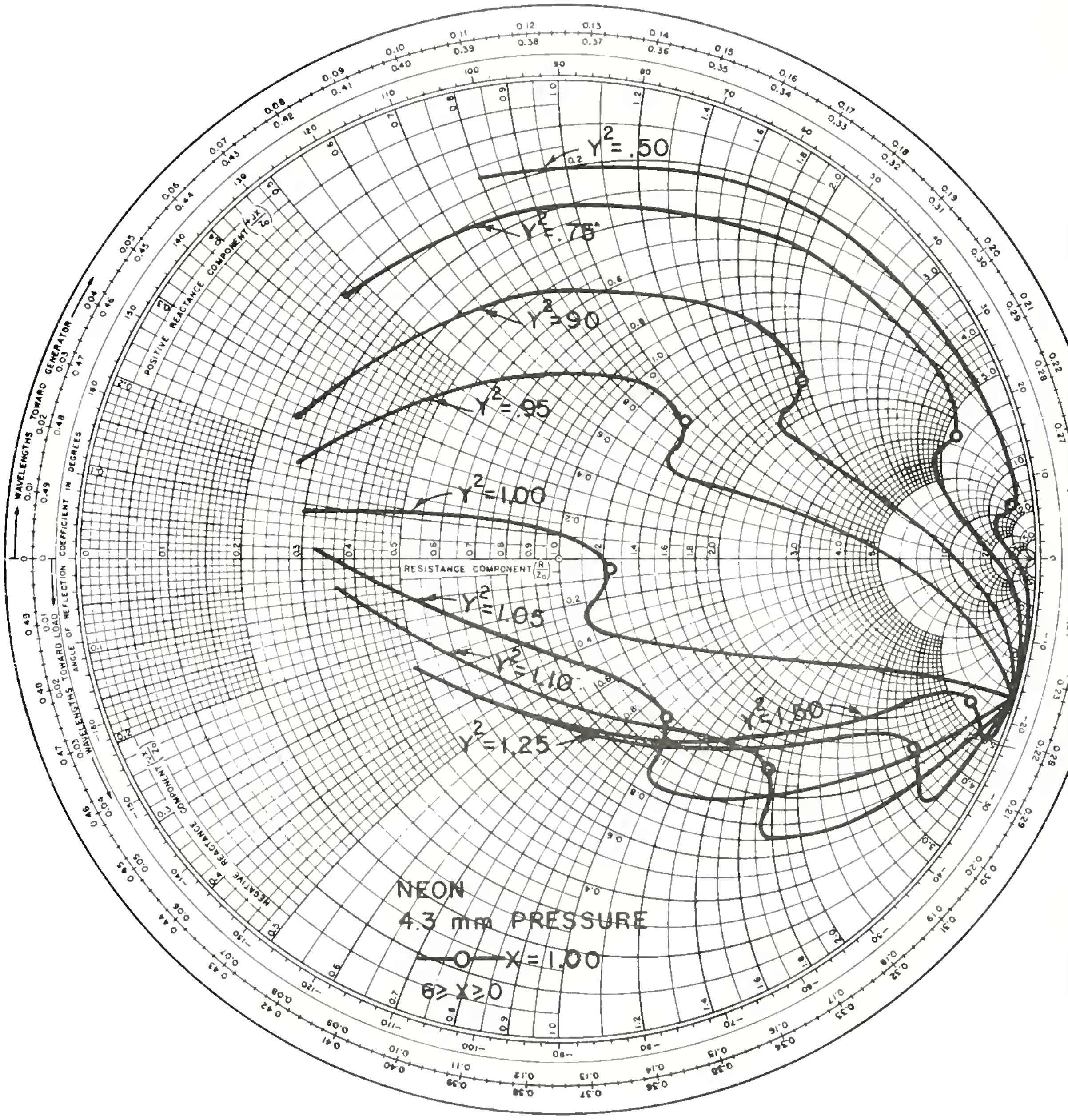

Figure 4.2.4 Theoretical impedance loci for neon at 4.3 mm. pressure

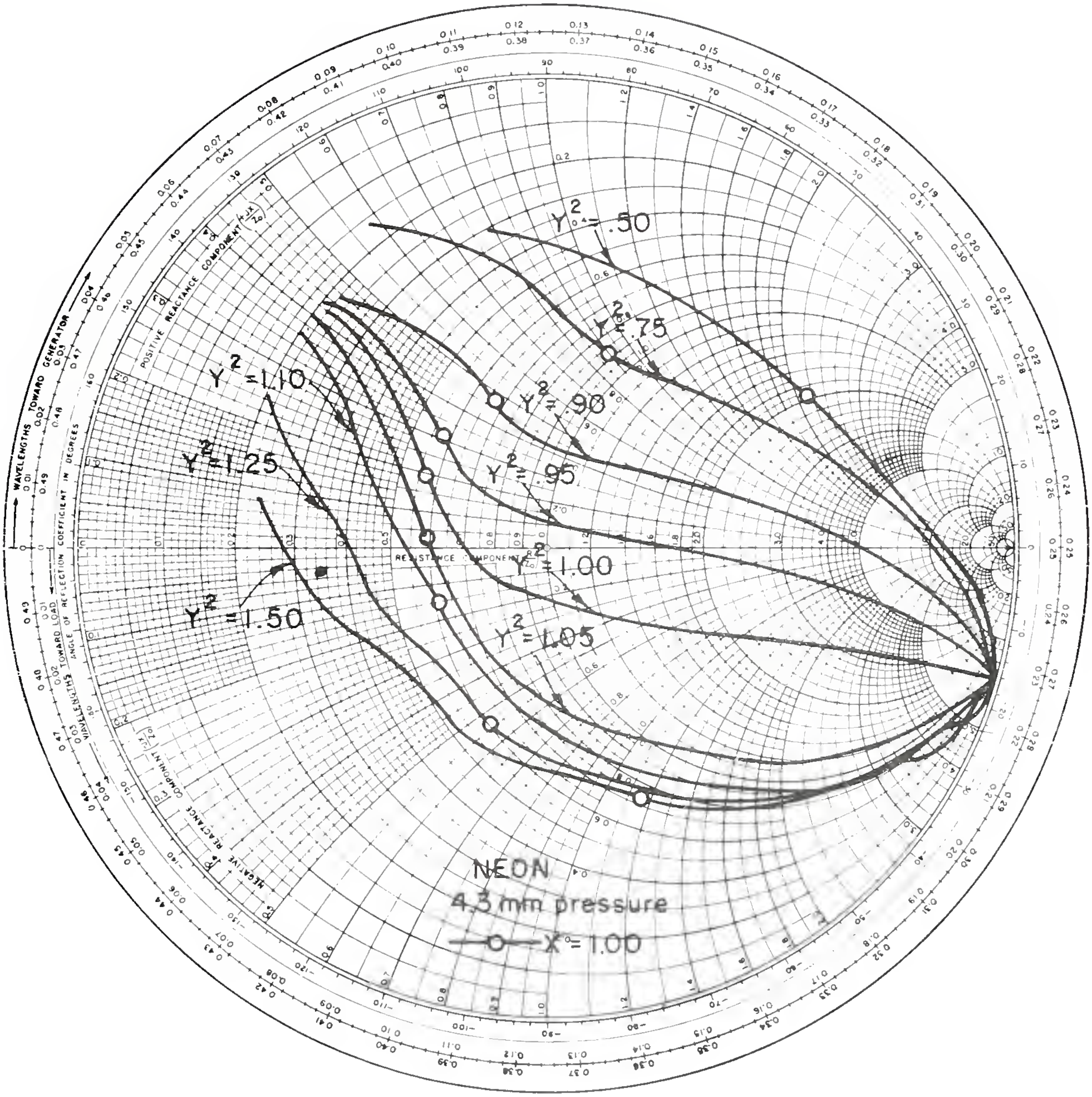

Figure 4.2.5 Experimental impedance loci for neon at 4.3 mm. pressure

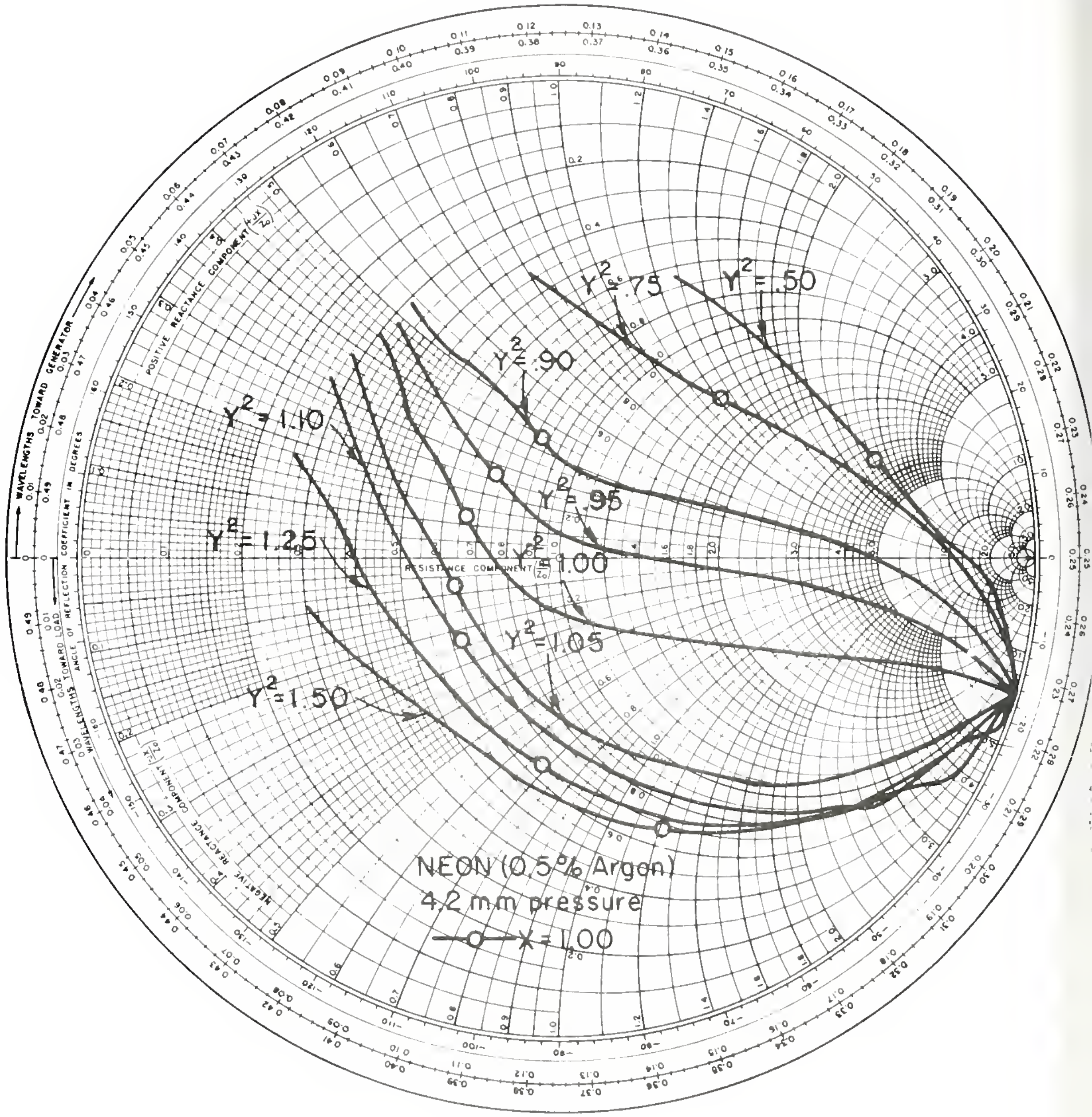

Figure 4.2.6 Experimental impedance loci for neon (0.5% argon) at 4.2 mm.pressure

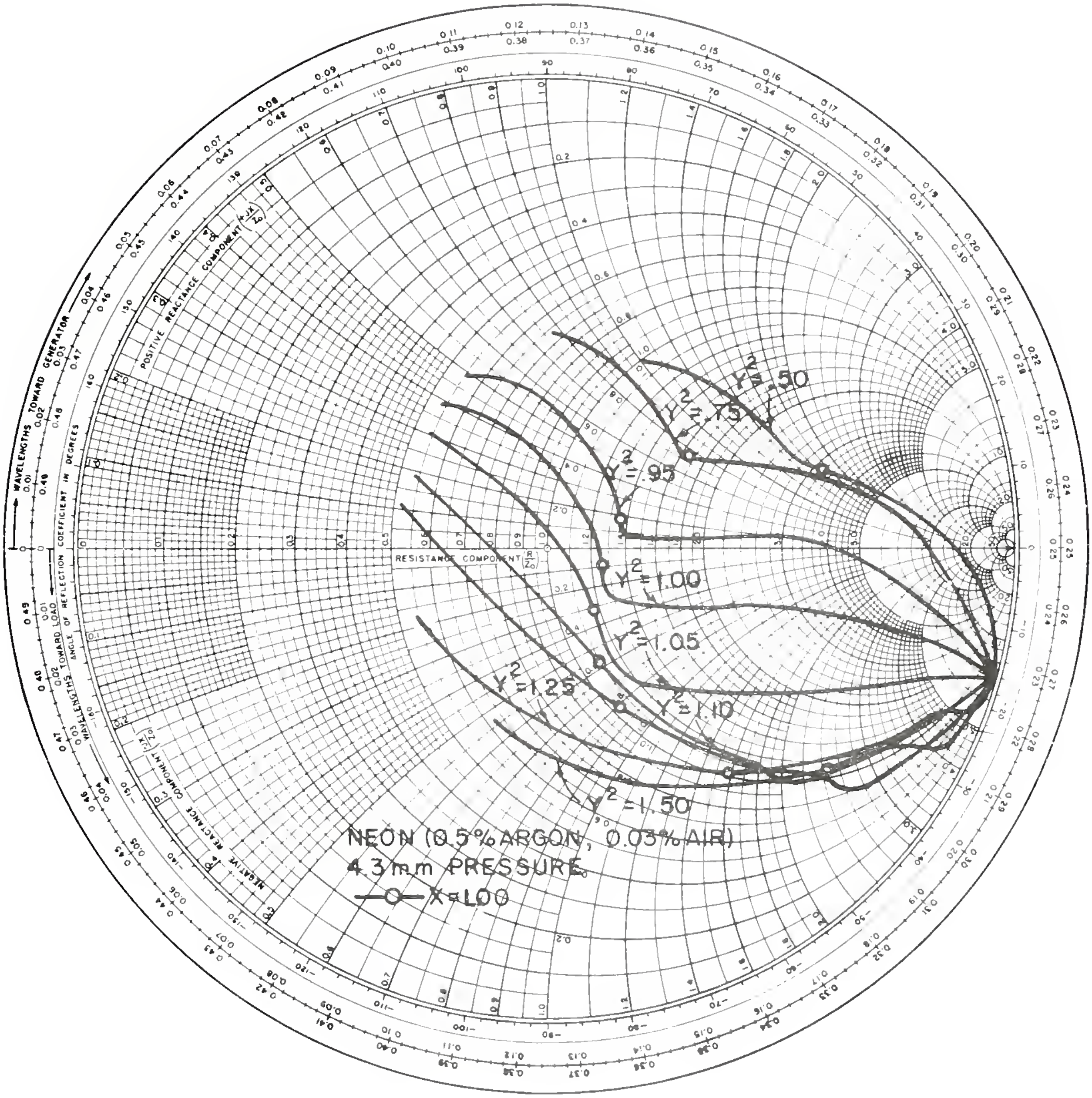

Figure 4.2.7 Experimental impedance loci for neon (0.5% argon, 0.03% air) at 4.3 mm. pressure

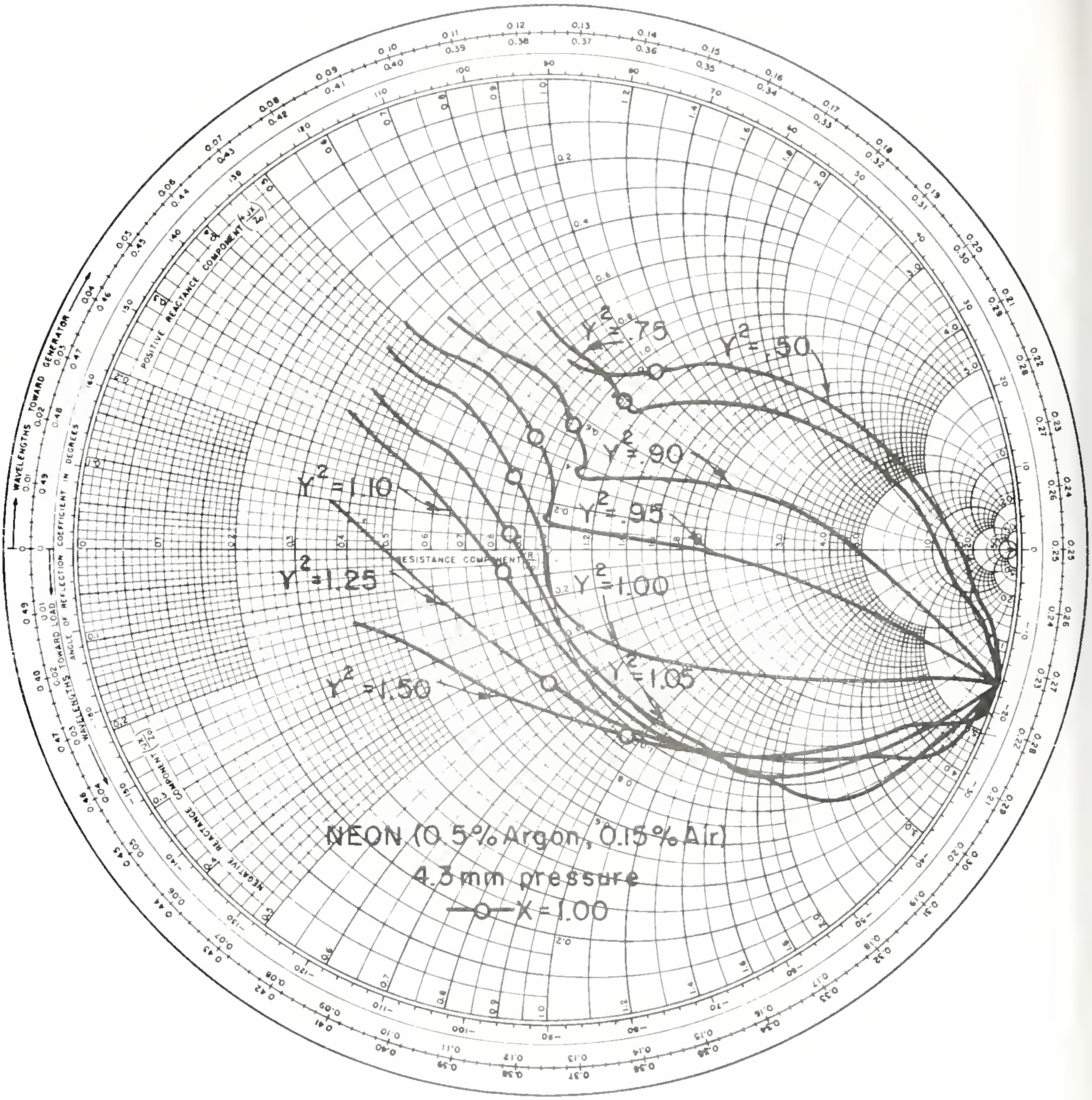

Figure 4.2.8 Experimental impedance loci for neon (0.5% argon, 0.15% air) at 4.3 mm. pressure

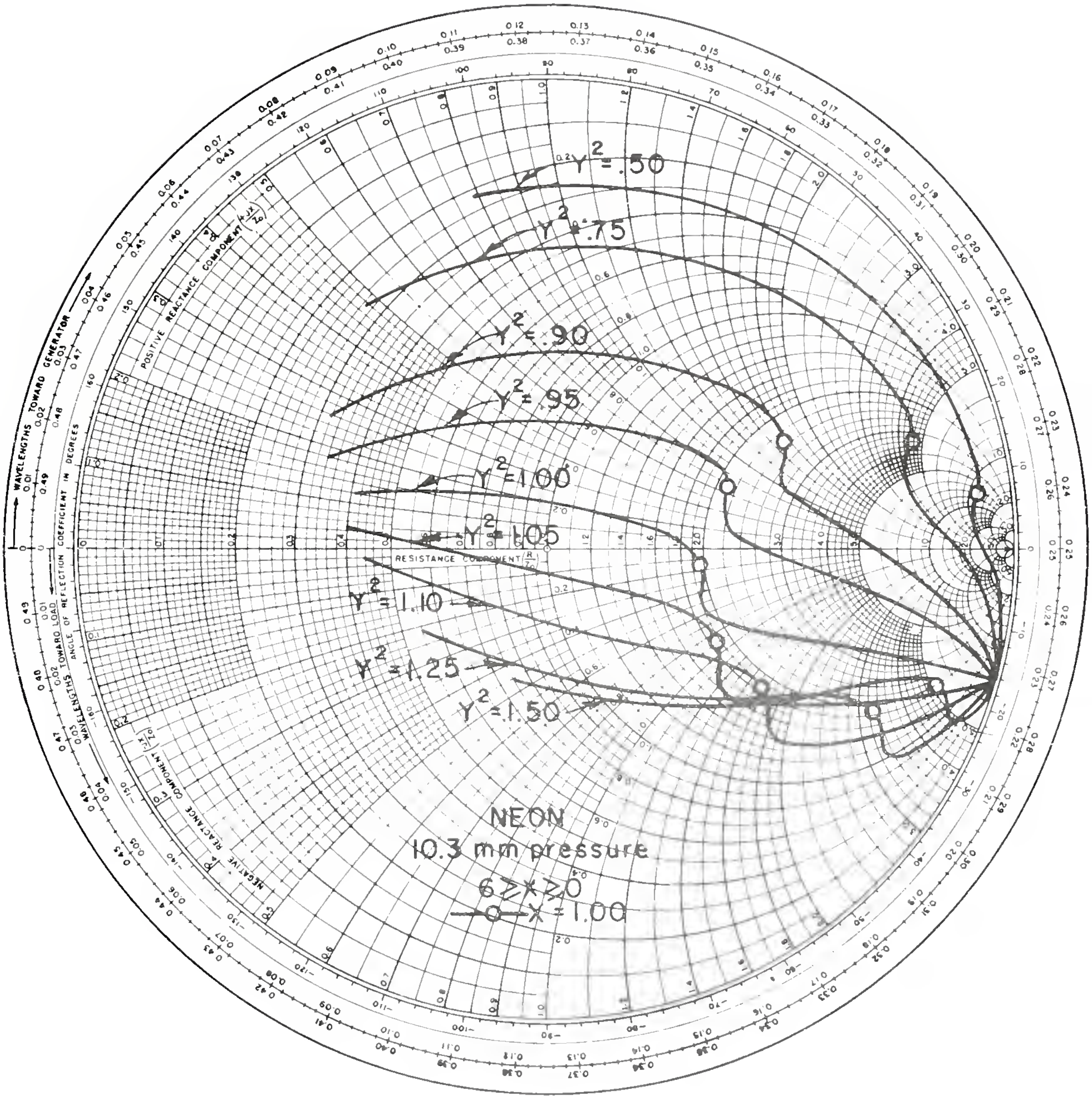

Figure 4.2.9 Theoretical impedance loci for neon at 10.3 mm. pressure

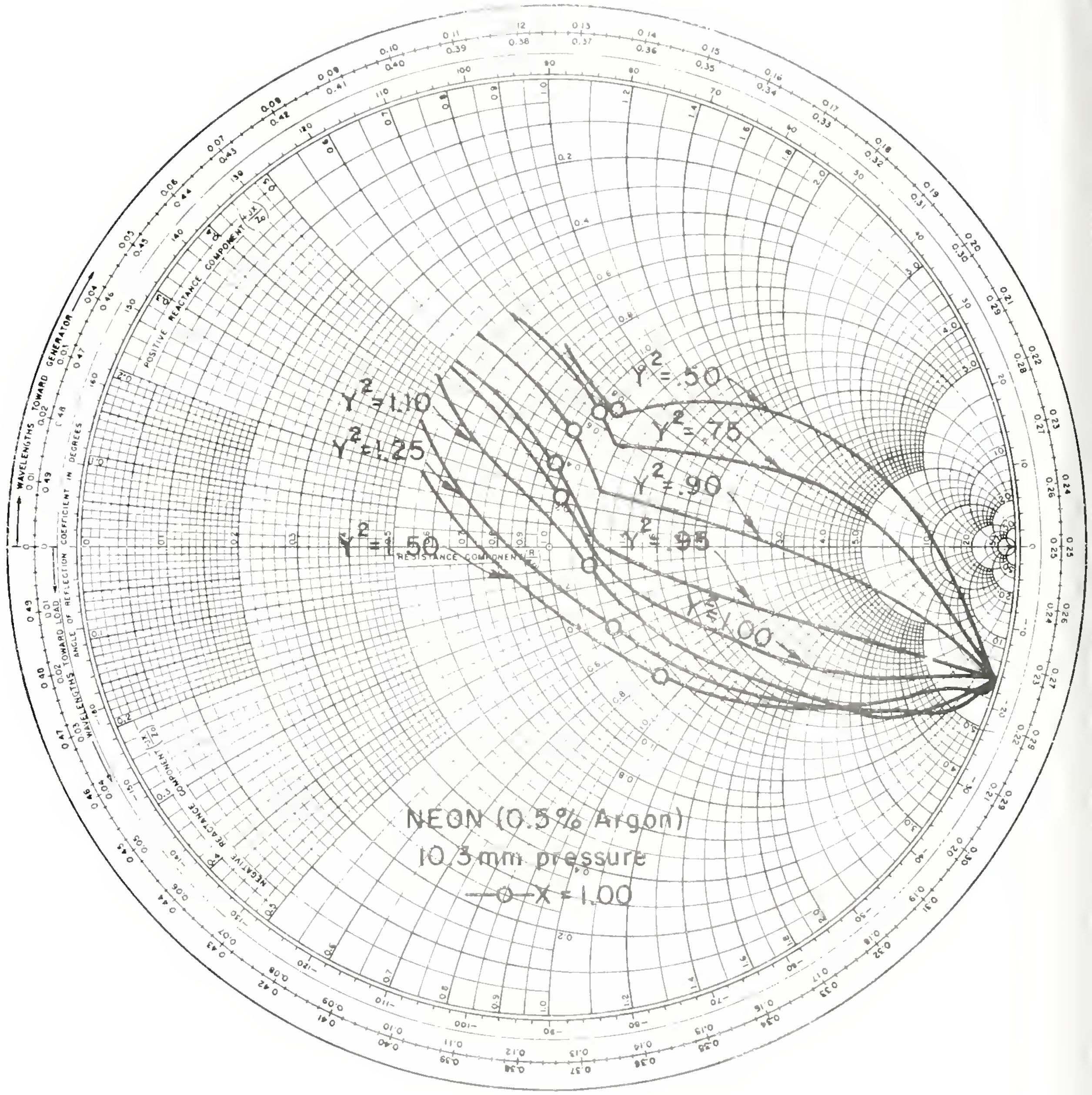

Figure 4.2.10 Experimental impedance loci for neon (0.5% argon) at 10.3 mm. pressure

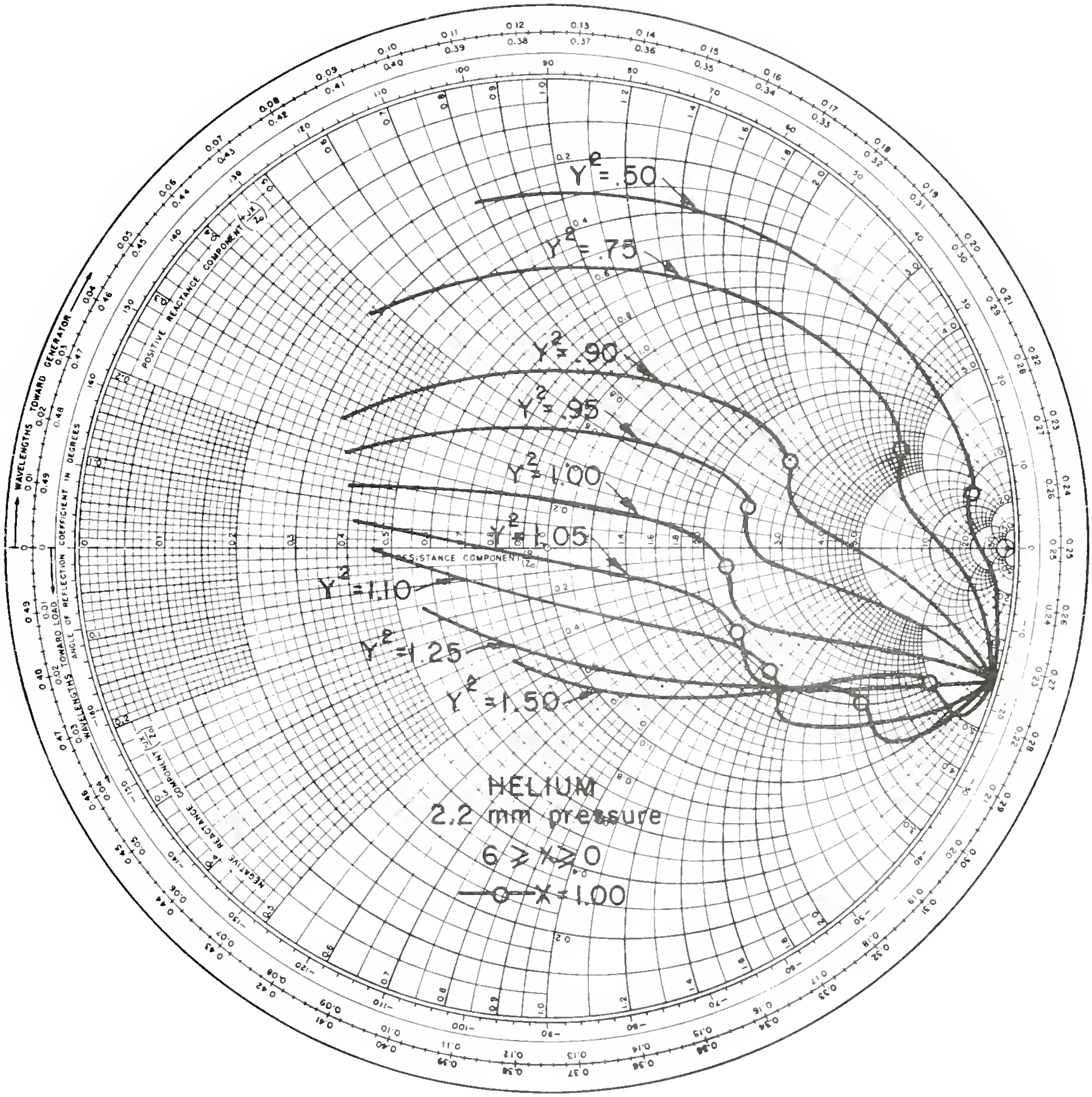

Figure 4.2.11 Theoretical impedance loci for helium at 2.2 mm. pressure

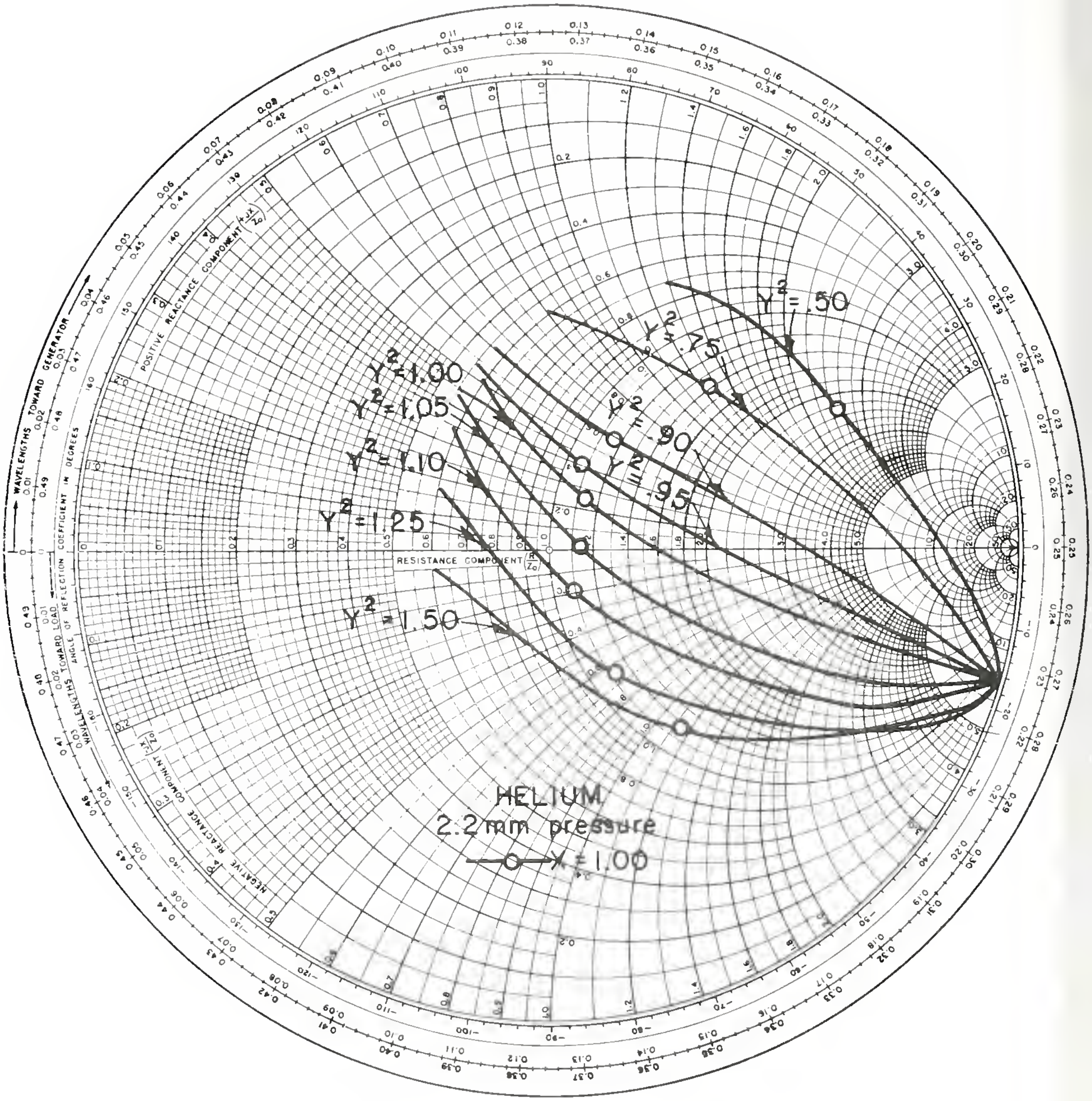

Figure 4.2.12 Experimental impedance loci for helium at 2.2 mm. pressure

circular path as the DC magnetic field changes

It should be noted that the line $X + Y^2 = 1$ is also an elliptic-hyperbolic boundary for $X < 1$, $Y^2 < 1$ (Refer to Figure 2.1.1). The points $X = 1 - Y^2$ are not marked on the theoretical impedance loci but they are close to the real axis for small values of Y^2 and are all capacitive. The Smith chart graphs reveal no unusual behaviour at $X = 1 - Y^2$

In general there is good qualitative agreement between experiment and theory. The movement of the impedance loci from the top of the Smith chart to the bottom with increasing magnetic field is evident in every experiment. Movement of the loci to the right and toward the real axis with increasing collision frequency also is evident. In all cases (theoretical and experimental) the cyclotron resonance locus ($Y^2 = 1$) meets the rim of the Smith chart at right angles.

In each experiment, the points $X = 1$ follow an approximately circular path. Since these points were determined at zero magentic field and since an increasing magnetic field tends to increase the time required for afterglow decay, the points $X = 1$ are in error for $Y^2 > 0$ Furthermore the magnitude of the error increases as Y^2 increases Thus the true plasma resonance points are somewhat to the right of the indicated points and the necessary correction increases with increasing magnetic field

In Section 3.3 it was found that a non-uniform electron density tends to move the impedance locus for $Y^2 = 0$ away from the rim of the Smith chart and toward the real axis Such an effect is evident in every experimental Smith chart at low values of Y^2 Agreement with the theory is somewhat better at high values of Y^2, presumably because the magnetic field tends to reduce diffusion to the probe surface (transverse diffusion). A reduction in diffusion renders the plasma more uniform and uniformity is assumed in the theory.

The kinks at X = 1 are visible in many of the experimental loci. At high magnetic fields, the kinks are to the right of the plasma resonance points obtained at zero magnetic field. As discussed above, this is probably caused by the extended decay period of a plasma in a magnetic field. The theory predicts a smoothing out of the kinks as gas pressure is increased and this effect is noticeable if Figure 4.2.2 is compared with Figure 4.2.5. However, a non-uniform plasma density also would tend to smooth out the kinks and the degree of uniformity depends on the plasma decay processes which in turn are pressure-dependent. Thus it is very difficult to identify the cause of a smoothing effect in the impedance loci when the gas pressure is changed.

The addition of a small quantity of Argon (to increase the rate at which the electrons approach thermal equilibrium) apparently has little effect. This can be seen by comparing Figure 4.2.3 with Figure 4.2.2 and Figure 4.2.6 with Figure 4.2.5.

In contrast to the case of argon, the addition of a very small amount of air has a pronounced effect on the impedance loci (see Figures 4.2.7 and 4.2.8). The effect of the addition of air is to bring the experimental results into much closer agreement with the theory, expecially in the regions of the plasma resonance kinks. The air percentages indicated on the graphs are rough approximations obtained by extrapolating the leakage graph of Figure 4.1.7 to 5 hours (.03% air at 4.3 mm) and to

25 hours (.15% air at 4.3 mm). It is suggested that the addition of air tends to cause the predominance of volume processes (recombination, attachment) in the afterglow decay. This should produce a more uniform plasma and hence better agreement between theory and experiment. The argument for additional decay processes is supported by the fact that the addition of air shortens the overall decay period by a factor ranging from 1/5 to 1/10. Most of this shortening is in the early part of the afterglow when the electron density is high. Since the recombination decay rate is proportional to the square of electron density, the early afterglow shortening is a further argument for the addition of volume decay processes.

The impedance loci for helium (Figure 4.2.12) exhibit no kinks at all. In contrast the experiment in neon at 10.3 mm (Figure 4.2.10) displays kinks which are definite although considerably smoothed in comparison with the theory (Figure 4.2.9). The two cases compared have similar collision frequencies as is shown in the collision frequency table given earlier in this section. This tends to confirm the earlier assertion that neon is preferable to helium in an experiment of this type.

5. CONCLUSIONS

A formulation for electromagnetic theory in a magnetoplasma is obtained. This formulation is in terms of a scalar potential and a vector potential. A modified Coulomb gauge condition is selected, the choice being made so that the quasi-static electric field is displayed as a distinct part of the total electric field. The total electric field is expanded in such a manner as to facilitate making a low frequency approximation (the expansion is similar to the expansions used by Mittra and Deschamps[1] and also Kogelnik[26]). In the low frequency approximation, it is shown that only the quasi-static electric field remains. Furthermore in the low frequency approximation, part of the magnetic field is shown to arise from currents induced in the magnetoplasma by the quasi-static electric field. This induced magnetic field is not present in isotropic media.

The quasi-static electric field of a short dipole antenna is calculated and in the lossless case the field is found to contain conical discontinuities emanating from the ends and center of the dipole. These discontinuities occur only when the quasi-static differential equation is hyperbolic and they lie along members of the family of characteristic surfaces of the differential equation.

The quasi-static electric field is used to obtain an expression for the input impedance of the dipole for any orientation with respect to the DC magnetic field. Under lossless, hyperbolic conditions it is found that the input impedance has a positive real part. Integration of the Poynting vector over a surface surrounding the dipole indicates that real outward power flow is present and that it arises from the induced magnetic field mentioned above. It is concluded that the quasi-static theory predicts a form of radiation from a short dipole in a magnetoplasma.

The results summarized above are based on the assumption that the current distribution is triangular and that a filamentary current is an adequate representation of the dipole current for electric field calculations. The influence of this assumption is estimated by carrying out impedance calculations for two different current distributions. The first distribution is triangular but the current is assumed to be spread over the cylindrical surface of the dipole. The second distribution is filamentary and such that the slope of the current is zero at the ends of the dipole and at the center. These two assumed currents give impedances which are essentially identical to the impedance as originally derived.

The quasi-static differential equation can be reduced to Poisson's equation by a simple dimensional scaling. It is shown that a cylindrical dipole in a magnetoplasma has a free space equivalent with a different length and a distorted cross section. Furthermore, it is shown that the scaling principle can be used to derive the dipole impedance formula.

A first order correction to the quasi-static impedance theory is computed. The correction is found to be small in many cases of interest, including the laboratory experiment used to test the theory.

The generation of longitudinal plasma waves is considered but only for the isotropic case. Plasma waves are found to affect impedance appreciably only in the vicinity of plasma resonance. In the laboratory plasma, the collision frequency is high enough to mask completely any impedance effect due to plasma wave generation.

The effect of a non-uniform electron density is considered by calculating the impedance of a non-uniform, isotropic plasma between parallel plane electrodes. Non-uniformity is found to have little effect as long as no part of the plasma is in a state of plasma resonance. If some region is in resonance, the effect on impedance is similar to the effect of increasing the collision frequency

A series of experiments is described in which impedance measurements are made on a cylindrical probe immersed in a pulsed, decaying plasma. A DC magnetic field permeates the plasma and is parallel to the dipole axis. The electron density in the vicinity of the probe is measured using the "Resonance Probe" technique. Good qualitative agreement between measured and theoretical impedance is obtained. Quantitative agreement is only fair, probably because the plasma is quite non-uniform. In some of the experiments, a small amount of air was allowed to mix with the neon (neon was used in almost all of the experiments). Addition of the air resulted in greatly improved agreement between theory and experiment. It is suggested that the presence of air enhanced volume decay processes in the discharge afterglow and thus prpduced a more uniform plasma.

REFERENCES

1. R. Mittra and G. A. Deschamps, "Field Solution for a Dipole in an Anisotropic Medium", Proceedings of the Symposium on Electromagnetic Theory and Antennas, Copenhagen, Denmark, 1962.

2. B. P. Kononov, A. A. Rukhadze, G. V. Solodukhov, "Electric Field of a Radiator in a Plasma in an External Magnetic Field", Soviet Physics-Technical Physics 6 #5, pp. 405-410, November 1961.

3. J. C. Katzin and M. Katzin, "The Impedance of a Cylindrical Dipole in a Homogeneous Anisotropic Ionosphere", Electromagnetic Research Corp., Report No. NAS 585-2, September 26, 1961.

4. H. A. Whale, "The Impedance of an Electrically Short Antenna in the Ionosphere", Presented at the conference on "The Ionosphere", London, Goddard Space Flight Center Report X-615-62-88, July 1962.

5. E. N. Bramley, "The Impedance of a Short Cylindrical Dipole in the Ionosphere", Planet. Space Sci., 9, pp. 445-454.

6. T. R. Kaiser, "The Admittance of an Electric Dipole in a Magneto-Ionic Environment", Planet. Space Sci., 9, pp. 639-657, 1962.

7. R. King and C. W. Harrison, "Half-Wave Cylindrical Antenna in a Dissipative Medium: Current and Impedance", J. of Res. NBS (D) 64 D No. 4, p. 365, July-August 1960.

8. G. A. Deschamps, "Impedance of an Antenna in a Conducting Medium", Transactions IRE, AP-10, #5, pp. 648-650, September 1962.

9. A. W. Trivelpiece and R. W. Gould, "Space Charge Waves in Cylindrical Plasma Columns", J.A.P. 30 #11, p. 1784, November 1959.

10. A. W. Trivelpiece, A. Ignatius, and P. C. Holscher, "Backward Waves in Longitudinally Magnetized Ferrite Rods", J.A.P. 32 #2, pp. 259-267, February 1961.

11. R. W. Damon, and J. R. Eshbach, "Magnetostatic Modes of a Ferromagnetic Slab", J.A.P. Supplement to Vol. 31 #5, p. 104S-105S, May 1960.

12. R. I. Joseph, and E. Schlömann, "Theory of Magnetostatic Modes in Long, Axially Magnetized Cylinders", J.A.P. 32 #6, pp. 1001-1005, June 1961.

13. M. H. Cohen, "Radiation in Plasmas", Part I Phys. Rev. 123 #3, pp. 711-721, Part II Phys. Rev. 126 #2, pp. 389-397, Part III Phys. Rev. 126 #2, pp. 398-404.

14. I. N. Sneddon, "Elements of Partial Differential Equations", McGraw-Hill Book Co., 1957.

15. J. H. Richmond, "A Reaction Theorem and Its Application to Antenna Impedance Calculations", IRE-PGAP, AP-9 #6, pp. 515-520, November 1961.

16. S. A. Schelkunoff, H. T. Friis, "Antennas: Theory and Practice", Chapter 10, John Wiley and Sons Inc., 1952.

17 R. A. Hurd, "On the Possibility of Intrinsic Loss Occurring at the Edges of Ferrites", Canadian Journal of Physics, 40, pp. 1067-1076, 1962.

18. Y. T. Lo, " A Note on the Cylindrical Antenna of Non-Circular Cross Section", Jour. App. Phys., 24, #10, pp. 1338-1339, October 1953.

19. A. Hessel and I. Shmoys, "Excitation of Plasma Waves by a Dipole in a Homogeneous Isotropic Plasma", Electromagnetics and Fluid Dynamics of Gaseous Plasma, pp. 173-183, Polytechnic Press, 1962, MRI Symposia Series Vol. XI.

20. K. Takayama, H. Ikegami, and S. Miyazaki, "Plasma Resonance in a Radio Frequency Probe", Phys. Rev. Lett, 5 #6, pp. 238-240, September 15, 1960.

21. E. L. Ginzton, "Microwave Measurements", McGraw—Hill Book Co., 1957.

22. L. Goldstein, "Electrical Discharges in Gases and Modern Electronics", Advances in Electronics and Electron Physics, Vol. VII, Academic Press, 1955.

23. S. C. Brown, "Basic Data of Plasma Physics", Technology Press and Wiley, 1959.

24. A. A. Dougal, and L. Goldstein, "Energy Exchange Processes Through Coulomb Collisions in Gaseous Discharge Plasma Studied by Microwave Interaction Techniques", University of Illinois, Gaseous Electronics Laboratory, Scientific Report No. 1, Contract No. AF19(604)-2152.

25. W. Pfister, "Studies of the Refractive Index in the Ionosphere: The Effect of the Collision Frequency and of Ions", The Physics of the Ionosphere - Report of the 1954 Cambridge Conference, pp. 394-401.

26. H. Kogelnik, "On Electromagnetic Radiation in Magneto-Ionic Media", NBS Journal of Research, Vol. 64D, No. 5, pp. 515-523, September-October, 1960

ADDITIONAL REFERENCES ON RELATED TOPICS

A-1 E. Arbel, "Radiation from a Point Source in an Anisotropic Medium", Polytechnic Institute of Brooklyn, Research Report PIB MRI-861-60, November 2, 1960.

A-2 E. Arbel, L. B. Felsen, "On Electromagnetic Green's Functions for Uniaxially Anisotropic Regions , Polytechnic Institute of Brooklyn Research Report PIB MRI-985-61, February 26, 1962.

A-3 H. H. Kuehl, "Electromagnetic Radiation from an Electric Dipole in a Cold, Anisotropic Plasma", Phys. of Fluids, 5, #9, pp. 1095-1103, September, 1962.

A-4 J. R. Herman, "Theoretical Determination of the Impedance Characteristics of a Capacitive Ionosphere Rocket Probe", Penn. State University, Ionosphere Research Laboratory, Scientific Report No. 180, March 1, 1963.

APPENDIX

THE MODIFIED COULOMB GAUGE CONDITION

The gauge condition used in Section 2.1 is

$$\nabla \cdot K \overline{A} = 0 \tag{A.1}$$

This will be referred to as the modified Coulomb gauge condition because of its similarity to the Coulomb gauge condition

$$\nabla \cdot \overline{A} = 0 \tag{A.2}$$

which is mentioned in various texts.

In general, a particular gauge condition is chosen in order to simplify some aspect of electromagnetic theory. It is necessary to show that the choice of gauge condition has no effect on the field solution for $\overline{E}$ and $\overline{H}$ and that it is always possible to find potentials which satisfy the gauge condition. Suppose that $\overline{A}$ and Ψ are potentials which satisfy Maxwell's equations through the relations

$$\overline{E} = -\nabla\Psi - j\omega\overline{A} \tag{A.3}$$

$$\mu_o \overline{H} = \nabla \times \overline{A} \tag{A.4}$$

It is assumed that no restriction (such as a gauge condition) has been applied to $\overline{A}$ and Ψ. It is known that Maxwell's equations are invariant under a gauge transformation of the type

$$\overline{A}' = \overline{A} + \nabla\beta \tag{A.5}$$

$$\Psi' = \Psi - j\omega\beta \tag{A.6}$$

in which A', Ψ' are the new potentials and β is the gauge function. If it is required that the new potentials satisfy the modified Coulomb gauge condition, Equation (A.1) becomes

$$\nabla \cdot K \nabla \beta = - \nabla \cdot K \overline{A} \tag{A.7}$$

Equation (A.7) has the same form as the quasi-static equation for the scalar potential and solutions for this equation may be obtained easily. Thus a gauge function β can always be found such that the gauge condition is satisfied. Furthermore the invariance of Maxwell's equations under a gauge transformation assures that the field solutions are unaffected by the choice of of gauge condition.

UNIVERSITY OF ILLINOIS-URBANA
3 0112 101625298